THE PLANT CELL

The Plant Cell, 2025, **37**, koaf178

https://doi.org/10.1093/plcell/koaf178
Advance access publication 18 July 2025
Research Article

Jasmonate signaling coordinates with the SOD7–KLU pathway to regulate seed size in *Arabidopsis thaliana*

Juping Zhang,[1,2] Jian Yao,[3] Kunrong He,[1,4] Chunlan Yu,[1] Jie Du,[1] Jiancan Du,[1] Qiantang Fu,[1] Ruifeng Yao,[5,6] Gregg A. Howe,[3] Xiao Han,[1,*] Yanru Hu[1,5,6,*]

[1]CAS Key Laboratory of Tropical Plant Resources and Sustainable Use, Xishuangbanna Tropical Botanical Garden, Chinese Academy of Sciences, Kunming, Yunnan 650223, China
[2]College of Life Sciences, University of Chinese Academy of Sciences, Beijing 100049, China
[3]Department of Energy, Plant Research Laboratory, Michigan State University, East Lansing, MI 48824, USA
[4]State Key Laboratory of Tree Genetics and Breeding, Co-Innovation Center for Sustainable Forestry in Southern China, Nanjing Forestry University, Nanjing 210037, China
[5]State Key Laboratory of Chemo and Biosensing, Hunan Key Laboratory of Plant Functional Genomics and Developmental Regulation, Hunan Research Center of the Basic Discipline for Cell Signaling, College of Biology, Hunan University, Changsha 410082, China
[6]Yuelushan Laboratory, Changsha 410128, China
*Author for correspondence: huyanru@hnu.edu.cn (Y.H.), hanxiao@xtbg.ac.cn (X.H.)
The author responsible for distribution of materials integral to the findings presented in this article in accordance with the policy described in the Instructions for Authors (https://academic.oup.com/plcell/pages/General-Instructions) is: Yanru Hu (huyanru@hnu.edu.cn).

Abstract

Seed size is crucial for crop yield and plant ecological fitness. The phytohormone jasmonate regulates *Arabidopsis thaliana* seed size, but the underlying molecular mechanisms remain elusive. Here, we established that CORONATINE INSENSITIVE1 (COI1)-mediated jasmonate signaling acts maternally to repress seed growth. Accordingly, jasmonate signaling suppresses the expression of *KLUH* (*KLU*), encoding an inducer of integument cell proliferation. KLU regulates the effects of COI1-mediated signaling on seed size. The JASMONATE ZIM-DOMAIN (JAZ) repressors of jasmonate signaling interact with SUPPRESSOR OF DA1-1 (SOD7) and DEVELOPMENT-RELATED PcG TARGET IN THE APEX4 (DPA4), two transcription factors that directly repress *KLU*. Overexpression of *SOD7* largely rescues the seed size phenotype of *coi1* mutants and *JAZ1*-overexpressing *JAZ1-ΔJas* plants. Furthermore, SOD7 associates with MYC2 and MYC4, two master transcriptional regulators of jasmonate signaling. SOD7 and MYC2 synergistically decrease *KLU* transcription and inhibit seed growth, while JAZ1 interferes with their transcriptional activities and physical interaction. Notably, jasmonate signaling considerably impacts seed size under salinity stress, primarily through SOD7 and KLU. Collectively, our findings suggest that the JAZ repressors and MYC transcription factors of the jasmonate signaling pathway coordinate with the SOD7/DPA4–KLU pathway to incorporate jasmonate signals into seed development.

Introduction

Seed size in flowering plants is a critical factor influencing ecological fitness as well as an important agronomic trait directly related to crop yield (Moles et al. 2005; Fan et al. 2006; Song et al. 2007; Orsi and Tanksley 2009; Gegas et al. 2010; Linkies et al. 2010; Zuo and Li 2014; Li and Li 2016; Li et al. 2019; Zhang et al. 2023). The mature seed of angiosperms consists of the following three genetically distinct components: the seed coat, the embryo, and the endosperm. The seed coat, which is the outermost layer of the seed, is derived from the maternal sporophytic integuments of the ovule (Haughn and Chaudhury 2005). The diploid embryo is produced from the fertilized egg cell, whereas the triploid endosperm originates from the fertilized central cell (Lopes and Larkins 1993; Reiser and Fischer 1993; Chaudhury and Berger 2001; He et al. 2017). Therefore, seed size is tightly modulated by the coordinated development of maternal and zygotic tissues (Garcia et al. 2005). Previous studies using genetic and molecular approaches identified a number of regulators that control seed size in *Arabidopsis thaliana* (Li and Li 2016; Li et al. 2019). For example, the cytochrome P450 KLUH (KLU)/CYP78A5 stimulates seed growth by promoting cell proliferation in the maternal integuments (Anastasiou et al. 2007; Adamski et al. 2009). Compared with the seeds of Columbia-0 (Col-0) wild type, the seeds of the loss-of-function *klu* mutants are smaller because of the premature arrest of cell proliferation, whereas the seeds of plants overexpressing *KLU* are larger (Anastasiou et al. 2007; Adamski et al. 2009). KLU has also been suggested to regulate the formation and size of other organs, such as leaves and floral organs (Wang et al. 2008; Eriksson et al. 2010; Zhao et al. 2018). Subsequent research revealed that *KLU* transcription is directly repressed by the B3 domain transcription factors SUPPRESSOR OF DA1-1 (SOD7) and DEVELOPMENT-RELATED PcG TARGET IN THE APEX4 (DPA4), which suppress seed and organ growth (Zhang et al. 2015a). Some key regulators, such as HAIKU1 (IKU1), IKU2, MINISEED3 (MINI3), and SHORT HYPOCOTYL UNDER BLUE1 (SHB1), modulate seed growth by influencing cell elongation or proliferation in zygotic tissues (Scott et al. 1998; Garcia et al. 2003; Luo et al. 2005; Xiao et al. 2006; Zhou et al. 2009; Wang et al. 2010; Kang et al. 2013). Plant hormones, such as auxin, cytokinins, and abscisic acid (ABA), also have important roles in seed growth (McCarty 1995; Finkelstein et al. 2002; Riefler et al. 2005; Hutchison et al. 2006 ; Schruff et al. 2006; Kanno et al. 2010; Jiang et al. 2013; Li et al. 2013; Cheng et al. 2014; Gomez et al. 2016; Figueiredo and

Received January 29, 2025. Accepted May 7, 2025.

Köhler 2018; Hu et al. 2018; Robert et al. 2018; Zhang et al. 2020a Gomez et al. 2023).

The fatty acid–derived hormone jasmonate is ubiquitous in the plant kingdom; it is essential for a variety of physiological processes (Wasternack and Hause 2013; Chini et al. 2016; Huang et al. 2017; Zhang et al. 2017a; Guo et al. 2018a; Han et al. 2018 , 2023a; Howe et al. 2018; Zhou et al. 2019; Wasternack 2020; Cao et al. 2022; Hu et al. 2023). In plants, jasmonate (i.e. jasmonate-isoleucine) induces the formation of the CORONATINE INSENSITIVE1 (COI1)-JASMONATE ZIM-DOMAIN (JAZ) co-receptor (Xie et al. 1998; Xu et al. 2002; Chini et al. 2007; Thines et al. 2007; Fonseca et al. 2009; Yan et al. 2009). COI1 also associates with Arabidopsis SKP1-LIKE (ASK1 and ASK2), CULLIN1, and RING-BOX1 (RBX1) to form the SCF^{COI1} complex (Xu et al. 2002). Following the perception of jasmonate, JAZ proteins, which are crucial suppressors of jasmonate signaling, are recruited by the SCF^{COI1} complex for the subsequent degradation via the 26S proteasome pathway (Chini et al. 2007; Thines et al. 2007; Sheard et al. 2010; Yan et al. 2013; Wu et al. 2020; Li et al. 2021; Hu et al. 2023). The JAZ proteins negatively modulate various jasmonate-related processes by interacting with and repressing downstream transcription factors from multiple families (Fernández-Calvo et al. 2011; Kazan and Manners 2013; Chini et al. 2016; Mao et al. 2017). The basic helix-loop-helix (bHLH) transcription factors MYC2, MYC3, and MYC4 are the most comprehensively characterized JAZ-binding proteins that mediate a subset of jasmonate responses (e.g. root elongation inhibition and stress responses) (Boter et al. 2004; Lorenzo et al. 2004; Dombrecht et al. 2007; Cheng et al. 2011; Fernández-Calvo et al. 2011; Qi et al. 2015; Liu et al. 2019; Wang et al. 2019; Zander et al. 2020; Zhai et al. 2020; He et al. 2023). In Arabidopsis, deficiencies in jasmonate biosynthesis or signaling alter several developmental processes, such as root hair elongation, trichome initiation, and stamen development (Sanders et al. 2000; Stintzi and Browse 2000; Balbi and Devoto 2008; Qi et al. 2011, 2015; Song et al. 2011; Chini et al. 2016; Guo et al. 2018a; Han et al. 2018 , 2020; Mei et al. 2023).

Accumulating evidence has highlighted a close connection between jasmonate signaling pathway and seed size control (Eltayeb Habora et al. 2013; Wasternack et al. 2013; Wasternack and Hause 2013; Cai et al. 2014; Zhao et al. 2014; Guo et al. 2018b; Chen et al. 2020; Liu et al. 2020; Hu et al. 2021; Huang et al. 2023; Zhang et al. 2023). For example, exogenous application of jasmonate repressed Arabidopsis seed size in a COI1-dependent manner (Hu et al. 2021). Consistently, loss-of-function *coi1* mutants exhibit large seed size, whereas *jaz6* and higher order *jaz* mutant, such as *jazQ* (*jaz* quintuple) and *jazD* (*jaz* decuple), produce seeds that are smaller than wild type (Guo et al. 2018b; Liu et al. 2020; Hu et al. 2021). Further analyses revealed that COI1 suppresses cell proliferation within the integument (Hu et al. 2021). Moreover, the downstream MYC transcription factors also influence seed size (Liu et al. 2020; Hu et al. 2021). These MYC factors interact with MEDIATOR25 (MED25), KINASE-INDUCIBLE DOMAIN INTERACTING 8/9 (KIX8/9), and/or PEAPOD1/2 (PPD1/2) to regulate seed size (Liu et al. 2020; Hu et al. 2021). Similar to the seed size increase in Arabidopsis *coi1* mutants, the rice *OsCOI1-RNAi* lines also displayed larger grains than wild type (Yang et al. 2012; Hu et al. 2021). The role of OsCOI1/2 in seed and spikelet development has been recently confirmed using *Oscoi1/2* loss-of-function mutants (Nguyen et al. 2023; Wang et al. 2023). The influence of endogenous jasmonate levels on seed size is also evident in wheat. A premature stop mutation in *ketoacylthiolase 2B* (*KAT-2B*), which is involved in β-oxidation during jasmonate synthesis, leads to the grain defect in wheat seed (Chen et al. 2020). During our previous studies on jasmonate-related growth and tolerance (Hu et al. 2013; Han et al. 2018, 2020, 2023b; He et al. 2023; Mei et al. 2023), we also observed that Arabidopsis *coi1* mutants have larger seeds than the wild-type controls, which is consistent with the findings of a recent study (Hu et al. 2021). However, the genetic mechanism mediating the effects of jasmonate on seed size warrants further investigation.

In this study, we report that the seed phenotype of *coi1* was largely rescued by the *klu* mutation. Further investigation into the underlying mechanism revealed that several JAZ proteins physically interact with the transcription factors SOD7 and DPA4, which both repress *KLU* expression. Genetic analyses demonstrated that overexpression of *SOD7* suppresses the seed size phenotype of jasmonate-insensitive mutants. We provide evidence that JAZ proteins disrupt the ability of SOD7 to modulate *KLU* expression and that SOD7 and DPA4 interact with the transcription factors MYC2 and MYC4. Intriguingly, SOD7 and MYC2 reciprocally enhance their enrichment at the *KLU* promoter region, thereby suppressing *KLU* expression in a synergistic manner. MYC2 and SOD7 jointly inhibit seed growth, whereas JAZ1 interferes with their transcriptional activities and physical interaction. We also show that the jasmonate pathway negatively influences the stability of the KLU protein and impacts seed size under salinity stress conditions, primarily through the actions of SOD7 and KLU. Collectively, our study provides insights into how seed development is controlled through the integration of the jasmonate and SOD7/DPA4–KLU signaling pathways.

Results

COI1/JAZ-mediated endogenous jasmonate signaling acts maternally to decrease the seed size

During our analysis of jasmonate signaling, we observed that mutations in the jasmonate receptor COI1 lead to the formation of large seeds, indicative of the repressive effect of jasmonate signaling on seed growth. To clarify how jasmonate signaling influences seed size at the molecular level, we initially confirmed the regulatory roles of the COI1 receptor and JAZ repressors in the jasmonate pathway. Similar to the results of an earlier study by Hu et al. (2021), the seeds of the leaky loss-of-function *coi1-2* and *coi1-16* mutants were considerably larger and heavier than the Col-0 wild-type seeds (Fig. 1, A, E, and F). In mature Arabidopsis seeds, the embryo accounts for most of the seed volume. Both *coi1-2* and *coi1-16* had larger embryos than the Col-0 control (Fig. 1B). The changes in seed size were also reflected in the size of the seedlings. Similarly, the *coi1-2* and *coi1-16* cotyledons were clearly larger than the Col-0 cotyledons (Fig. 1, C and G). In addition, the *coi1-2* and *coi1-16* mutants had larger leaves and petals than the Col-0 plants (Fig. 1, D and H; Supplementary Fig. S1, A and B). Accordingly, COI1 appears to negatively affect seed size.

The JAZ proteins suppress various responses to jasmonate via direct interactions with the COI1 receptor and downstream transcription factors (Chini et al. 2007; Thines et al. 2007). Previous studies showed that the loss-of-function *jaz6*, *jazQ* quintuple mutant, and *jazD* decuple mutant produce seeds that are smaller than wild type (Guo et al. 2018b; Liu et al. 2020; Hu et al. 2021). We confirmed this phenotype for *jazQ* and also found that that *jazQ* embryos are smaller the Col-0 control (Fig. 1, A, B, E, and F). Additionally, the *jazQ* cotyledons, leaves, and petals were also significantly smaller than those of the Col-0 plants (Fig. 1, C, D, G, and

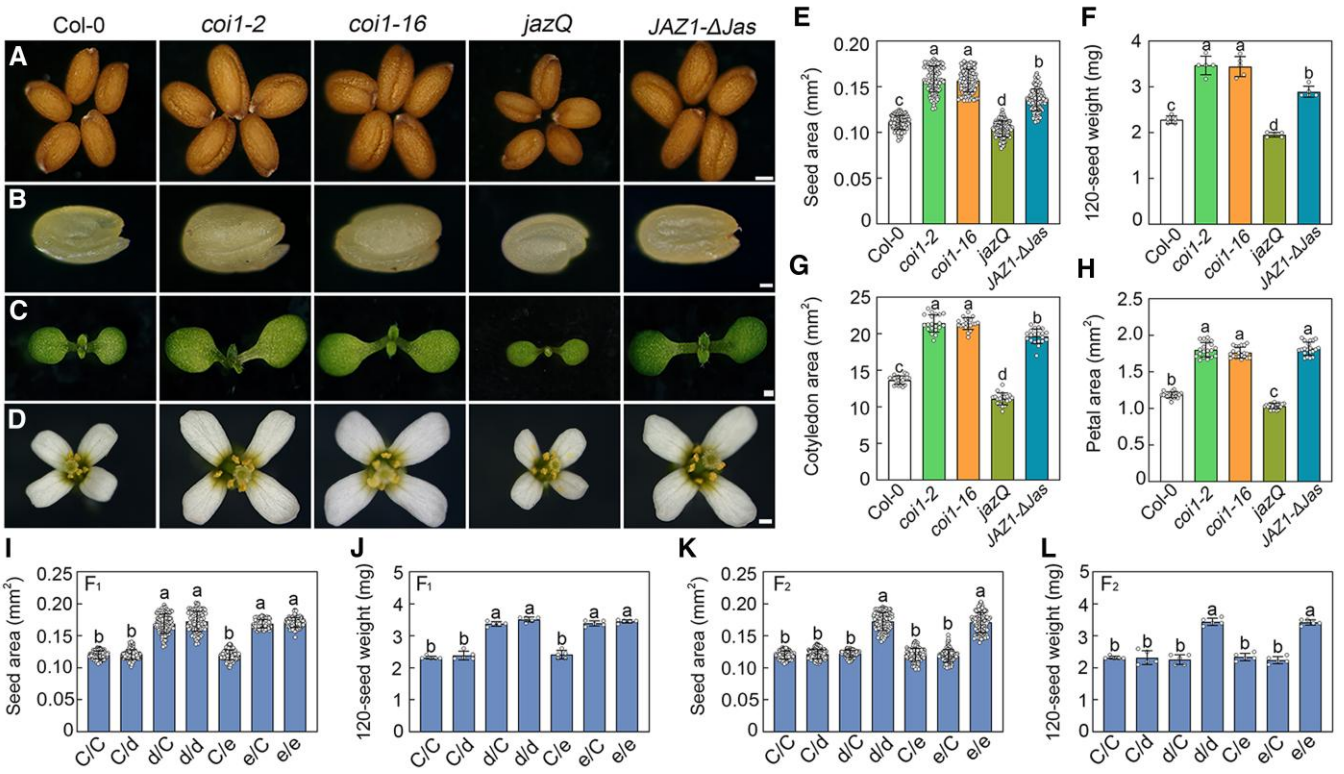

Figure 1. The COI1/JAZ-mediated jasmonate signaling inhibits seed size through maternal tissue. **A)** to **D)** Seeds **(A)**, mature embryos **(B)**, 10-d-old seedlings **(C)**, and flowers **(D)** of wild type (Col-0), *coi1-2*, *coi1-16*, *jazQ*, and *JAZ1-ΔJas* (from left to right). **E)** Seed area of Col-0, *coi1-2*, *coi1-16*, *jazQ*, and *JAZ1-ΔJas* ($n = 120$ seeds from 80 independent plants). **F)** Seed weight of Col-0, *coi1-2*, *coi1-16*, *jazQ*, and *JAZ1-ΔJas*. The weight of 120 dry seeds pooled from more than 80 independent plants was measured for each sample per replicate. Experiments were performed 5 times by analyzing different batches of seeds ($n = 5$). **G)** Cotyledon area of 10-d-old Col-0, *coi1-2*, *coi1-16*, *jazQ*, and *JAZ1-ΔJas* seedlings ($n = 20$ representative seedlings). **H)** Petal area of Col-0, *coi1-2*, *coi1-16*, *jazQ*, and *JAZ1-ΔJas*. Petals of 20 different representative flowers from different plants were used to measure petal area ($n = 20$ petals). **I)** Area of Col-0 × Col-0 (C/C) F_1, Col-0 × *coi1-2* (C/d) F_1, *coi1-2* × Col-0 (d/C) F_1, *coi1-2* *coi1-2* (d/d) F_1, Col-0 × *coi1-16* (C/e) F_1, *coi1-16* × Col-0 (e/C) F_1, and *coi1-16* × *coi1-16* (e/e) F_1 seeds. **J)** Weight of Col-0 × Col-0 (C/C) F_1, Col-0 × *coi1-2* (C/d) F_1, *coi1-2* × Col-0 (d/C) F_1, *coi1-2* × *coi1-2* (d/d) F_1, Col-0 × *coi1-16* (C/e) F_1, *coi1-16* × Col-0 (e/C) F_1, and *coi1-16* × *coi1-16* (e/e) F_1 seeds. **K)** Area of Col-0 × Col-0 (C/C) F_2, Col-0 × *coi1-2* (C/d) F_2, *coi1-2* × Col-0 (d/C) F_2, *coi1-2* × *coi1-2* (d/d) F_2, Col-0 × *coi1-16* (C/e) F_2, *coi1-16* × Col-0 (e/C) F_2, and *coi1-16* × *coi1-16* (e/e) F_2 seeds. **L)** Weight of Col-0 × Col-0 (C/C) F_2, Col-0 × *coi1-2* (C/d) F_2, *coi1-2* × Col-0 (d/C) F_2, *coi1-2* × *coi1-2* (d/d) F_2, Col-0 × *coi1-16* (C/e) F_2, *coi1-16* × Col-0 (e/C) F_2, and *coi1-16* × *coi1-16* (e/e) F_2 seeds. Values in **(E)** to **(L)** are means ± SD. Bars with different letters are significantly different from each other ($P < 0.05$). Data were analyzed by a one-way ANOVA using Tukey's HSD test ($P < 0.05$). The statistical analyses described apply to all statistical analyses presented in this figure. Scale bars = 0.2 mm in **(A)**, 0.1 mm in **(B)**, 1 mm in **(C)**, and 0.5 mm in **(D)**.

H; Supplementary Fig. S1, A and B). In contrast, a *JAZ1-ΔJas* heterozygous transgenic plant that overexpressed a 3Myc-JAZ1 fused protein with Jas domain deletion (Han et al. 2018) had larger seeds, embryos, cotyledons, leaves, and petals than the Col-0 plants (Fig. 1, A to H; Supplementary Fig. S1, A and B). These results are consistent with the view that the canonical jasmonate signaling pathway inhibits seed growth in Arabidopsis.

The size of seeds is markedly impacted by plant fertility. Mutant or transgenic plants with impaired jasmonate signaling, such as *coi1-2*, *coi1-16*, and *JAZ1-ΔJas*, exhibit increased seed size but also show compromised fertility (Fig. 1; Farmer and Dubugnon 2009; Yang et al. 2012; Lee et al. 2015; Hu et al. 2021). To eliminate the influence of plant fertility on seed size, as previously reported by Hu et al. (2021), we conducted hand pollination on the flowers of *coi1-2* and *coi1-16* mutants, utilizing their own viable pollen collected at a later stage of inflorescence development. This procedure successfully restored their fertility to levels comparable with those observed in Col-0 plants (Supplementary Fig. S2, A to C). Consistent with the findings of Hu et al. (2021), when the fertility of *coi1-2* and *coi1-16* mutants was restored to the levels of Col-0 plants, with similar numbers of siliques per plant and seeds per silique compared with Col-0, the seed weight of the fertile-rescued *coi1-2* (designated as *coi1-2R*) and fertile-rescued *coi1-16* (*coi1-16R*) remained significantly heavier than that of Col-0 (Supplementary Fig. S2, A to D). Our parallel experiments revealed that similar results were achieved when the *JAZ1-ΔJas* flowers were pollinated using Col-0 pollen (Supplementary Fig. S2, A to D). These findings provide further evidence that the attenuation of jasmonate signaling leads to the production of larger seeds in *coi1-2*, *coi1-16*, and *JAZ1-ΔJas* plants.

Hu et al. (2021) recently showed that COI1 suppresses cell proliferation in the integuments. Specifically, the integument has more cells in the *coi1-2* ovule than in the Col-0 ovule, suggesting that jasmonate signaling may affect maternal tissues to control seed size (Li et al. 2004). To test this possibility, we performed reciprocal crosses between Col-0 and *coi1-2* or *coi1-16* plants. The effects of the *coi1* mutation on seed growth were detectable only when the *coi1* mutants were used as the maternal parent (Fig. 1, I and J). The Col-0 plants pollinated with the *coi1* mutant pollen formed seeds that were similar in size to the seeds of the self-pollinated Col-0 plants (Fig. 1, I and J). However, the seeds of the *coi1* plants pollinated with the Col-0 pollen were comparable in size to the seeds of the self-pollinated *coi1* plants (Fig. 1, I and J). Hence, COI1 is likely required in the sporophytic tissue of the

maternal plant to determine seed size. We subsequently measured the size of the Col-0 × Col-0 F_2, Col-0 × *coi1-2* F_2, *coi1-2* × Col-0 F_2, *coi1-2* × *coi1-2* F_2, Col-0 × *coi1-16* F_2, *coi1-16* × Col-0 F_2, and *coi1-16* × *coi1-16* F_2 seeds. The *coi1-2* × *coi1-2* F_2 and *coi1-16* × *coi1-16* F_2 seeds were larger than the Col-0 seeds, whereas the Col-0 × *coi1-2* or *coi1-16* F_2 and *coi1-2* or *coi1-16* × Col-0 F_2 seeds were similar in size to the Col-0 seeds (Fig. 1, K and L). Thus, the embryo and endosperm *coi1* genotypes do not affect seed size, supporting the notion that COI1-mediated jasmonate signaling modulates maternal tissues to control seed size.

To further substantiate the involvement of jasmonate signaling in regulating seed growth, we investigated the expression patterns of *COI1* and *JAZ* during seed development. Analysis of RNA-seq data obtained from public databases suggested that genes related to jasmonate signaling, such as *COI1* and *JAZ*, are expressed during various stages of seed development (Liu et al. 2020; Zhang et al. 2020b; Supplementary Fig. S3). In line with these findings, our quantitative real-time PCR (RT-qPCR) analyses revealed that *COI1* and *JAZ* are differentially expressed across developmental stages, ranging from 1 to 11 d after pollination (DAP; Supplementary Fig. S4). To gain a more detailed understanding of the temporal and spatial expression patterns of *COI1* and *JAZ* during seed development, we cloned their putative promoter sequences and fused them with the sequence encoding green fluorescent protein (GFP). This resulted in the generation of *pCOI1:GFP* and *pJAZ:GFP* constructs, which were subsequently transformed into the Col-0 plants. During the analyzed stages of seed development (5 to 13 DAP), *COI1* was highly expressed, notably in the integuments (Fig. 2; Supplementary Figs. S5 to S7). Similarly, multiple *JAZ* genes, including *JAZ1*, *JAZ2*, *JAZ3*, *JAZ4*, *JAZ6*, *JAZ8*, *JAZ9*, and *JAZ10*, exhibited high expression levels in the integuments during certain stages of seed development (Fig. 2; Supplementary Figs. S5 to S7). Thus, the expression of *COI1* and *JAZ* in the integuments aligns with the role of COI1/JAZ-mediated jasmonate signaling in the maternal control of seed size.

KLU is required for the repressive effect of COI1 on seed growth

Previous studies showed that the cytochrome P450 KLU monooxygenase is a major stimulator of cell proliferation in maternal integuments (Anastasiou et al. 2007; Adamski et al. 2009; Zhang et al. 2015a). The *klu* mutant plants reportedly produce small seeds because of the decreased cell proliferation in the integuments, which is in contrast to the relatively large seeds of transgenic plants overexpressing *KLU* (Anastasiou et al. 2007; Adamski et al. 2009; Zhang et al. 2015a). Because COI1-mediated jasmonate signaling negatively regulates cell proliferation in integuments and controls seed size by affecting maternal tissues (Fig. 1; Hu et al. 2021), we speculated that it may modulate *KLU* expression. Thus, we performed RT-qPCR analyses to examine the *KLU* transcript levels in the *coi1-2*, *coi1-16*, *JAZ1-ΔJas*, and *jazQ* plants. The *KLU* expression level was clearly higher in the *coi1-2*, *coi1-16*, and *JAZ1-ΔJas* gynoecia than in the wild type (Fig. 3A). Conversely, the *KLU* expression level was lower in the *jazQ* gynoecia than in the Col-0 gynoecia (Fig. 3A). Accordingly, jasmonate signaling negatively regulates *KLU* expression, implying jasmonate signaling is involved in *KLU*-mediated seed growth.

To further elucidate the relationship between jasmonate signaling and *KLU* expression, we analyzed the genetic interaction between *COI1* and *KLU* to determine whether they function in a common pathway. The *coi1-2* and *coi1-16* plants were crossed with the *klu-11* mutant (Nobusawa et al. 2021) to generate the *coi1-2 klu-11* and *coi1-16 klu-11* double mutants, respectively. Phenotypic analyses showed that the *coi1-2 klu-11* and *coi1-16 klu-11* seeds were significantly smaller and lighter than the *coi1-2* and *coi1-16* seeds, similar to the Col-0 seeds (Fig. 3, B, F, and G). Moreover, the *coi1-2 klu-11* and *coi1-16 klu-11* plants had smaller embryos than the *coi1-2* and *coi1-16* plants (Fig. 3C). Our observations also revealed that the fertility levels of *coi1-2 klu-11* and *coi1-16 klu-11* were comparable with those of *coi1-2* and *coi1-16*, as evidenced by similar numbers of siliques per plant and seeds per silique (Supplementary Fig. S2, E to H), which rules out fertility as a contributing factor. Furthermore, the *coi1-2 klu-11* and *coi1-16 klu-11* cotyledons, leaves, and petals were much smaller than those of the *coi1-2* and *coi1-16* plants (Fig. 3, D, E, H, and I; Supplementary Fig. S1, C and D). Therefore, disrupting KLU can largely restore the seed size phenotype of the *coi1* mutants, suggesting that KLU is essential for the repressive effect of COI1-mediated signaling on seed growth.

JAZ proteins physically interact with SOD7 and DPA4, which suppress *KLU* expression

An earlier study showed that the B3 domain transcription factors SOD7 and DPA4 bind directly to the *KLU* promoter and repress *KLU* expression (Zhang et al. 2015a). Considering that COI1-mediated jasmonate signaling also represses *KLU* transcript levels, we wondered whether the effects of jasmonate signaling in this process are mediated through SOD7 and DPA4. Because JAZ repressors interact with several transcription factors during jasmonate responses (Kazan and Manners 2013; Schweizer et al. 2013; Guo et al. 2018b), we hypothesized that SOD7 and DPA4 may directly bind JAZ repressors. To test this hypothesis, we first performed yeast two-hybrid (Y2H) analyses. Y2H assays showed that the C-terminal region of SOD7 ($SOD7^{151-268}$) interacts with JAZ1, JAZ3, JAZ4, JAZ6, JAZ7, JAZ9, and JAZ11 (Fig. 4A). Similarly, the C-terminal region ($DPA4^{154-282}$) of DPA4 interacted with JAZ4, JAZ5, JAZ6, JAZ7, JAZ9, JAZ10, JAZ11, and JAZ12 in yeast cells (Fig. 4A). Further mapping revealed that the ZIM domain (amino acids 122 to 154) of JAZ1 was responsible for the association with SOD7 (Fig. 4B).

To verify the interactions between JAZ repressors and SOD7/DPA4 in plant cells, we conducted bimolecular fluorescence complementation (BiFC) assays in *Nicotiana benthamiana*. The full-length sequence encoding JAZ1 or JAZ9 was ligated to the sequence encoding the C-terminal fragment of the yellow fluorescent protein (cYFP) for the subsequent expression of the fusion proteins (JAZ1-cYFP or JAZ9-cYFP) under the control of the cauliflower mosaic virus (CaMV) 35S promoter (*Pro35S*). The sequences encoding SOD7 and DPA4 were fused to the sequence encoding the N-terminal fragment of YFP (nYFP) to produce SOD7-nYFP and DPA4-nYFP, respectively. When JAZ1-cYFP was co-expressed with SOD7-nYFP in *N. benthamiana*, strong YFP fluorescence was detected in the nucleus of the transformed cells stained with 4′,6-diamidino-2-phenylindole (DAPI) (Fig. 4C; Supplementary Fig. S8A). Similarly, the YFP signal was detectable in *N. benthamiana* leaf cells co-infiltrated with JAZ9-cYFP and SOD7-nYFP or DPA4-nYFP (Fig. 4C; Supplementary Fig. S8A). The YFP signal was also observed in *N. benthamiana* leaves when JAZ1-cYFP was co-expressed with the C-terminal region of SOD7 (amino acids 151 to 268) fused to nYFP ($SOD7^{151-268}$-nYFP; Fig. 4C; Supplementary Fig. S8A). However, fluorescence was undetectable in the negative controls in which JAZ8-cYFP (full-length JAZ8 fused to cYFP) was co-expressed with SOD7-nYFP and DPA4-nYFP or $SOD7^{1-150}$-nYFP (N-terminal amino acids 1 to 150 of SOD7 fused

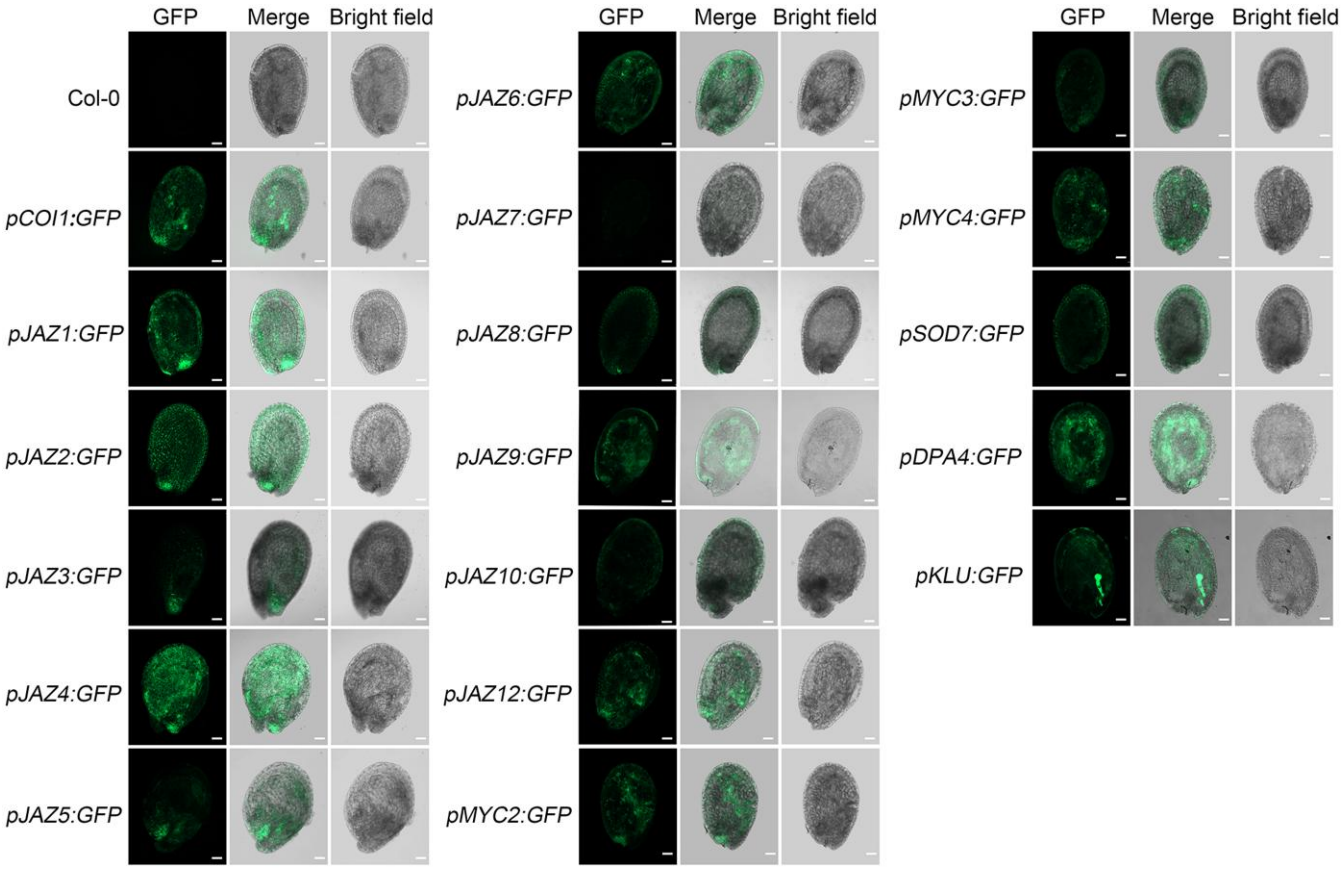

Figure 2. Expression analysis of *COI1*, *JAZ*, and *MYC* genes in developing seeds (5 DAP). The putative promoter sequences of *COI1*, *JAZ*, and *MYC*, as well as those of *SOD7* and *DPA4*, were cloned and then fused with the sequence encoding GFP. This resulted in the generation of *pCOI1:GFP*, *pJAZ:GFP*, *pMYC:GFP*, *pSOD7:GFP*, *pDPA4:GFP*, and *pKLU:GFP* constructs, which were subsequently transformed into the wild-type (Col-0) plants. To observe GFP fluorescence, the developing seeds of *pCOI1:GFP*, *pJAZ:GFP*, *pMYC:GFP*, *pSOD7:GFP*, *pDPA4:GFP*, and *pKLU:GFP* transgenic plants were examined 5 DAP. The Col-0 developing seeds were also detected and served as a negative control. Experiments were conducted 3 times, analyzing different batches of plants, and yielded similar results each time. Scale bars = 50 μm. DAP, days after pollination.

to nYFP) was co-expressed with JAZ1-cYFP (Fig. 4C). In addition to the BiFC assays, co-immunoprecipitation (CoIP) assays were conducted to produce further evidence of the physical interaction between JAZ1 and SOD7 in transgenic Arabidopsis plants simultaneously overexpressing JAZ1 and SOD7 proteins (Fig. 4D). These experimental findings demonstrate that SOD7 and DPA4 physically interact with several JAZ repressors.

Overexpression of *SOD7* largely restores the seed size phenotype of the *coi1* mutants and *JAZ1-ΔJas* transgenic plants, whereas JAZ1 has an inhibitory effect on the SOD7 function

The JAZ proteins negatively modulate jasmonate signaling by interacting with and suppressing the functions of multiple transcription factors. Additionally, they are stabilized and accumulate to high levels in the *coi1* mutants, wherein they inhibit various jasmonate responses (Chini et al. 2007; Thines et al. 2007; Katsir et al. 2008; Fonseca et al. 2009; Kazan and Manners 2013; Guo et al. 2018b; Howe et al. 2018). Because JAZ repressors interact with SOD7 and DPA4, we reasoned that the accumulation of JAZ proteins might impede the functions of these two transcription factors, thereby leading to increased *KLU* expression and large seeds. Hence, we assessed whether the overexpression of *SOD7* rescues the seed size phenotype of the *coi1-2* and *coi1-16* mutants. The *coi1-2* and *coi1-16* mutants were crossed with *SOD7*-overexpressing (*SOD7-OE-8* and *SOD7-OE-23*) transgenic plants to generate *coi1-2 SOD7-OE-8*, *coi1-16 SOD7-OE-8*, *coi1-2 SOD7-OE-23*, and *coi1-16 SOD7-OE-23* plants. As expected, the seeds of the *SOD7-OE-8* and *SOD7-OE-23* plants were smaller than those of the Col-0 controls (Fig. 5A; Supplementary Fig. S9; Zhang et al. 2015a). Further phenotypic analyses showed that the seeds of *coi1-2 SOD7-OE-8*, *coi1-16 SOD7-OE-8*, *coi1-2 SOD7-OE-23*, and *coi1-16 SOD7-OE-23* plants were smaller and lighter than the *coi1-2* and *coi1-16* seeds, similar to the Col-0 seeds (Fig. 5, A, E, and F; Supplementary Fig. S9). Moreover, the *coi1-2 SOD7-OE-8*, *coi1-16 SOD7-OE-8*, *coi1-2 SOD7-OE-23*, and *coi1-16 SOD7-OE-23* embryos were considerably smaller than the *coi1-2* and *coi1-16* embryos (Fig. 5B; Supplementary Fig. S9). We also observed that the fertility levels of the *coi1-2 SOD7-OE-8* and *coi1-16 SOD7-OE-8* plants were similar to those of *coi1-2* and *coi1-16* (Supplementary Fig. S2, I to L), thus eliminating the possibility of fertility being a contributing factor. In addition, the *coi1-2 SOD7-OE-8*, *coi1-16 SOD7-OE-8*, *coi1-2 SOD7-OE-23*, and *coi1-16 SOD7-OE-23* cotyledons, leaves, and petals were smaller than the corresponding tissues of the *coi1-2* and *coi1-16* plants (Fig. 5, C, D, G, and H; Supplementary Figs. S9 and S10, A to D). Thus, the overexpression of *SOD7* largely restored the seed phenotypes of the *coi1-2* and *coi1-16* mutants.

To further dissect the interaction between JAZ repressors and SOD7, we tested whether the seed size phenotype of the JAZ1-overaccumulating *JAZ1-ΔJas* plants is rescued by *SOD7* overexpression. The results demonstrate that overexpression of *SOD7* repressed the large-seed phenotype of the *JAZ1-ΔJas* heterozygous

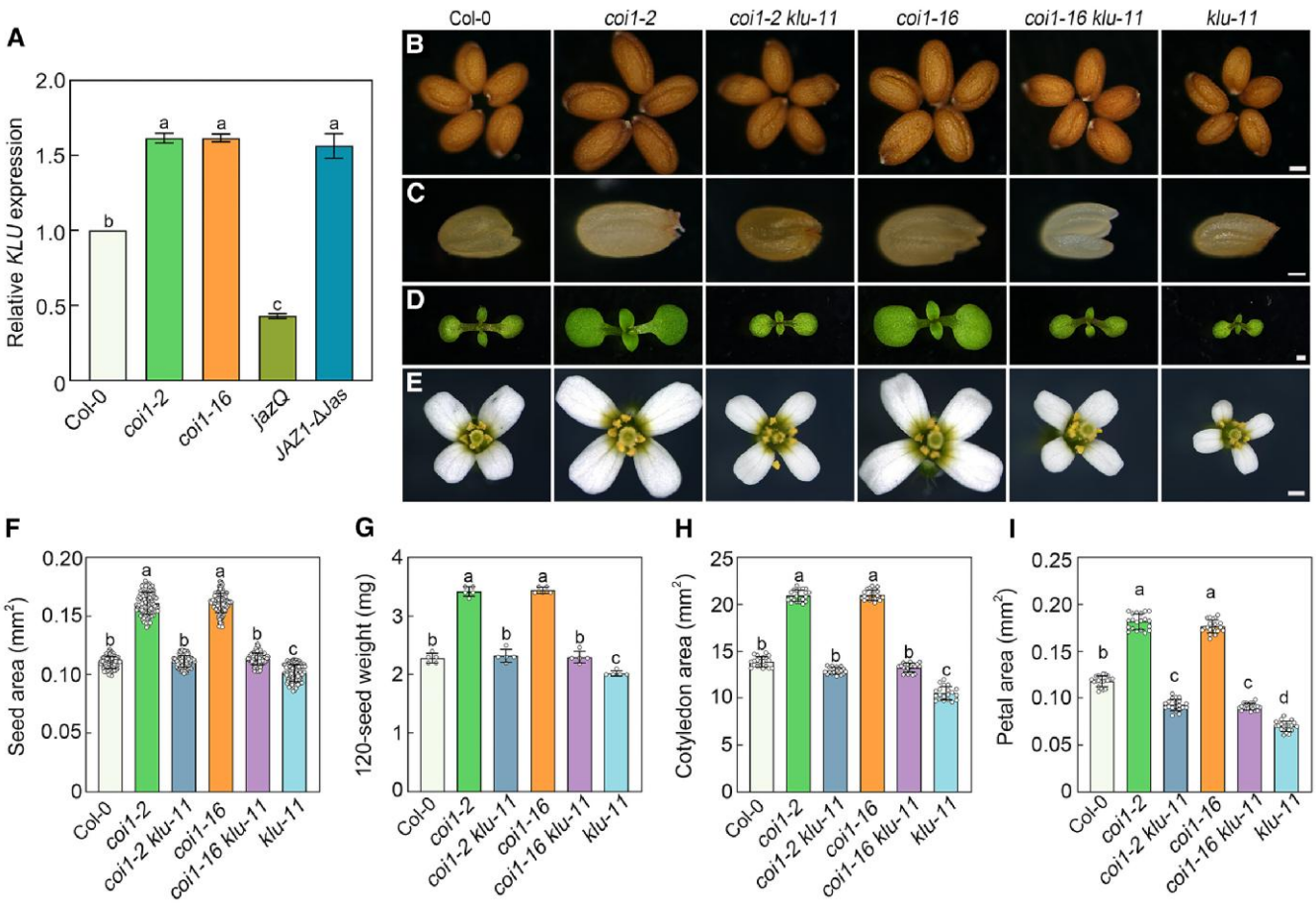

Figure 3. Knockout of *KLU* largely restores the seed size phenotype of *coi1-2* and *coi1-16*. **A)** RT-qPCR analyses of *KLU* expression levels in the wild type (Col-0), *coi1-2*, *coi1-16*, *jazQ*, and *JAZ1-ΔJas* gynoecia. Total RNA was extracted from pools of dissected gynoecia from 60 oldest unopened flower buds of different plants for each sample per replicate. The RT-qPCR analyses were completed using 3 biological replicates by analyzing different batches of gynoecia, each with 3 technical replicates. Data are means ± SD. **B)** to **E)** Seeds **(B)**, mature embryos **(C)**, 10-d-old seedlings **(D)**, and flowers **(E)** of Col-0, *coi1-2*, *coi1-2 klu-11*, *coi1-16*, *coi1-16 klu-11*, and *klu-11* (from left to right). **F)** Seed area of Col-0, *coi1-2*, *coi1-2 klu-11*, *coi1-16*, *coi1-16 klu-11*, and *klu-11* ($n = 120$ seeds from 80 independent plants). **G)** Seed weight of Col-0, *coi1-2*, *coi1-2 klu-11*, *coi1-16*, *coi1-16 klu-11*, and *klu-11*. The weight of 120 dry seeds pooled from more than 80 independent plants was measured for each sample per replicate. Experiments were performed 5 times by analyzing different batches of seeds ($n = 5$). **H)** Cotyledon area of the 10-d-old Col-0, *coi1-2*, *coi1-2 klu-11*, *coi1-16*, *coi1-16 klu-11*, and *klu-11* seedlings ($n = 20$ representative seedlings). **I)** Petal area of Col-0, *coi1-2*, *coi1-2 klu-11*, *coi1-16*, *coi1-16 klu-11*, and *klu-11*. Petals of 20 different representative flowers from different plants were used to measure petal area ($n = 20$ petals). Values in **(F)** to **(I)** are means ± SD. Bars with different letters are significantly different from each other ($P < 0.05$). Data were analyzed by a one-way ANOVA using Tukey's HSD test ($P < 0.05$). The statistical analyses described apply to all statistical analyses presented in this figure. Scale bars = 0.2 mm in **(B)**, 0.1 mm in **(C)**, 1 mm in **(D)**, and 0.5 mm in **(E)**.

plants (Fig. 6, A, E, and F). The *JAZ1-ΔJas SOD7-OE-8* and *JAZ1-ΔJas SOD7-OE-23* plants simultaneously overexpressing *JAZ1* and *SOD7* produced smaller seeds, embryos, cotyledons, leaves, and petals than the *JAZ1-ΔJas* plants (Fig. 6, B, C, D, G, and H, Supplementary Fig. S10, E and F). These observations imply that SOD7 functions downstream of the COI1/JAZ-mediated jasmonate pathway during the modulation of seed size.

A previous study showed that expression of *KLU* from the promoter of *INNER NO OUTER* (*pINO*), a key regulator of ovule integument formation, resulted in the production of enlarged seeds in the Col-0 background (Villanueva et al. 1999; Adamski et al. 2009). Interestingly, we discovered that the expression of *KLU* from the *INO* promoter also led to the production of enlarged seeds in the *jazQ* background (specifically in lines *pINO:KLU jazQ-17* and *pINO:KLU jazQ-21*), similar to the effect observed when *KLU* expression was driven by *Pro35S* (in line *KLU-OE jazQ-1*; Fig. 6, I and J). These findings suggest that the elevated accumulation of KLU effectively restored the reduced seed size phenotype of *jazQ*, thus providing further evidence for the idea that SOD7/KLU operates downstream of the COI1/JAZ-mediated pathway in regulating seed size.

Having ascertained that SOD7 physically associates with JAZ proteins and contributes to jasmonate signaling-controlled seed size, we analyzed the effects of JAZ proteins on SOD7 stability and function. Initial experiments showed that the accumulation of a SOD7-Flag fusion protein was not obviously affected in the *coi1* or *JAZ1-ΔJas* genetic backgrounds (Supplementary Fig. S11, A and B). Chromatin immunoprecipitation (ChIP) assays involving *JAZ1-ΔJas SOD7-OE-8* plants were next conducted to determine whether JAZ1 affects the binding of SOD7 to the promoter region of *KLU* (referred to as the *PF1* fragment by Zhang et al. 2015a; Supplementary Table S1). The ChIP assays revealed a clear decrease in the enrichment of SOD7 at the *KLU* promoter in the *JAZ1-ΔJas SOD7-OE-8* plants (relative to the enrichment in the *SOD7-OE-8* plants; Fig. 6K), suggesting JAZ1 interferes with the binding of SOD7 to the *KLU* promoter. To further investigate the effects of JAZ proteins on SOD7, we performed dual-luciferase (LUC) reporter assays using Col-0 Arabidopsis mesophyll

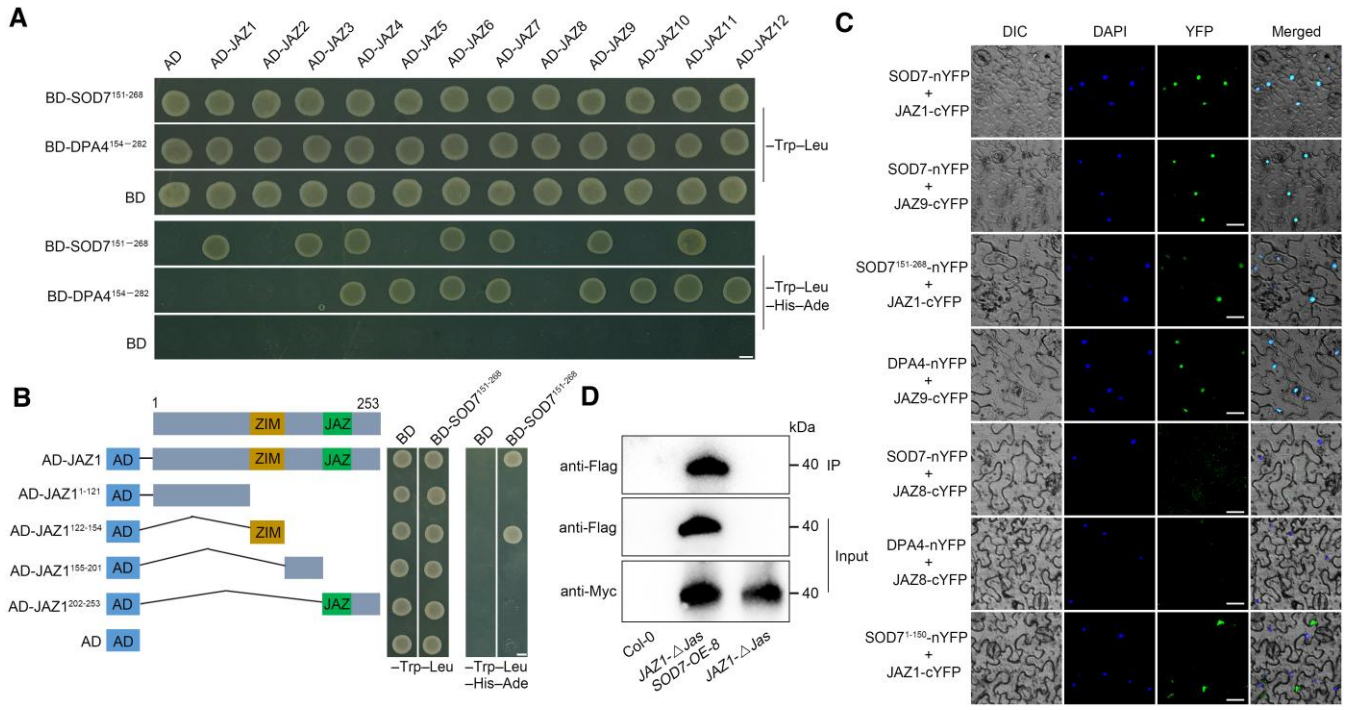

Figure 4. Physical associations of JAZ repressors with SOD7 and DPA4 transcription factors. **A)** Y2H assays. Protein interactions were indicated by the ability of yeast cells to grow on dropout medium lacking Leu, Trp, His, and Ade after a 4-d incubation. pGBKT7 (BD) and pGADT7 (AD) were used as negative controls. Bar = 2.5 mm. **B)** Y2H assay showing that the ZIM domain of JAZ1 is essential for the interaction with SOD7. Left: diagram of the full-length and truncated JAZ1 constructs with specific deletions. Right: interactions are indicated by the ability of yeast cells to grow on the dropout medium lacking Leu, Trp, His, and Ade after a 4-d incubation. BD and AD were used as negative controls. Bars = 2.5 mm. **C)** BiFC assays. Fluorescence was detected in the nuclear compartment of transformed *N. benthamiana* cells as a result of co-expressing of JAZ1-cYFP (or JAZ9-cYFP) with SOD7-nYFP, DPA4-nYFP, or SOD7$^{151\text{-}268}$-nYFP (a sequence encoding the C-terminal portion of SOD7 fused to nYFP) under the control of the CaMV 35S promoter (*Pro35S*). In negative controls, JAZ8-cYFP was co-expressed with SOD7-nYFP or DPA4-nYFP, or SOD7$^{1\text{-}150}$-nYFP (a sequence encoding the N-terminal portion of SOD7 fused to nYFP) was co-expressed with JAZ1-cYFP; no signal was detected. Nuclei are indicated by DAPI staining. Bars = 15 μm. **D)** Co-IP assays. Total proteins were extracted from 10-d-old transgenic Arabidopsis seedlings simultaneously overexpressing *JAZ1* and *SOD7* (*JAZ1-ΔJas SOD7-OE-8*) under the control of *Pro35S*. The *JAZ1-ΔJas SOD7-OE-8* plants were generated by introducing *SOD7* overexpression (containing a functional *2Flag-SOD7* construct driven by *Pro35S*) into *JAZ1-ΔJas* plants overexpressing a 3Myc-JAZ1 fused protein with Jas domain deletion. 3Myc-JAZ1 protein was immunoprecipitated using an anti-Myc antibody (1:250) and the CoIP 2Flag-SOD7 protein was detected using an anti-Flag antibody (1:10,000). Protein input for 3Myc-JAZ1 in the immunoprecipitated complexes was also analyzed and shown. Experiments were performed 3 times with similar results. DIC, differential interference contrast. DAPI, 4′,6-diamidino-2-phenylindole. YFP, yellow fluorescence protein. IP, immunoprecipitation.

protoplasts (Yoo et al. 2007). The effector constructs comprised *GFP*, *JAZ1*, *JAZ9*, or *SOD7* under the control of *Pro35S*, whereas the reporter construct consisted of the *KLU* promoter fused to *LUC* (Supplementary Fig. S12A). Compared with the effect of GFP alone, the presence of SOD7 obviously decreased the expression of *LUC* driven by the *KLU* promoter (Fig. 6L; Supplementary Fig. S12B). However, the *LUC* expression level was higher in the presence of both SOD7 and JAZ1 than in the presence of SOD7 alone (Fig. 6L; Supplementary Fig. S12B). Similar results were obtained when JAZ9 was co-expressed with SOD7 (Fig. 6L; Supplementary Fig. S12B). These observations imply that the inhibitory effect of SOD7 on *KLU* expression is attenuated by JAZ repressors.

SOD7 physically associates with MYC2 and MYC4

The bHLH transcription factors MYC2, MYC3, and MYC4 are the most extensively studied JAZ-binding factors that regulate diverse jasmonate responses (Dombrecht et al. 2007; Chen et al. 2012; Qi et al. 2015; Liu et al. 2019; You et al. 2019; He et al. 2023; Wang et al. 2024). Interestingly, recent studies have demonstrated that these MYC transcription factors also influence seed size (Liu et al. 2020; Hu et al. 2021; Guo et al. 2022). Considering that SOD7 and JAZ repressors combine to control seed size, we wondered whether SOD7 also interacts with MYC transcription factors. Thus, the sequences encoding the C-terminal regions of MYC2, MYC3, and MYC4 were ligated with the sequence encoding the Gal4 DNA-binding domain in the bait vector to produce BD-MYC2$^{189\text{-}624}$, BD-MYC3$^{375\text{-}593}$, and BD-MYC4$^{171\text{-}590}$, respectively, whereas the sequence encoding SOD7 was fused to the sequence encoding the Gal4 activation domain in the prey vector (AD-SOD7). The Y2H assay results indicated that SOD7 interacts with MYC2 and MYC4 in yeast cells (Fig. 7A; Supplementary Fig. S8B). However, no obvious interaction was detected between SOD7 and MYC3 in yeast (Supplementary Fig. S8B). We also characterized the MYC2 domain(s) responsible for the association with SOD7. The MYC2 protein was divided into the N-terminal fragment (including the TAD domain; amino acid residues 1 to 188), the mid-terminal fragment (amino acid residues 189 to 445), and the fragment with the bHLH domain (amino acid residues 446 to 624). Both the N-terminal and mid-terminal fragments of MYC2 interacted with SOD7 (Fig. 7A). To identify the SOD7 domain involved in the interaction, we divided SOD7 into the N-terminal fragment (containing the B3 domain; amino acid residues 1 to 150) and the C-terminal fragment (amino acid residues 151 to 268). The subsequent analysis demonstrated that the N-terminal fragment of SOD7 is required for the interaction with MYC2 (Fig. 7B).

To confirm SOD7 and MYC2 interact in plant cells, we performed in vivo BiFC assays in *N. benthamiana*. Sequences encoding the full-length or truncated SOD7 were fused to the sequence

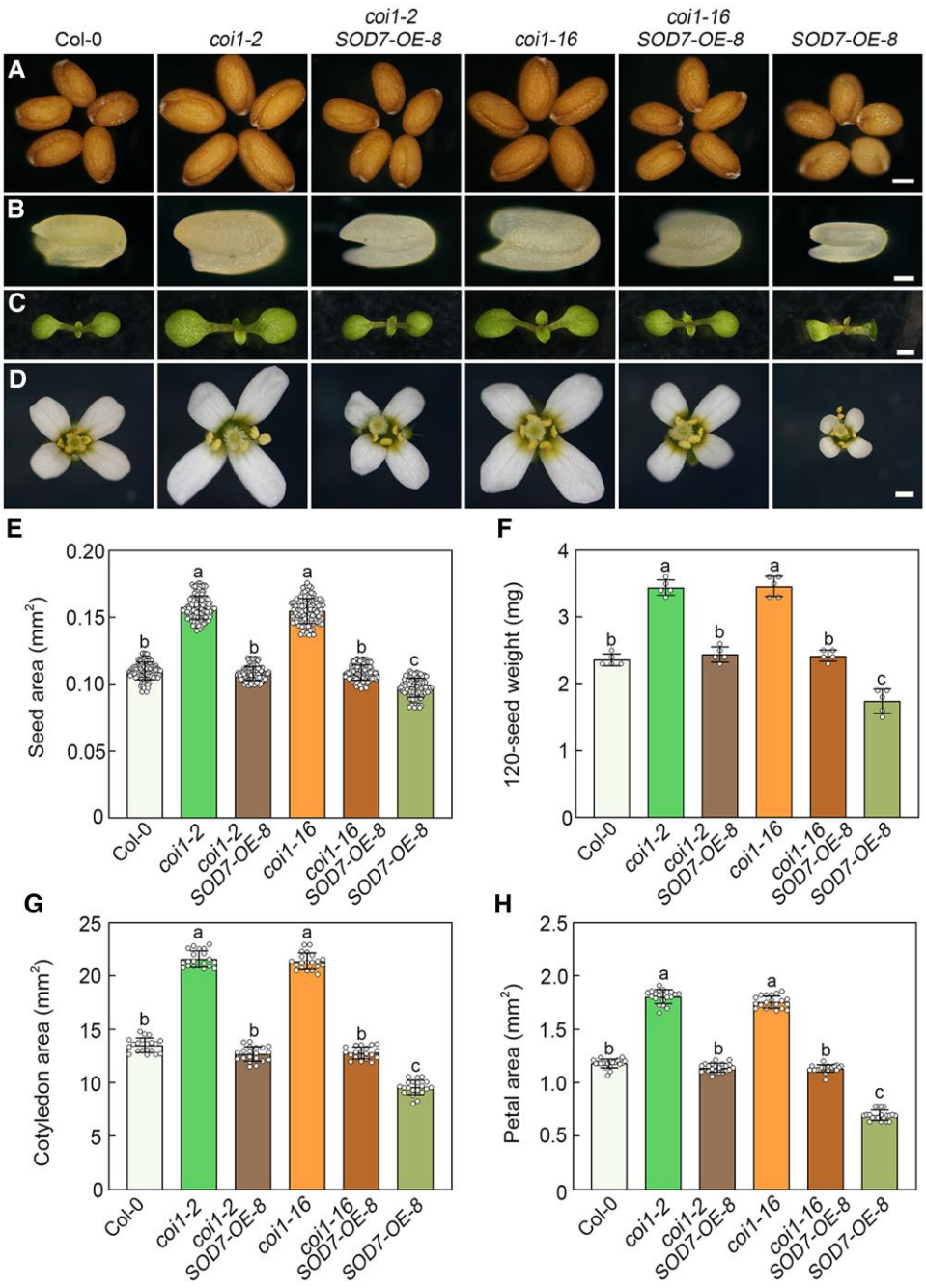

Figure 5. Overexpression of *SOD7* largely rescues the large-seed phenotype of *coi1-2* and *coi1-16*. **A)** to **D)** Seeds **(A)**, mature embryos **(B)**, 10-d-old seedlings **(C)**, and flowers **(D)** of wild type (Col-0), *coi1-2*, *coi1-2 SOD7-OE-8*, *coi1-16*, *coi1-16 SOD7-OE-8*, and *SOD7-OE-8* (from left to right). **E)** Seed area of Col-0, *coi1-2*, *coi1-2 SOD7-OE-8*, *coi1-16*, *coi1-16 SOD7-OE-8*, and *SOD7-OE-8* ($n = 120$ seeds from 80 independent plants). **F)** Seed weight of Col-0, *coi1-2*, *coi1-2 SOD7-OE-8*, *coi1-16*, *coi1-16 SOD7-OE-8*, and *SOD7-OE-8*. The weight of 120 dry seeds pooled from more than 80 independent plants was measured for each sample per replicate. Experiments were performed 5 times by analyzing different batches of seeds ($n = 5$). **G)** Cotyledon area of 10-d-old Col-0, *coi1-2*, *coi1-2 SOD7-OE-8*, *coi1-16*, *coi1-16 SOD7-OE-8*, and *SOD7-OE-8* seedlings ($n = 20$ representative seedlings). **H)** Petal area of Col-0, *coi1-2*, *coi1-2 SOD7-OE-8*, *coi1-16*, *coi1-16 SOD7-OE-8*, and *SOD7-OE-8*. Petals of 20 different representative flowers from different plants were used to measure petal area ($n = 20$ petals). Values in **(E)** to **(H)** are means ± SD. Bars with different letters are significantly different from each other ($P < 0.05$). Data were analyzed by a one-way ANOVA using Tukey's HSD test ($P < 0.05$). The statistical analyses described apply to all statistical analyses presented in this figure. Scale bars = 0.2 mm in **(A)**, 0.1 mm in **(B)**, 1 mm in **(C)**, and 0.5 mm in **(D)**.

encoding cYFP for the expression of SOD7-cYFP, SOD7$^{1\text{-}150}$-cYFP, and SOD7$^{151\text{-}268}$-cYFP under the control of *Pro35S*. Next, the sequence encoding the full-length MYC2 as well as the sequence encoding the C-terminal of MYC2 (amino acid residues 446 to 624) were ligated to the sequence encoding nYFP to generate MYC2-nYFP and MYC2$^{446\text{-}624}$-nYFP. Among the DAPI-stained samples, strong YFP fluorescence was detected in the nucleus of transformed *N. benthamiana* leaf cells when MYC2-nYFP was co-expressed with SOD7-cYFP or SOD7$^{1\text{-}150}$-cYFP (Fig. 7C; Supplementary Fig. S8C). Fluorescence was not observed in the negative controls in which MYC2-nYFP was co-expressed with SOD7$^{151\text{-}268}$-cYFP or MYC2$^{446\text{-}624}$-nYFP was co-expressed with SOD7-cYFP (Fig. 7C; Supplementary Fig. S8C). The interaction was further verified by conducting CoIP assays involving the

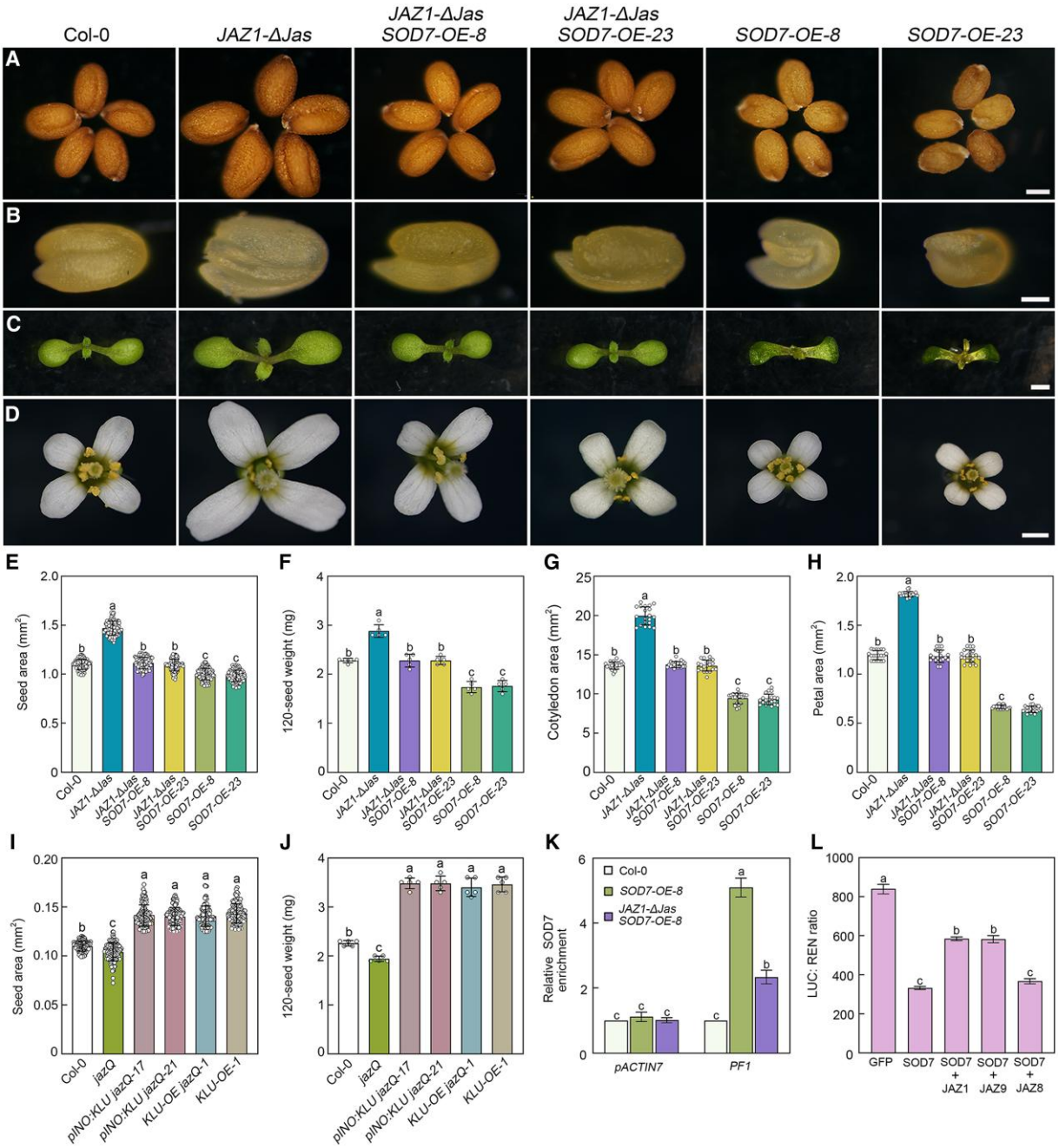

Figure 6. Overexpression of *SOD7* largely restores the phenotype of *JAZ1-ΔJas* in terms of seed size, whereas JAZ proteins interfere with the transcriptional function of SOD7. **A)** to **D)** Seeds **(A)**, mature embryos **(B)**, 10-d-old seedlings **(C)**, and flowers **(D)** of wild type (Col-0), *JAZ1-ΔJas*, *JAZ1-ΔJas SOD7-OE-8*, *JAZ1-ΔJas SOD7-OE-23*, *SOD7-OE-8*, and *SOD7-OE-23* (from left to right). **E)** Seed area of Col-0, *JAZ1-ΔJas*, *JAZ1-ΔJas SOD7-OE-8*, *JAZ1-ΔJas SOD7-OE-23*, *SOD7-OE-8*, and *SOD7-OE-23* ($n = 120$ seeds from 80 independent plants). **F)** Seed weight of Col-0, *JAZ1-ΔJas*, *JAZ1-ΔJas SOD7-OE-8*, *JAZ1-ΔJas SOD7-OE-23*, *SOD7-OE-8* and *SOD7-OE-23*. The weight of 120 dry seeds pooled from more than 80 independent plants was measured for each sample per replicate. Experiments were performed 5 times by analyzing different batches of seeds ($n = 5$). **G)** Cotyledon area of 10-d-old Col-0, *JAZ1-ΔJas*, *JAZ1-ΔJas SOD7-OE-8*, *JAZ1-ΔJas SOD7-OE-23*, *SOD7-OE-8* and *SOD7-OE-23* seedlings ($n = 20$ representative seedlings). **H)** Petal area of Col-0, *JAZ1-ΔJas*, *JAZ1-ΔJas SOD7-OE-8*, *JAZ1-ΔJas SOD7-OE-23*, *SOD7-OE-8* and *SOD7-OE-23*. Petals of 20 different representative flowers from different plants were used to measure petal area ($n = 20$ petals). **I)** Seed area of Col-0, *jazQ*, *pINO:KLU jazQ-17*, *pINO:KLU jazQ-21*, *KLU-OE jazQ-1*, and *KLU-OE-1* ($n = 120$ seeds from 80 independent plants). **J)** Seed weight of Col-0, *jazQ*, *pINO:KLU jazQ-17*, *pINO:KLU jazQ-21*, *KLU-OE jazQ-1*, and *KLU-OE-1*. The weight of 120 dry seeds pooled from more than 80 independent plants was measured for each sample per replicate. Experiments were performed 5 times by analyzing different batches of seeds ($n = 5$). Values in **(E)** to **(J)** are means ± SD. Scale bars = 0.2 mm in **(A)**, 0.1 mm in **(B)**, 1 mm in **(C)**, and 0.5 mm in **(D)**. **K)** ChIP-qPCR analyses of the enrichment of SOD7 at the promoter region (*PF1*) of *KLU* after the attenuation by JAZ1. Ten-day-old Col-0, *SOD7-OE-8*, and *JAZ1-ΔJas SOD7-OE-8* seedlings grown on half-strength MS medium were used for ChIP analyses. More than 50 seedlings for each sample were pooled for ChIP assays using an anti-Flag antibody. qPCR data from the ChIP assays with the *ACTIN7* untranslated region sequence (*pACTIN7*) as a negative control. Experiments were performed 3 times by using different batches of seedlings. Data are means ± SD. **L)** Transient dual-luciferase reporter assays demonstrated that JAZ repressors interfered with the transcriptional function of SOD7 in repressing *KLU* expression. Experiments were performed 3 times by using different batches of plants; each replication was from different Col-0 leaves of more than 60 plants. Data are the mean ± SD of 3 independent biological replicates. Bars with different letters are significantly different from each other ($P < 0.05$). Data shown in **(K)** was analyzed by a two-way ANOVA, and others were analyzed by a one-way ANOVA using Tukey's HSD test ($P < 0.05$). LUC, firefly luciferase; REN, renilla luciferase.

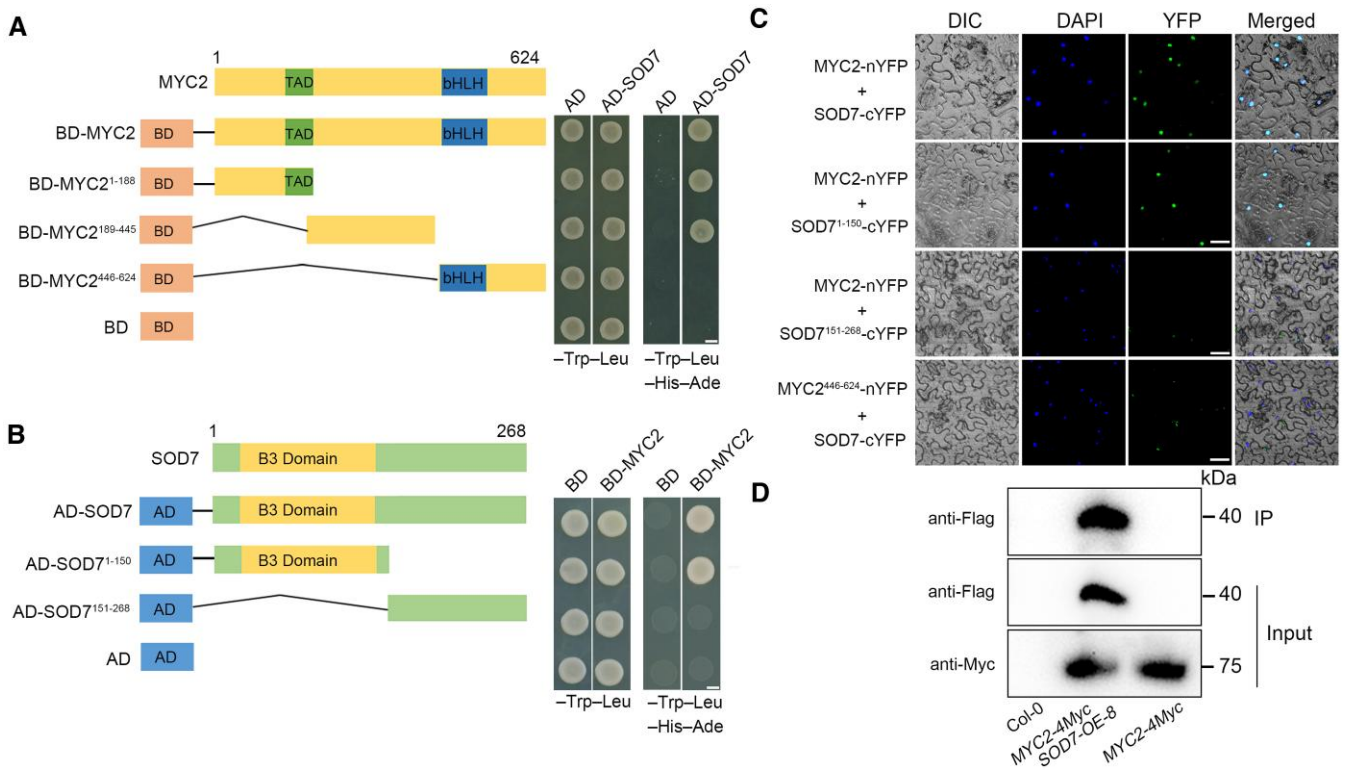

Figure 7. MYC2 physically associates with SOD7. **A)** Mapping the SOD7-interacting domain of MYC2 using an Y2H assay. Interaction is indicated by the ability of yeast cells to grow on dropout medium lacking Leu, Trp, His, and Ade and containing 20 mM 3-aminotriazole after a 4-d incubation. pGBKT7 (BD) and pGADT7 (AD) vectors were used as negative controls. Bar = 2.5 mm. **B)** Mapping the MYC2-interacting domain of SOD7 using an Y2H assay. Interaction is indicated by the ability of yeast cells to grow on dropout medium lacking Leu, Trp, His, and Ade after a 4-d incubation. BD and AD vectors were used as negative controls. Bar = 2.5 mm. **C)** BiFC analyses. The fluorescence detected in the nucleus of transformed *N. benthamiana* cells co-expressing MYC2-nYFP with SOD7-cYFP or SOD7$^{1\text{-}150}$-cYFP under the control of the CaMV 35S promoter (*Pro35S*). No signal was observed in the negative controls where MYC2-nYFP and SOD7$^{151\text{-}268}$-cYFP or MYC2$^{446\text{-}624}$-nYFP and SOD7-cYFP co-expressed. Nuclei are indicated by DAPI staining. Bars = 15 μm. **D)** CoIP assays. Total proteins were extracted from 10-d-old transgenic Arabidopsis seedlings simultaneously overexpressing *MYC2* and *SOD7* (*MYC2-4Myc SOD7-OE-8*) under the control of *Pro35S*. The *MYC2-4Myc SOD7-OE-8* plants were derived from a cross between the *SOD7-OE-8* plants (containing a functional *2Flag-SOD7* construct driven by *Pro35S*) and the transgenic plants overexpressing a functional *MYC2-4Myc* construct under the control of *Pro35S* (*MYC2-4Myc*). MYC2-4Myc was immunoprecipitated using an anti-Myc antibody (1:250) and the CoIP 2Flag-SOD7 protein was detected using an anti-Flag antibody (1:10,000). Protein input for MYC2-4Myc in the immunoprecipitated complexes was also detected and is shown. Experiments were performed 3 times with similar results. DIC, differential interference contrast; DAPI, 4′,6-diamidino-2-phenylindole; YFP, yellow fluorescence protein; IP, immunoprecipitation.

proteins extracted from Arabidopsis plants simultaneously overexpressing *MYC2* and *SOD7* (*MYC2-4Myc SOD7-OE-8*; Fig. 7D), which were derived from a cross between the *SOD7-OE-8* plants (containing a functional *2Flag-SOD7* construct driven by *Pro35S*) and the transgenic plants overexpressing a functional *MYC2-4Myc* construct under the control of *Pro35S* (*MYC2-4Myc*; Chen et al. 2011, 2012; Zhai et al. 2013; He et al. 2023). Collectively, these results demonstrate that SOD7 physically associates with the MYC2 and MYC4 transcription factors in the nuclei of plant cells.

SOD7 and MYC proteins synergistically control seed size

Recent studies revealed that MYC proteins repress integument cell proliferation during seed development (Liu et al. 2020; Hu et al. 2021). Given the physical interaction between SOD7 and MYC, which both negatively modulate seed size (Zhang et al. 2015a; Liu et al. 2020; Hu et al. 2021), we examined the functional relationship between SOD7 and MYC by testing whether the overexpression of *SOD7* rescues the seed size phenotype of the *myc2 myc3 myc4* (*myc234*) triple mutant. We crossed the *myc234* mutant with the *SOD7*-overexpressing *SOD7-OE-8* and *SOD7-OE-23* transgenic plants to generate *myc234 SOD7-OE-8* and *myc234 SOD7-OE-23* plants. In accordance with the results of previous studies (Liu et al. 2020; Hu et al. 2021), the *myc234* triple mutant produced larger seeds than the Col-0 control (Supplementary Fig. S13A). The seeds of the *myc234 SOD7-OE-8* and *myc234 SOD7-OE-23* plants were much smaller and lighter than the *myc234* seeds (Supplementary Fig. S13, A, E, and F; Supplementary Data Set 1). Moreover, the *myc234 SOD7-OE-8* and *myc234 SOD7-OE-23* plants had smaller embryos, cotyledons, leaves, and petals than the *myc234* mutant (Supplementary Figs. S13, B, C, D, G, and H and S14, A and B; Supplementary Data Set 1). Accordingly, the excessive accumulation of SOD7 largely suppressed the large-seed phenotype of *myc234* plants.

On the basis of the genetic association between *SOD7* and *MYC*, we speculated whether SOD7 functions synergistically with MYC to suppress seed growth. To test this possibility, we used the CRISPR-Cas9 gene-editing system to mutate *SOD7* in the Col-0 and *myc234* backgrounds, producing the loss-of-function *sod7*^{CR} single mutant and *myc234 sod7*^{CR}*-1* and *myc234 sod7*^{CR}*-21* quadruple mutants. The coding regions of *SOD7* in *sod7*^{CR} and *myc234 sod7*^{CR}*-21* exhibited a base deletion that leads to a frameshift mutation, while the *SOD7* coding region

in *myc234 sod7*^{CR}*-1* harbored a base insertion that also induces a frameshift mutation, ultimately resulting in premature termination of translation in both cases (Supplementary Fig. S15, A and B). The phenotypic analyses indicated that the *myc234 sod7*^{CR}*-1* and *myc234 sod7*^{CR}*-21* seeds were larger and heavier than the *myc234* and *sod7*^{CR} seeds (Fig. 8, A, E, and F; Supplementary Data Set 1). Moreover, both *myc234 sod7*^{CR}*-1* and *myc234 sod7*^{CR}*-21* had larger embryos than *myc234* and *sod7*^{CR} (Fig. 8B). The *myc234 sod7*^{CR}*-1* and *myc234 sod7*^{CR}*-21* cotyledons, leaves, and petals were also larger than those of the *myc234* and *sod7*^{CR} mutant (Fig. 8, C, D, G, and H; Supplementary Fig. S14, C and D; Supplementary Data Set 1). To further assess the synergistic interaction between SOD7 and MYC2 in seed size regulation, we examined the phenotype of *MYC2-4Myc SOD7-OE-8* and *MYC2-GFP SOD7-OE-8* plants simultaneously overexpressing *MYC2* and *SOD7*. As shown in Fig. 8, I and J, seeds of the *MYC2-4Myc SOD7-OE-8* and *MYC2-GFP SOD7-OE-8* plants were significantly smaller and lighter than *MYC2-4Myc*, *MYC2-GFP*, and *SOD7-OE-8* seeds. These observations are consistent with the idea that SOD7 works in concert with MYC proteins to negatively modulate seed size.

The negative effects of MYC transcription factors on seed size are associated with inhibited *KLU* expression

Having confirmed SOD7 and MYC transcription factors suppress seed growth, we hypothesized that these transcription factors may cooperatively inhibit *KLU* expression. To test this hypothesis, we first analyzed *KLU* expression in the *myc234*, *SOD7-OE-8*, *SOD7-OE-23*, *myc234 SOD7-OE-8*, and *myc234 SOD7-OE-23* plants. Compared with the corresponding expression in the Col-0 gynoecia, *KLU* was expressed at lower levels in *SOD7-OE-8* and *SOD7-OE-23* gynoecia, but at higher levels in *myc234* mutant gynoecia (Fig. 9A; Supplementary Data Set 1). The *KLU* expression level in *myc234 SOD7-OE-8* (or *myc234 SOD7-OE-23*) plants was between that in the *myc234* and *SOD7-OE-8* (or *SOD7-OE-23*) plants (Fig. 9A; Supplementary Data Set 1). Accordingly, the MYC transcription factors repressed the expression of *KLU* and the overaccumulation of SOD7 largely rescued the effect of *MYC* mutations on *KLU* expression. To further confirm the regulatory effects of SOD7 and MYC transcription factors on *KLU* expression, we examined *KLU* expression in the *myc234 sod7*^{CR}*-1* and *myc234 sod7*^{CR}*-21* plants. The *KLU* transcript levels were significantly higher in the *myc234 sod7*^{CR}*-1* and *myc234 sod7*^{CR}*-21* gynoecia than in the *myc234* gynoecia (Fig. 9B). These results suggest SOD7 and MYC transcription factors synergistically suppress *KLU* expression.

Because MYC transcription factors can modulate *KLU* expression, we further dissected the possible relationship between MYC and KLU. The *myc234* plants were crossed with *klu-11* to generate *klu-11 myc234* quadruple mutant plants. Phenotypic analyses showed that the *klu-11 myc234* seeds were significantly smaller and lighter than the *myc234* seeds (Fig. 9, C, G, and H). Similarly, the *klu-11 myc234* embryos were smaller than the *myc234* embryos (Fig. 9D). In addition, the *klu-11 myc234* plants had smaller cotyledons, leaves, and petals than the *myc234* plants (Fig. 9, E, F, I, and J; Supplementary Fig. S14, E and F). Therefore, the knockout of *KLU* largely repressed the seed size phenotypes of the *myc234* triple mutant, implying that the MYC transcription factors negatively modulate seed growth in part by inhibiting *KLU* expression.

SOD7 and MYC2 reciprocally enhance their suppressive effects on *KLU* expression

To further elucidate the biochemical mechanisms underlying the synergistic effects of SOD7 and MYC transcription factors on seed size, we analyzed whether SOD7 and MYC2 reciprocally affect their roles in modulating *KLU* expression. We initially conducted yeast one-hybrid (Y1H) analyses to assess whether MYC2 binds to the *KLU* promoter region to directly regulate expression. Previous studies revealed that MYC2 binds to the MYC-recognition sequence (CANNTG; also known as the E-box) in the promoters of downstream target genes (Dombrecht et al. 2007; Fernández-Calvo et al. 2011; Wang et al. 2017). Sequence analyses identified 4 putative E-box elements in the *KLU* promoter region (2,000 bp segment upstream of the translation start site), raising the possibility that MYC2 interacts with these motifs. The putative E-box elements in the *KLU* promoter were cloned into the pAbAi vector to generate pAbAi-pKLU-1, pAbAi-pKLU-2, pAbAi-pKLU-3, and pAbAi-pKLU-4 (Fig. 10A). The full-length *MYC2* coding sequence was introduced into the pGADT7 vector to produce the AD-MYC2 construct. The Y1H assay results reflected the association between MYC2 and the *KLU* promoter region (*pKLU-1*) in yeast cells (Fig. 10A). To verify this observation, we performed ChIP assays involving *MYC2*-overexpressing *MYC2-4Myc* plants (Chen et al. 2011, 2012). As shown in Fig. 10B, MYC2 was highly enriched at the *KLU* promoter fragment with an E-box element (*pKLU-a*; Supplementary Table S2). Collectively, these results suggest that MYC2 directly associates with the *KLU* promoter in vivo.

Next, we investigated whether the binding of MYC2 to the *KLU* promoter region is influenced by SOD7. Specifically, ChIP assays were conducted using *MYC2-4Myc SOD7-OE-8* transgenic plants that simultaneously overaccumulated MYC2 and SOD7. The enrichment of MYC2 at the *KLU* promoter region (*pKLU-a*; Supplementary Table S2) was greater in the *MYC2-4Myc SOD7-OE-8* plants than in the *MYC2-4Myc* plants (Fig. 10C). To determine whether this observation was due to altered *MYC2* expression in the transgenic lines, we compared the *MYC2* expression levels in the *MYC2-4Myc* and *MYC2-4Myc SOD7-OE-8* plants. A similar *MYC2* expression level was detected in both transgenic lines (Supplementary Fig. S16A). These observations imply that SOD7 enhances the binding of MYC2 to the *KLU* promoter region. Moreover, our parallel experiments showed that the enrichment of SOD7 at the *KLU* promoter region (referred to as the *PF1* fragment by Zhang et al. 2015a; Supplementary Table S1) was much higher in the *MYC2-4Myc SOD7-OE-8* plants than in the *SOD7-OE-8* plants (Fig. 10D). However, the *SOD7* transcript level was similar in the *MYC2-4Myc SOD7-OE-8* and *SOD7-OE-8* plants (Supplementary Fig. S16B). We also observed that the *SOD7* expression levels in the *myc234* and *MYC2*-overexpressing plants did not differ significantly from the *SOD7* expression level in the Col-0 plants (Supplementary Fig. S16C). In addition, the stability of SOD7 was unchanged in the *myc234* and *MYC2*-overexpressing plants (Supplementary Fig. S11C). These results suggest that SOD7 and MYC2 reciprocally enhance their enrichment at the *KLU* promoter region.

To further elucidate the relationship between SOD7 and MYC2, we performed dual-luciferase reporter assays using Col-0 mesophyll protoplasts (Yoo et al. 2007). Compared with the effect of GFP alone, the co-expression of MYC2 or SOD7 with GFP substantially decreased the expression of *LUC* driven by the *KLU* promoter (Fig. 10E; Supplementary Fig. S12, C and D; Supplementary Data Set 1). Additionally, *LUC* expression under the control of the *KLU* promoter was significantly lower when SOD7 and MYC2 were co-expressed than when SOD7 and GFP or MYC2 and GFP were co-expressed (Fig. 10E; Supplementary Fig. S12, C and D; Supplementary Data Set 1). Similar results were obtained when MYC4 was co-expressed with SOD7 (Fig. 10E; Supplementary Fig. S12E; Supplementary Data Set 1). These findings imply that

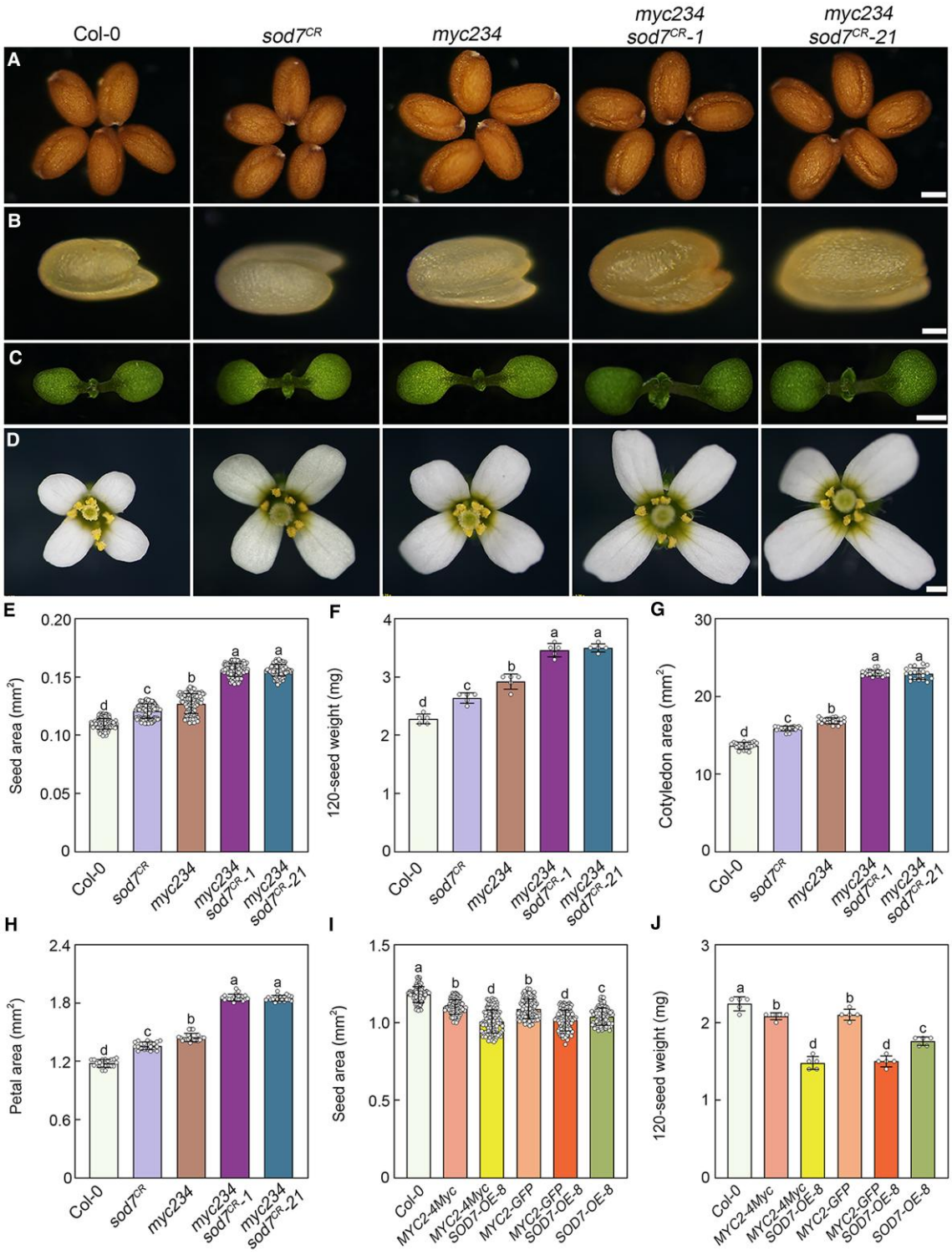

Figure 8. The synergistic function of SOD7 and MYC2 in seed size regulation. **A)** to **D)** Seeds **(A)**, mature embryos **(B)**, 10-d-old seedlings **(C)**, and flowers (**D**) of wild type (Col-0), *myc234*, *sod7*^{CR}, *myc234 sod7*^{CR}-1, and *myc234 sod7*^{CR}-*21* (from left to right). **E)** Seed area of Col-0, *myc234*, *sod7*^{CR}, *myc234 sod7*^{CR}-1, and *myc234 sod7*^{CR}-*21* ($n = 120$ seeds from 80 independent plants). **F)** Seed weight of Col-0, *myc234*, *sod7*^{CR}, *myc234 sod7*^{CR}-1, and *myc234 sod7*^{CR}-*21*. The weight of 120 dry seeds pooled from more than 80 independent plants was measured for each sample per replicate. Experiments were performed 5 times by analyzing different batches of seeds ($n = 5$). **G)** Cotyledon area of 10-d-old Col-0, *myc234*, *sod7*^{CR}, *myc234 sod7*^{CR}-1, and *myc234 sod7*^{CR}-*21* seedlings ($n = 20$ representative seedlings). **H)** Petal area of Col-0, *myc234*, *sod7*^{CR}, *myc234 sod7*^{CR}-1, and *myc234 sod7*^{CR}-*21*. Petals of 20 different representative flowers from different plants were used to measure petal area ($n = 20$ petals). **I)** Seed area of Col-0, *MYC2-4Myc*, *MYC2-4Myc SOD7-OE-8*, *MYC2-GFP*, and *MYC2-GFP SOD7-OE-8* ($n = 120$ seeds from 80 independent plants). **J)** Seed weight of Col-0, *MYC2-4Myc*, *MYC2-4Myc SOD7-OE-8*, *MYC2-GFP*, and *MYC2-GFP SOD7-OE-8*. The weight of 120 dry seeds pooled from more than 80 independent plants was measured for each sample per replicate. Experiments were performed 5 times by analyzing different batches of seeds ($n = 5$). Values in **(E)** to **(J)** are means ± SD. Bars with different letters are significantly different from each other ($P < 0.05$). Data were analyzed by a one-way ANOVA using Tukey's HSD test ($P < 0.05$). The statistical analyses described apply to all statistical analyses presented in this figure. Scale bars = 0.2 mm in **(A)**, 0.1 mm in **B)**, 1 mm in **(C)**, and 0.5 mm in **(D)**.

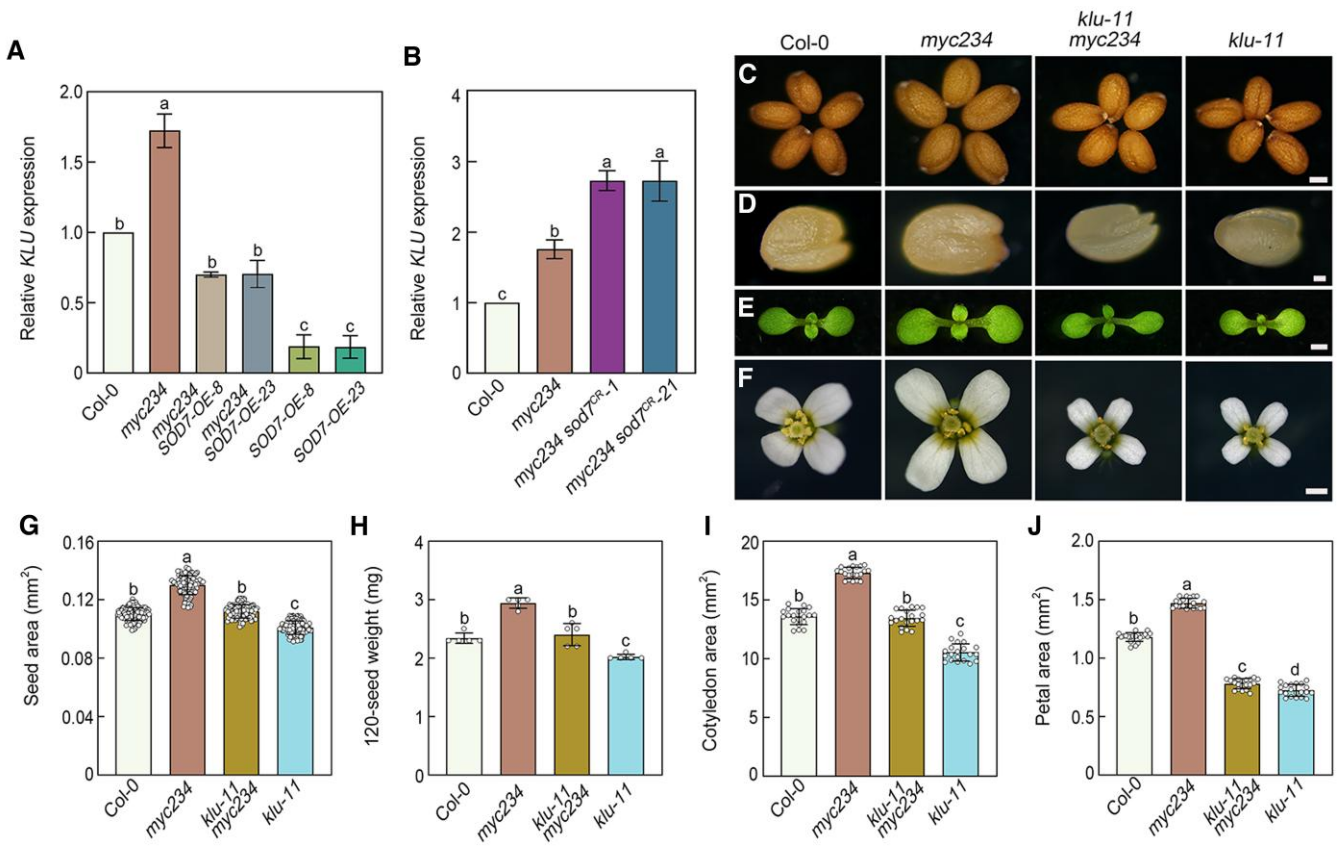

Figure 9. The negative effects of MYC transcription factors on seed size are associated with inhibited *KLU* expression. **A)** RT-qPCR analyses of *KLU* expression levels in the wild type (Col-0), *myc234*, *myc234 SOD7-OE-8*, *myc234 SOD7-OE-23*, *SOD7-OE-8*, and *SOD7-OE-23* gynoecia. **B)** RT-qPCR analyses of *KLU* expression levels in the Col-0, *myc234*, *myc234 sod7*^{CR}*-1*, and *myc234 sod7*^{CR}*-21* gynoecia. Total RNA was extracted from pools of dissected gynoecia from 60 oldest unopened flower buds of different plants for each sample per replicate. The RT-qPCR analyses were completed using 3 biological replicates by analyzing different batches of gynoecia, each with 3 technical replicates. **C)** to **F)** Seeds **(C)**, mature embryos **(D)**, 10-d-old seedlings **(E)**, and flowers **(F)** of Col-0, *myc234*, *klu-11 myc234*, and *klu-11* (from left to right). **G)** Seed area of Col-0, *myc234*, *klu-11 myc234*, and *klu-11* ($n = 120$ seeds from 80 independent plants). **H)** Seed weight of Col-0, *myc234*, *klu-11 myc234*, and *klu-11*. The weight of 120 dry seeds pooled from more than 80 independent plants was measured for each sample per replicate. Experiments were performed 5 times by analyzing different batches of seeds ($n = 5$). **I)** Cotyledon area of the 10-d-old Col-0, *myc234*, *klu-11 myc234*, and *klu-11* seedlings ($n = 20$ representative seedlings). **J)** Petal area of the Col-0, *myc234*, *klu-11 myc234*, and *klu-11*. Petals of 20 different representative flowers from different plants were used to measure petal area ($n = 20$ petals). Values in **(G)** to **(J)** are means ± SD. Bars with different letters are significantly different from each other ($P < 0.05$). Data were analyzed by a one-way ANOVA using Tukey's HSD test ($P < 0.05$). The statistical analyses described apply to all statistical analyses presented in this figure. Scale bars = 0.2 mm in **(C)**, 0.1 mm in **(D)**, 1 mm in **(E)**, and 0.5 mm in **(F)**.

SOD7 inhibits *KLU* transcription in conjunction with either MYC2 or MYC4. To further verify SOD7 and MYC2 synergistically repress *KLU* expression, we examined the *KLU* expression level in transgenic plants simultaneously expressing *SOD7* and *MYC2*, including the *MYC2-4Myc SOD7-OE-8* and *MYC2-GFP SOD7-OE-8* plants developed by crossing *SOD7-OE-8* plants with *MYC2*-overexpressing *MYC2-GFP* plants (Chen et al. 2012). The *KLU* transcript levels were much lower in the *MYC2-4Myc SOD7-OE-8* and *MYC2-GFP SOD7-OE-8* gynoecia than in the *MYC2-4Myc*, *MYC2-GFP*, and *SOD7-OE-8* gynoecia (Fig. 10F; Supplementary Data Set 1). These observations support the notion that SOD7 and MYC2 act synergistically to inhibit *KLU* expression.

Considering JAZ proteins physically interact with SOD7 and MYC2, we completed dual-luciferase reporter assays to analyze the effect of JAZ1 on these two transcription factors in Col-0 mesophyll protoplasts (Yoo et al. 2007). When JAZ1 was co-expressed with SOD7 and/or MYC2, the *KLU* promoter-driven *LUC* expression level increased (relative to the expression level in protoplasts with SOD7 and/or MYC2; Fig. 10G; Supplementary Fig. S12, F and G). Thus, JAZ1 appears to affect the ability of SOD7 and MYC2 to modulate *KLU* expression. To confirm the regulatory effect of JAZ1 on SOD7 and MYC2, we examined the effects of SOD7 and MYC2 on *KLU* transcription in *JAZ1-ΔJas* protoplasts. The expression of *LUC* driven by the *KLU* promoter was higher in the *SOD7*- and/or *MYC2*-expressing *JAZ1-ΔJas* protoplasts than in the Col-0 protoplasts (Fig. 10H; Supplementary Fig. S12, H and I), providing further evidence that JAZ1 inhibits the ability of SOD7 and MYC2 to modulate *KLU* transcription. To further uncover the regulatory relationship among JAZ1, SOD7, and MYC2, we conducted the BiFC assays to detect the interaction between SOD7 and MYC2 with or without JAZ1. When JAZ1 was co-expressed with MYC2-nYFP and SOD7-cYFP, the YFP fluorescence signal was dramatically reduced in leaves of *N. benthamiana* (Fig. 10I; Supplementary Fig. S17). As a negative control, when GUS (β-glucuronidase) was co-expressed with MYC2-nYFP and SOD7-cYFP, the YFP fluorescence intensity was not obviously changed (Fig. 10I; Supplementary Fig. S17). These observations suggest that JAZ1 interferes with the physical interaction between SOD7 and MYC2.

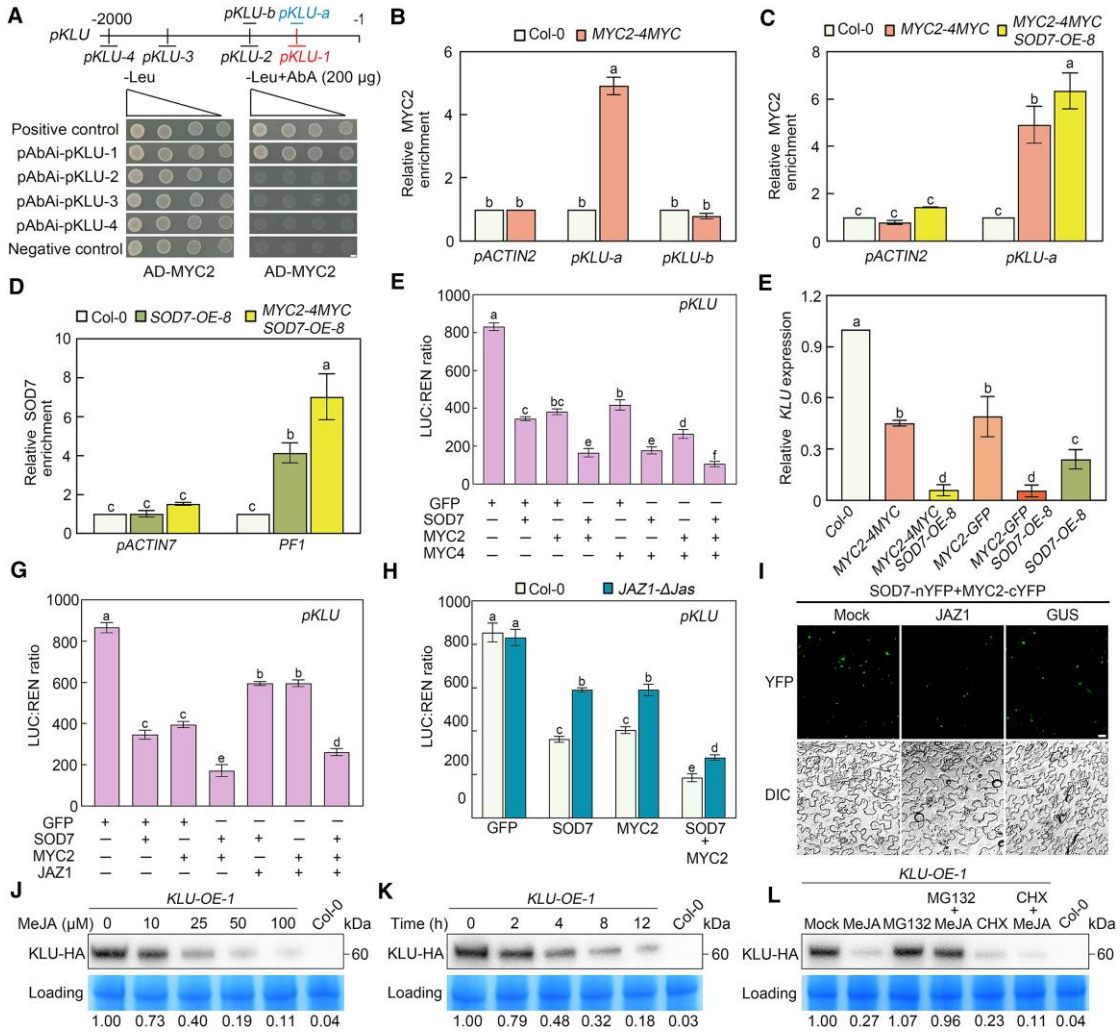

Figure 10. SOD7 and MYC2 reciprocally stimulate each other's transcriptional functions in suppressing *KLU* expression. **A)** Y1H analyses of the binding of MYC2 to the *KLU* promoter regions in yeast cells. The empty triangle represents the range of yeast concentrations from the dilutions 10^0 ($OD_{600} = 0.8$) to 10^{-3}. pGADT7-p53 + pAbAi-p53 was used as a positive control and pGADT7 + pAbAi-p53 was used as a negative control. The red font indicates the MYC2-binding site on the *KLU* promoter. The blue font marks the position of *pKLU-a*, as illustrated in **(B)**. Bar = 2.5 mm. **B)** ChIP analyses of the enrichment of MYC2 in the regions (*pKLU-a* and *pKLU-b* shown in **(A)** of *KLU* promoter. Ten-day-old wild-type (Col-0) and *MYC2-4Myc* seedlings grown on half-strength MS medium were used in ChIP assays. More than 50 seedlings for each sample were pooled for ChIP assays using an anti-Myc antibody. qPCR data from the ChIP assays with the *ACTIN2* untranslated region sequence (*pACTIN2*) were used as a negative control. Experiments were performed 3 times by using different batches of seedlings. **C)** ChIP-qPCR analyses of the enrichment of MYC2 in the *KLU* promoter (*pKLU-a*) after the enhancement by SOD7. Ten-day-old Col-0, *MYC2-4Myc*, and *MYC2-4Myc SOD7-OE-8* seedlings were used in ChIP assays. More than 50 seedlings for each sample were pooled for ChIP assays using an anti-Myc antibody. qPCR data from the ChIP assays with the *ACTIN2* untranslated region sequence (*pACTIN2*) were used as a negative control. Experiments were performed 3 times by using different batches of seedlings. **D)** ChIP-qPCR analyses of the enrichment of SOD7 to the *KLU* promoter (*PF1*) after the enhancement by MYC2. Ten-day-old Col-0, *SOD7-OE-8*, and *MYC2-4Myc SOD7-OE-8* seedlings were used in ChIP assays. More than 50 seedlings for each sample were pooled for ChIP assays using an anti-Flag antibody. qPCR data from the ChIP assays with the *ACTIN7* untranslated region sequence (*pACTIN7*) as a negative control. Experiments were performed 3 times by using different batches of seedlings. **E)** Transient dual-luciferase reporter assays indicating that MYC acts synergistically with SOD7 to repress the transcription of *KLU*. Experiments were performed 3 times by using different batches of plants; each replication was from different Col-0 leaves of more than 60 plants. **F)** RT-qPCR analyses of *KLU* in the Col-0, *MYC2-4Myc*, *MYC2-4Myc SOD7-OE-8*, *MYC2-GFP*, *MYC2-GFP SOD7-OE-8*, and *SOD7-OE-8* gynoecia. Total RNA was extracted from pools of dissected gynoecia from 60 oldest unopened flower buds of different plants for each sample per replicate. The RT-qPCR analyses were completed using 3 biological replicates by analyzing different batches of gynoecia, each with 3 technical replicates. **G)** and **H)** Transient dual-luciferase reporter assays indicating that transcriptional function of MYC2 in concert with SOD7 is repressed by JAZ1. Experiments were performed 3 times by using different batches of plants; each replication was from different Col-0 and *JAZ1-ΔJas* leaves of more than 60 plants. Data shown in **(E)** to **(G)** were analyzed by a one-way ANOVA, and others were analyzed by a two-way ANOVA using Tukey's HSD test ($P < 0.05$). Values presented in this figure are means ± SD. Bars with different letters are significantly different from each other ($P < 0.05$). **I)** BiFC analyses showing that JAZ1 diminishes the interaction between SOD7 and MYC2. As a negative control, GUS (β-Glucuronidase) was co-expressed with SOD7-nYFP and MYC2-cYFP. Fluorescence was detected 48 h after co-expression of MYC2-nYFP + SOD7-cYFP (Mock), JAZ1 + MYC2-nYFP + SOD7-cYFP (JAZ1), or GUS + MYC2-nYFP + SOD7-cYFP (GUS). Bars = 15 μm. **J)** to **L)** Analysis of jasmonate effect on KLU abundance. Whole proteins were extracted from 8-d-old *KLU-OE-1* transgenic seedlings grown under long-day conditions. Methyl jasmonate (MeJA) concentration gradient treatment **(J)**: seedlings were treated with 0, 10, 25, 50, or 100 μM MeJA and harvested at 8 h post-treatment. Time course with 25 μM MeJA treatment **(K)**: seedlings were treated with 25 μM MeJA and harvested at various time points from 0 to 12 h post-treatment. Proteasome inhibitor (MG132), and protein synthesis inhibitor (CHX) treatment **(L)**: seedlings were treated with 25 μM MeJA and/or 100 μM MG132 or 100 μM CHX for 8 h before sample harvest (including a mock treatment as control). The KLU-HA fusion protein was detected by immunoblotting using an anti-HA antibody (1:10,000). All experiments were repeated 3 times with similar results. Relative protein levels of KLU-HA were quantified by ImageJ. LUC, firefly luciferase; REN, renilla luciferase; DIC, differential interference contrast; YFP, yellow fluorescence protein; MeJA, methyl jasmonate; MG132, carbobenzoxy-Leu-Leu-leucinal; CHX, cycloheximide.

After ascertaining that *KLU* expression is synergistically repressed by both MYC2 and SOD7 and that JAZ1 inhibits their transcriptional activities and physical interaction, we sought to investigate whether jasmonate also affects KLU protein abundance. For this purpose, we generated transgenic plants (designated as *KLU-OE*) in the Col-0 background, which overexpress a fusion protein comprising full-length KLU and a 2HA tag, under the control of *Pro35S*. As shown in Fig. 10J, we observed a clear decrease in KLU-HA fusion protein levels in *KLU-OE-1* seedlings with increasing concentrations of MeJA. Furthermore, the accumulation of KLU-HA decreased as the duration of MeJA treatment was extended (Fig. 10K). Crucially, the abundance of KLU-HA was higher in seedlings treated with both MeJA and the proteasome inhibitor MG132 compared with those treated with MeJA alone (Fig. 10L), suggesting that jasmonate induces the degradation of KLU-HA via the 26S proteasome pathway. In addition, the simultaneous application of MeJA and the protein synthesis inhibitor cycloheximide (CHX) led to a further reduction in KLU-HA levels (Fig. 10L). As a control, the transcript abundance of the exogenously introduced *KLU-2HA* transgene in *KLU-OE-1* seedlings was not influenced by MeJA (Supplementary Fig. S18, A and B). Collectively, these results suggest that jasmonate negatively regulates the stability of KLU.

Jasmonate signaling influences seed size under salinity stress via SOD7 and KLU

Considering that jasmonate signaling and the SOD7–KLU pathway collaborate to regulate seed size, we sought to determine whether jasmonate modulates seed size under specific environmental conditions, such as salinity stress. To delve deeper into the regulatory effects of jasmonate on seed size, we treated 14-d-old soil grown under a long-day photoperiod with 75 mM NaCl (applied through irrigation) until seed maturity and subsequently analyzed the seed size phenotypes. As shown in Fig. 11, A to E, the seeds of Col-0 plants were markedly smaller and lighter under salinity stress compared with control conditions. Similarly, the seeds of *coi1-2*, *coi1-16*, *JAZ1-ΔJas*, and *myc234* plants also exhibited reduced weight and size upon salt treatment (Fig. 11, A to E). However, when compared with the Col-0 plants, the changes in seed area and weight upon salt treatment were much less pronounced in the *coi1-2*, *coi1-16*, *JAZ1-ΔJas*, and *myc234* plants (Fig. 11, C and E). These results suggest that the COI1-mediated jasmonate signaling pathway plays a crucial role in the inhibition of seed size under salinity stress conditions. Similarly, to gain further insights into the involvement of SOD7 and KLU in regulating seed size during salinity stress, we performed a comparable analysis of the seed phenotypes of several mutant or transgenic plants subjected to salt treatment, including *klu-11*, *sod7*^{CR}, *SOD7-OE-8*, and *SOD7-OE-23*. Upon exposure to salinity stress, we observed that the alterations in seed size and weight were less significant in these SOD7/KLU-associated mutants or transgenic plants compared with the Col-0 controls (Fig. 11, F to J). These findings demonstrate that SOD7 and KLU are also essential for the regulation of seed size in response to salt stress.

Given the established mechanism linking jasmonate signaling and the SOD7–KLU pathway in mediating seed size, we aimed to explore the potential genetic relationship between these two pathways by assessing seed size phenotypes of diverse genetic materials subjected to salinity stress conditions. As shown in Fig. 11, K to O, the changes in seed area and weight in response to salt treatment were comparable in *coi1-2 klu-11* and *coi1-2*, *SOD7-OE-8* to those observed in *coi1-2*, *klu-11*, and *SOD7-OE-8* alone. Furthermore, the changes in seed size in *myc234 klu-11* under salt treatment were significantly diminished compared with Col-0 plants, mirroring the phenotypes seen in both *myc234* and *klu-11* plants (Fig. 11, P to T). Notably, the alterations in seed size of *myc234 sod7*^{CR} seeds were much less than those of *myc234* and *sod7*^{CR} seeds (Fig. 11, P to T). Collectively, these observations underscore the synergistic interplay between the jasmonate signaling and the SOD7–KLU pathway in the regulation of seed size under salt stress conditions.

Discussion

The integration of jasmonate signaling and SOD7–KLU pathway in the control of seed size

The phytohormone jasmonate is a crucial signaling molecule that affects a variety of physiological processes in plants (Wasternack and Hause 2013; Zhang et al. 2017a; Howe et al. 2018; Cao et al. 2022; Li et al. 2024). Jasmonate also modulates seed development in Arabidopsis and several crops (Wasternack et al. 2013; Huo et al. 2017; Chen et al. 2020; Hu et al. 2021; Wang et al. 2023; Fig. 1). However, the molecular mechanisms underlying jasmonate signaling-regulated seed growth have not been thoroughly characterized. In line with the results of a recent study by Hu et al. (2021), we observed that alterations in the COI1 receptor or the accumulation of JAZ1, which inhibits jasmonate signaling, result in an increase in seed size (Fig. 1, A, B, E, and F). Consistent with this finding, jasmonate signaling represses the expression of *KLU*, which plays an essential role in modulating cell proliferation in the maternal sporophytic integuments and other tissues (Fig. 3A; Anastasiou et al. 2007; Adamski et al. 2009; Eriksson et al. 2010; Zhang et al. 2015a; Zhao et al. 2018; Poretska et al. 2020; Jiang et al. 2021; Nobusawa et al. 2021). Further genetic analyses suggested that KLU is necessary for the inhibitory effects of the COI1-mediated pathway on seed growth (Fig. 3, B to I). Moreover, the expression of *KLU*, controlled by the promoter of *INO* (a key regulator crucial for the formation of the ovule integument), rescues the reduced size phenotypes of *jazQ* seeds (Fig. 6, I and J), supporting the sufficiency of *KLU* expression in the jasmonate-mediated maternal seed size control pathway. Additionally, jasmonate has an adverse effect on the abundance of KLU (Fig. 10, J to L). Taken together, these findings demonstrate that jasmonate signaling negatively regulates both *KLU* expression and KLU stability, thereby suppressing seed development in Arabidopsis through its effects on maternal tissues. Nevertheless, since KLU encodes a putative cytochrome P450 monooxygenase with poorly defined substrates and products, it remains unclear whether jasmonate influences the enzymatic activity of KLU and how this modulation contributes to jasmonate-regulated seed size.

Jasmonate signal transduction involves substantial changes to cytogenetic programs associated with the complex interplay between positive and negative modulators. As critical repressors of the jasmonate pathway, JAZ proteins physically interact with multiple transcription factors and attenuate their functions to mediate jasmonate signaling. The bHLH transcription factors MYC2, bHLH17, and ROOT HAIR DEFECTIVE6 (RHD6) as well as essential components of the WD-repeat/bHLH/MYB transcriptional complexes, TARGET OF EAT1 (TOE1), YABBY1 (YAB1), CONSTANS (CO), and some other regulators are reportedly targeted by JAZ proteins during the modulation of various jasmonate-mediated processes (Boter et al. 2004; Lorenzo et al. 2004; Dombrecht et al. 2007; Cheng et al. 2009; Fernández-Calvo et al. 2011; Niu et al.

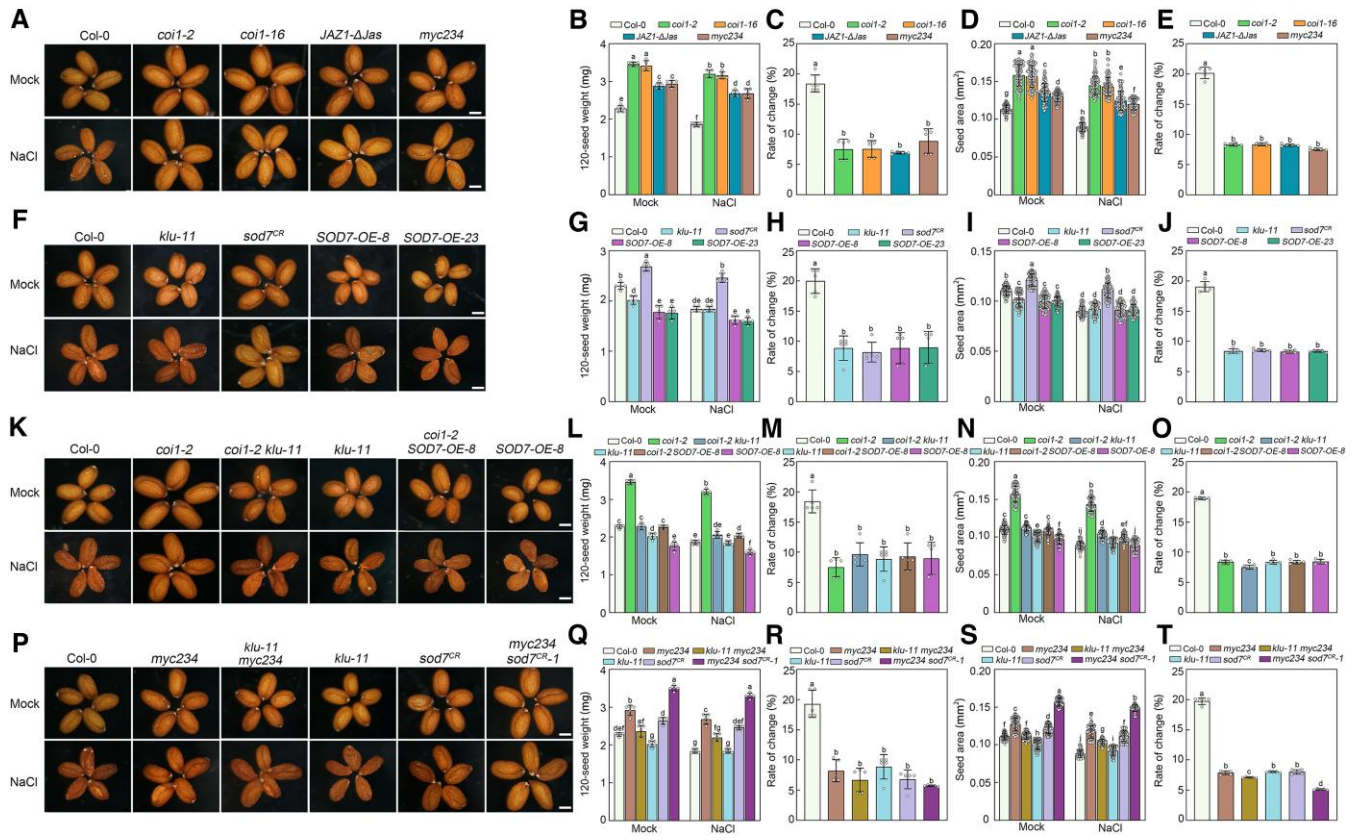

Figure 11. Jasmonate signaling modulates seed size under salinity stress via SOD7 and KLU. **A)**, **F)**, **K)**, and **P)** Seed phenotypes of wild type (Col-0), *coi1-2*, *coi1-16*, *JAZ1-ΔJas*, *myc234*, *klu-11*, *sod7*^{CR}, *SOD7-OE-8*, and *SOD7-OE-23* as well as various genetic materials in response to salinity stress. These plants were grown in soil under long-day conditions and subjected to treatment with 75 mM NaCl or a mock treatment (water) every 3 d, commencing from the 14th day of growth. The seed size of the plants was then compared between the stressed and mock-treated groups. The experiments were performed 5 times with similar results. **B)**, **G)**, **L)**, and **Q)** Seed weight of Col-0, *coi1-2*, *coi1-16*, *JAZ1-ΔJas*, *myc234*, *klu-11*, *sod7*^{CR}, *SOD7-OE-8*, and *SOD7-OE-23* as well as various genetic materials in response to salinity stress. The weight of 120 dry seeds pooled from more than 80 independent plants with or without 75 mM NaCl treatment. Experiments were performed 5 times by analyzing different batches of seeds. Data are means ± SD ($n = 5$). **C)**, **H)**, **M)**, and **R)** Percentage of seed weight changes in Col-0, *coi1-2*, *coi1-16*, *JAZ1-ΔJas*, *myc234*, *klu-11*, *sod7*^{CR}, *SOD7-OE-8*, and *SOD7-OE-23* as well as various genetic materials induced by salinity stress. The percentages mean the differences of seed weight with or without 75 mM NaCl treatment divided by seed weight without NaCl exposure. The data used to calculate percentage are from the corresponding panel **B)**, **G)**, **L)**, or **Q)**. Data are means ± SD ($n = 5$). **D)**, **I)**, **N)**, and **S)** Seed area of Col-0, *coi1-2*, *coi1-16*, *JAZ1-ΔJas*, *myc234*, *klu-11*, *sod7*^{CR}, *SOD7-OE-8*, and *SOD7-OE-23* as well as various genetic materials with or without 75 mM NaCl treatment ($n = 120$ seeds from 80 independent plants). Data are means ± SD. **E)**, **J)**, **O)**, and **T)** Percentage of seed area changes in Col-0, *coi1-2*, *coi1-16*, *JAZ1-ΔJas*, *myc234*, *klu-11*, *sod7*^{CR}, *SOD7-OE-8*, and *SOD7-OE-23* as well as various genetic materials induced by salinity stress. The percentages mean the differences of seed area with or without 75 mM NaCl treatment divided by seed area without NaCl exposure. The area of 120 dry seeds pooled from more than 80 independent plants was measured for each sample per replicate. Experiments were performed 5 times by analyzing different batches of seeds. Data are means ± SD ($n = 5$). Bars with different letters are significantly different from each other ($P < 0.05$). Data shown in **C**, **E**, **H**, **J**, **M**, **O**, **R**, and **T** were analyzed by a one-way ANOVA, and others were analyzed by a two-way ANOVA using Tukey's HSD test ($P < 0.05$). Scale bars = 0.2 mm in **(A)**, **(F)**, **(K)**, and **(P)**.

2011; Song et al. 2011, 2013, 2025; Kazan and Manners 2013; Schweizer et al. 2013; Jiang et al. 2014; Qi et al. 2014, 2015; Boter et al. 2015; Zhai et al. 2015; Han et al. 2020, 2023b; Serrano-Bueno et al. 2022; Sun et al. 2023; Lin et al. 2024; Zhang et al. 2024). Despite the identification of diverse transcription factors influencing jasmonate signaling, how the jasmonate signal is transduced to control specific context-dependent processes remains largely unclear. In the current study, SOD7 and DPA4 were found to interact with JAZ proteins (Fig. 4, A to D), implying SOD7 and DPA4 may function in the jasmonate signaling pathway. We also observed that the seed size phenotype of the *coi1* mutants and *JAZ1-ΔJas* transgenic plants was largely restored following the overexpression of *SOD7* (Figs. 5 and 6; Supplementary Fig. S9). Biochemical analyses showed that JAZ proteins restrict the ability of SOD7 to mediate *KLU* expression (Fig. 6, K and L). Hence, SOD7 and DPA4 are likely JAZ-binding transcription factors that contribute to jasmonate signaling-inhibited seed growth via direct protein–protein interactions.

Our further analyses revealed that the ZIM domain of JAZ1 is sufficient for its interaction with SOD7 (Fig. 4B). Likewise, JAZ proteins physically associate with ABSCISIC ACID INSENSITIVE3 (ABI3) and PHOSPHATE STARVATION RESPONSE1 (PHR1) through their ZIM domains (Pan et al. 2020; He et al. 2023). However, it is the Jas domain and/or the N-terminal cryptic MYC2-interacting domain (CMID) of JAZ proteins that mediate their interactions with MYC, INDUCER OF CBF EXPRESSION1 (ICE1), MYB75, and other identified transcription factors (Fernández-Calvo et al. 2011; Qi et al. 2011; Hu et al. 2013 , 2023; Moreno et al. 2013; Goossens et al. 2015; Chini et al. 2016). These findings underscore the diverse functional roles played by different domains of JAZ proteins in their interactions with downstream transcription factors. Ultimately, the modulation of JAZ proteins results in the

suppression of the transcriptional activities of these transcription factors (Figs. 6L and 10G; Chini et al. 2016). Furthermore, JAZ proteins can interfere with the enrichment of transcription factors, such as TOE1 and PHR1, on the promoter regions of target genes in vivo (Zhai et al. 2015; He et al. 2023). Consistent with this, our study also observed a reduction in SOD7 enrichment at the promoter region of *KLU* in the overaccumulation of JAZ1 (Fig. 6K). Additionally, JAZ proteins interfere with the interactions among various transcription factors, such as SOD7–MYC2, TT8–MYB75, and RHD6–RSL1 interactions (Fig. 10I; Qi et al. 2011; Han et al. 2020). Despite recent advancements, the biochemical mechanisms underlying JAZ-mediated inhibition of transcription factors remain incompletely understood. Previous research has shown that JAZ repressors, via their Jas and CMID domains, can bind to transcription factors like MYC3, causing pronounced conformational changes that alter the interactions with essential regulators like MED25 (Zhang et al. 2015b, 2017b; An et al. 2017). Thus, it is captivating to investigate whether JAZ repressors, through their ZIM domain, can similarly induce conformational changes in transcription factors like SOD7, ultimately leading to repression. JAZ proteins exert their inhibitory effects in conjunction with NOVEL INTERACTOR OF JAZ (NINJA) and TOPLESS (TPL) co-repressors (Pauwels et al. 2010; Shyu et al. 2012; Ke et al. 2015; Zhang et al. 2015b, 2017b; Howe et al. 2018; Zhou et al. 2023). Notably, the ZIM domain of JAZ proteins has been found to mediate both JAZ–JAZ and JAZ–NINJA interactions through separate surfaces (Zhou et al. 2023). Further exploration of the structural basis for ZIM domain–mediated interactions among JAZ, NINJA, TPL, and SOD7 may offer vital insights into the mechanism by which JAZ proteins regulate SOD7.

The precise transcriptional regulation of jasmonate signaling on seed size

Recent studies showed that MYC2, MYC3, and MYC4, which are 3 prominent transcription factors related to jasmonate signaling, suppress integument cell proliferation and negatively regulate seed size (Liu et al. 2020; Hu et al. 2021). Compared with the Col-0 control, the *MYC*-related mutant plants produce significantly larger seeds (Liu et al. 2020; Hu et al. 2021; Fig. 8, A to H). Interestingly, in the current study, SOD7 physically associated with MYC2 and MYC4 in plant cells (Fig. 7, A to D). Considering that both SOD7 and MYC transcription factors inhibit seed growth, we clarified their genetic and biochemical regulatory relationships. We determined that SOD7 works in concert with MYC proteins to control seed size. More specifically, the overexpression of *SOD7* largely rescued the seed size phenotype of the *myc234* mutant plants (Supplementary Fig. S13, A to H). Furthermore, the seeds of the *myc234 sod7*^{CR} quadruple mutant were significantly larger and heavier than those of the *myc234* mutant and *sod7*^{CR} mutant (Fig. 8, A, E, and F). In contrast, the seeds of *MYC2-4Myc SOD7-OE-8* and *MYC2-GFP SOD7-OE-8* plants simultaneously overexpressing *MYC2* and *SOD7* were much smaller and lighter than *MYC2-4Myc*, *MYC2-GFP*, and *SOD7-OE-8* seeds (Fig. 8, I and J). Consistent with these results, SOD7 and MYC2 reciprocally enhance their effects on *KLU* expression (Figs. 9, A and B and 10, A to F). According to the RT-qPCR data, *KLU* expression in the transgenic plants decreased more when both *SOD7* and *MYC2* were overexpressed than when only one of these genes was overexpressed (Fig. 10F). Therefore, we revealed a previously unknown signaling module in which SOD7 physically associates with MYC2 to synergistically repress *KLU* transcription, thereby negatively regulating seed size. However, the functions of these transcription factors are inhibited by JAZ proteins.

The mature seed of angiosperms is composed of 3 distinct components: the seed coat, embryo, and endosperm. Each tissue exhibits a certain degree of independence in its development, yet communication and coordination among these tissues are critical for proper seed development. Hu et al. (2021) demonstrated that COI1 inhibits cell proliferation in the integument. Their subsequent investigation into embryo development revealed that disrupting COI1 has no effect on embryogenesis. Our reciprocal cross experiments further suggest that the genotypes of *COI1* in the embryo and endosperm do not influence seed size (Fig. 1, I to L). Notably, using a GFP reporter driven by their native promoters, *COI1*, *JAZ1*, and *MYC* were found to be expressed in the integument during seed development, exhibiting expression patterns similar to those of *SOD7*, *DPA4*, and *KLU* (Fig. 2; Supplementary Figs. S5 to S7; Zhang et al. 2015a). These findings align with the concept that the COI1/JAZ-mediated jasmonate signaling regulates maternal tissues, thereby controlling seed growth. Nevertheless, gene expression analysis showed that *JAZ6* is expressed throughout the entire seed (Hu et al. 2021). Furthermore, the results obtained with the GFP reporter demonstrate that *COI1*, *JAZ*, and *MYC* are also expressed outside the integument during seed growth (Fig. 2; Supplementary Figs. S5 to S7). These observations suggest that jasmonate signaling is also generated and present in the embryo and endosperm, potentially challenging the notion of maternal control exerted by the jasmonate pathway during seed growth. Intriguingly, *SOD7*, *DPA4*, and *KLU* are also not specifically localized to the integument (Fig. 2; Supplementary Figs. S5 to S7; Zhang et al. 2015a). A plausible explanation is that other regulators present in the embryo and endosperm could effectively counteract the modulatory effects of jasmonate signaling and the SOD7/DPA4–KLU pathway. Alternatively, it is conceivable that the presence of jasmonate signaling and the SOD7/DPA4–KLU pathway in the embryo and endosperm may serve additional regulatory functions. Further research is necessary to elucidate the precise mechanisms by which seed size control is governed by jasmonate signaling and the SOD7/DPA4–KLU pathway in a maternal manner.

The seed size is markedly influenced by plant fertility, and a decline in plant fertility may lead to an enlargement of seed size. Mutants with reduced fertility in the jasmonate signaling pathway exhibit an increase in seed size (Fig. 1; Farmer and Dubugnon 2009; Yang et al. 2012; Lee et al. 2015; Hu et al. 2021). These observations hint at a role for jasmonate signaling in regulating the sink-source balance between plant reproduction and growth. However, despite rescuing the fertility of *coi1-2*, *coi1-16*, and *JAZ1-ΔJas* plants to the level of Col-0 plants, these mutant or transgenic plants still produce much larger seeds than those of Col-0 (Supplementary Fig. S2, A to D). Notably, we found that the fertility levels of *coi1-2 klu-11*, *coi1-16 klu-11*, *coi1-2 SOD7-OE-8*, and *coi1-16 SOD7-OE-8* plants were similar to those of *coi1-2* and *coi1-16* plants; yet, the seeds produced by the former were significantly smaller and lighter than those of the latter (Figs. 3 and 5; Supplementary Figs. S2, E to L and S9). These findings indicate that reduced fertility is not the primary factor determining the larger seed phenotype observed in *coi1-2*, *coi1-16*, and *JAZ1-ΔJas* plants, further supporting the notion that attenuated jasmonate signaling is responsible for the increased seed size. Besides inhibiting seed growth, jasmonate signaling also negatively impacts the size of various other organs, such as cotyledons, primary roots, leaves, and petals (Fig. 1; Supplementary Figs. S1 and S10; Staswick et al. 1992; Xie et al. 1998; Chen et al. 2011).

Conversely, jasmonate signaling can stimulate the development of certain tissues, including root hairs, trichomes, and filaments (McConn and Browse 1996; Sanders et al. 2000; Traw and Bergelson 2003; Li et al. 2004; Maes et al. 2008; Zhu et al. 2011; Han et al. 2020). The regulation of diverse organ and tissue development by jasmonate involves not only the core MYC factors but also potentially crucial tissue-specific transcriptional modulators, such as SOD7, MYB21, and RHD6 (Fig. 4; Chen et al. 2011; Qi et al. 2011; Song et al. 2011 , 2025; Han et al. 2020). Therefore, future research should delve deeper into investigating the exact mechanisms by which the canonical jasmonate signaling pathway regulates a wide array of tissues and cell types, especially under specific physiological and environmental conditions, encompassing intricate interactions among various transcription factors.

A complex jasmonate signaling network in the modulation of seed growth and germination

Although the overaccumulation of SOD7 largely suppressed the seed size phenotype of the *coi1-2*, *coi1-16*, *JAZ1-ΔJas*, and *myc234* plants, the *SOD7-OE* seeds differed in terms of size from the seeds of the *coi1-2 SOD7-OE*, *coi1-16 SOD7-OE*, *JAZ1-ΔJas SOD7-OE*, and *myc234 SOD7-OE* plants (Figs. 5 and 6; Supplementary Fig. S9). Similarly, there were differences in the sizes of the *klu-11* and *coi1-2 klu-11* (or *coi1-16 klu-11* and *klu-11 myc234*) seeds (Figs. 3 and 9). These observations imply that in addition to SOD7 and KLU, the jasmonate signaling pathway likely regulates seed growth through other components. Consistent with this possibility, MYC transcription factors can directly repress the expression of *GRF-INTERACTING FACTOR 1* (*GIF1*), which promotes seed growth by stimulating integument cell proliferation (Lee et al. 2014 ; Liu et al. 2020). Zheng et al. (2023) have revealed that SOD7 and DPA4 physically interact with and repress GIF1 in the control of seed size. These findings raise the possibility that jasmonate signaling also influences seed size via the regulations of MYC and SOD7/DPA4 on the GIF1-mediated pathway. Moreover, jasmonate signaling may synergize with the phytochrome B (phyB) pathway in suppressing seed growth, as evidenced by the partial rescue of the reduced seed size phenotype in *jazQ* mutants upon disruption of phyB (Supplementary Fig. S19; Campos et al. 2016). In addition, the CO transcription factor, which is a central regulator of the photoperiodic response pathway, positively modulates seed growth by promoting cell proliferation in the seed coat epidermis (Putterill et al. 1995; Simon et al. 1996; Suárez-López et al. 2001; Yu et al. 2023). Furthermore, CO was also identified as an interacting partner of JAZ repressors in the jasmonate signaling pathway (Serrano-Bueno et al. 2022; Han et al. 2023b). Consequently, jasmonate signaling appears to stimulate seed growth via CO. Nevertheless, the overall regulatory impacts of the jasmonate signaling network ultimately result in a reduction in seed size (Fig. 1; Hu et al. 2021). Further elucidating the potential relationships among these modulators may provide valuable insights into the molecular basis of the strict regulation and fine-tuning of the effects of jasmonate signaling on seed growth.

In addition to modulating seed growth, jasmonate also plays a critical role in the regulation of seed germination. For example, methyl jasmonate inhibits the seed germination of Arabidopsis and several crops (Wilen et al. 1991; Krock et al. 2002; Preston et al. 2002; Norastehnia et al. 2007; Barrero et al. 2009; Dave et al. 2011 , 2016; Pan et al. 2020 , 2023; Mei et al. 2023). Mechanistic investigations revealed jasmonate stimulates ABA signaling to delay seed germination (Ju et al. 2019; Pan et al. 2020; Mei et al. 2023). More specifically, JAZ proteins associated with jasmonate signaling physically interact with the ABI3 and ABI5 transcription factors (two key activators of ABA signaling) and disrupt the ABI3/ABI5-mediated transcriptional activation of downstream target genes (Ju et al. 2019; Pan et al. 2020; Mei et al. 2023; Varshney et al. 2023). Intriguingly, Chen et al. (2019) reported that the seeds of a quintuple mutant with mutations in *SOD7/DPA4* and related genes are hyposensitive to ABA during germination, suggestive of the stimulation of SOD7/DPA4 during ABA responses. Consistent with the findings of earlier research, we observed that the *SOD7-OE* seeds germinated more slowly and the resulting seedlings grew more slowly than the Col-0 seeds and seedlings after an ABA treatment or in response to salinity and osmotic stress (Supplementary Fig. S20). Considering jasmonate affects seed growth and germination and the interactive relationships among JAZ, SOD7, and ABI5 (Figs. 1 and 4; Supplementary Fig. S8D; Ju et al. 2019; Pan et al. 2020; Mei et al. 2023), we hypothesize that jasmonate signaling may regulate seed development and germination through intricate interactions involving JAZ, SOD7, ABI5, and potentially additional factors under specific natural environmental conditions. Consistent with this idea, we found that jasmonate signaling impacts seed size under salinity stress primarily via SOD7/KLU (Fig. 11). This strategy may allow plants to strike an appropriate balance between development and stress signaling pathways, optimizing growth and stress tolerance in response to prevailing conditions. Alternatively, the evolution of jasmonate-mediated seed size control could have been a mechanism to fine-tune nutrient distribution to seeds under stress conditions. While this hypothesis is certainly intriguing, future research is needed to provide additional experimental validation and clarification.

To better elucidate the molecular mechanism mediating the effects of jasmonate on seed size in Arabidopsis, we propose the following simplified model involving JAZ, SOD7/DPA4, MYC, and KLU (Fig. 12). In the absence of jasmonate perception, JAZ proteins accumulate and physically associate with SOD7/DPA4 and MYC, interfere with their transcriptional functions, and therefore upregulate the expression of *KLU* to promote integument cell proliferation and seed growth (Figs. 1, 3, 5, 8, and 9; Chini et al. 2007; Thines et al. 2007). In response to a jasmonate treatment or jasmonate biosynthesis induced during seed growth, the receptor COI1 perceives jasmonate and recruits JAZ repressors for the degradation via the SCF^{COI1}-26S proteasome pathway (Chini et al. 2007; Thines et al. 2007; Sheard et al. 2010; Yan et al. 2013; Li et al. 2021; Hu et al. 2023). The degradation of JAZ proteins facilitates the interaction between SOD7/DPA4 and MYC transcription factors, which subsequently negatively regulate the expression of *KLU* and inhibit seed growth by exerting effects on maternal tissues (Figs. 4, 7, 9, and 10). Our study has clarified the mechanism enabling JAZ repressors and MYC transcription factors in the jasmonate signaling to coordinate with the SOD7/DPA4–KLU pathway to integrate jasmonate signaling and the seed developmental process in Arabidopsis.

Materials and methods

Materials and plant growth conditions

Common chemicals were obtained from Shanghai Sangon (Shanghai, China), whereas Taq DNA polymerases were purchased from Takara Biotechnology (Dalian, China). The anti-Myc (catalog no. M4439) and anti-Flag (catalog no. H9658) antibodies used in this study were purchased from Sigma-Aldrich. The Col-0 and mutant *A. thaliana* plants had the Col-0 genetic

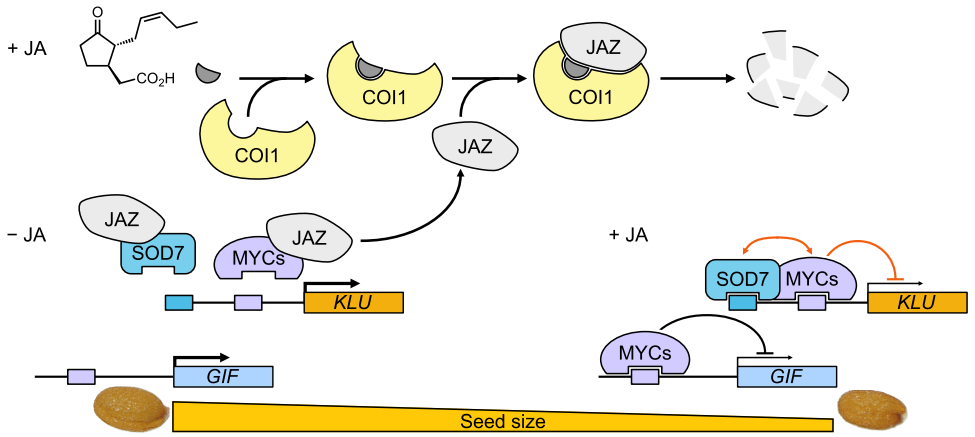

Figure 12. A working model for jasmonate signaling regulation of seed size involving JAZ, SOD7, MYC, and KLU. In response to a jasmonate treatment or jasmonate biosynthesis induced during seed growth, the receptor COI1 perceives jasmonate and recruits JAZ repressors for the degradation via the SCF^{COI1}-26S proteasome pathway. The degradation of JAZ proteins facilitates the interaction between SOD7 and MYC transcription factors, which subsequently negatively regulate the expression of *KLU* and inhibit seed growth by exerting effects on maternal tissues. Black lines indicate existing research. The regulatory relationships identified by our findings are shown by the orange lines. Pointed arrow, indicates promotion or activation. Flat arrow, indicates inhibition or repression.

background. The *coi1-2* (Xu et al. 2002), *coi1-16* (Pan et al. 2020), *JAZ1-ΔJas* (Han et al. 2018), *jazQ* (Campos et al. 2016), *myc234* (Fernández-Calvo et al. 2011), *MYC2-4Myc* (Chen et al. 2012), and *MYC2-GFP* (Chen et al. 2012) mutant or transgenic plants were described in earlier studies. The *klu-11* (SALK_024697C) mutant was obtained from The Arabidopsis Biological Resource Center at Ohio State University (http://abrc.osu.edu). To generate *SOD7-OE* and *KLU-OE* transgenic plants, the full-length sequences of *SOD7* (tagged with 2Flag) and *KLU* (tagged with 2HA) were inserted into the binary vector pOCA30 in the sense orientation for the subsequent expression under the control of *Pro35S* (Hu et al. 2013). The *JAZ1-ΔJas SOD7-OE-8*, which were generated by introducing *SOD7* overexpression (containing a functional *2Flag-SOD7* construct driven by *Pro35S*) into *JAZ1-ΔJas* plants (overexpressing a 3Myc-JAZ1 fused protein with Jas domain deletion; Han et al. 2018). In order to obtain the *pINO:KLU jazQ-17* and *pINO:KLU jazQ-21* transgenic plants, the putative promoter sequences (4,000 bp) of *INO* were first cloned and subsequently fused with the full-length sequences of *KLU*, which were then inserted into the PHB vector. This fusion construct, termed *pINO:KLU*, was then introduced into *jazQ* mutant plants through *Agrobacterium tumefaciens*–mediated transformation. The *MYC2-4Myc SOD7-OE-8* and *MYC2-GFP SOD7-OE-8* were generated by genetically crossing *MYC2-4Myc* or *MYC2-GFP* with *SOD7-OE-8*. Arabidopsis and *N. benthamiana* seeds were surface sterilized for 12 min in 20% (v/v) bleach and then sown on modified half-strength Murashige and Skoog (MS) medium and kept at 4 °C for a 3-d pregermination incubation. Arabidopsis and *N. benthamiana* plants were grown in an artificial growth chamber at 22 °C with a 16 h light (100 μE m^{-2} s^{-1} provided by white fluorescent bulbs, full wavelength)/8-h dark photoperiod.

Seed area and weight measurement

For each genotype, mature seeds were harvested from ~80 plants and pooled together. These seeds were then dried in a 37 °C incubator for 3 d before being used for area and weight measurements. To measure seed area, the seeds were imaged under the SZX16 microscope (Olympus, Tokyo, Japan). The area of each seed was subsequently analyzed using the ImageJ software, with a total of 120 seeds being analyzed per sample and per replicate. For seed weight measurement, a precise quantity of 120 dried mature seeds was randomly selected as a single sample and weighed using an analytical balance. This process was repeated independently by using different batches of seeds to ensure the reliability and reproducibility of the results.

Morphological analysis

The fully expanded cotyledons (10 d old) and petals were examined using a stereomicroscope and photographed, and then the areas of the cotyledons and petals were analyzed using the ImageJ software. Data were obtained for 20 cotyledons and 20 petals. The area of the fifth leaves was analyzed using the ImageJ software. Eight leaves from independent plants were used to measure the fifth leaf area.

Gene expression analysis in developing seeds by using the GFP reporter

The promoter regions of various genes, including *COI1* (3,000 bp), *JAZ1* (2,600 bp), *JAZ2* (2,600 bp), *JAZ3* (2,600 bp), *JAZ4* (2,600 bp), *JAZ5* (2,600 bp), *JAZ6* (2,600 bp), *JAZ7* (2,600 bp), *JAZ8* (2,800 bp), *JAZ9* (2,600 bp), *JAZ10* (2,600 bp), *JAZ12* (2,600 bp), *MYC2* (2,800 bp), *MYC3* (2,800 bp), *MYC4* (2,800 bp), *SOD7* (2,800 bp), *DPA4* (2,800 bp), and *KLU* (4,000 bp), were cloned into the PHG-GFP vector to generate the corresponding constructs: *pCOI1:GFP*, *pJAZ1:GFP*, *pJAZ2:GFP*, *pJAZ3:GFP*, *pJAZ4:GFP*, *pJAZ5:GFP*, *pJAZ6:GFP*, *pJAZ7:GFP*, *pJAZ8:GFP*, *pJAZ9:GFP*, *pJAZ10:GFP*, *pJAZ12:GFP*, *pMYC2:GFP*, *pMYC3:GFP*, *pMYC4:GFP*, *pSOD7:GFP*, *pDPA4:GFP*, and *pKLU:GFP*. These constructs were subsequently transferred into Col-0 plants through *A. tumefaciens*–mediated transformation. At various stages of seed development (5, 7, 9, and 13 DAP), developing seeds from the transgenic plants were isolated and screened using water. The GFP fluorescence in the developing seeds was then observed using confocal microscopy (LSM 900, Zeiss, Germany). The GFP signals were detected with an excitation wavelength of 488 nm (the intensity was 3% and the gain was 2) and an emission wavelength between 490 and 570 nm. This allowed for the visualization and analysis of the gene expression patterns of the respective genes during different stages of seed development.

Total RNA extraction and RT-qPCR

The TRIzol reagent (Invitrogen) was used to extract total RNA from pools of dissected gynoecia obtained from more than 60 of the oldest unopened flower buds (Adamski et al. 2009). Next, 1 μg DNase-treated RNA was reverse transcribed in a 20 μL reaction volume containing the oligo-$(dT)_{19}$ primer and Moloney murine leukemia virus reverse transcriptase (Fermentas, Hanover, MD, USA). The RT-qPCR analysis was performed using a 1.0 μL aliquot of the cDNA solution as well as the SYBR Premix Ex Taq kit (Takara Biotechnology) and LightCycler 480 real-time PCR system (Roche). The RT-qPCR analyses were completed using 3 biological replicates by analyzing different batches of gynoecia, each with 3 technical replicates. Target gene expression was analyzed relative to the expression of *ACTIN2* (AT3G18780) according to the $2^{-\Delta\Delta Ct}$ method. The gene-specific RT-qPCR primers are listed in Supplementary Table S3.

Y2H assays

To analyze the possible interactions of SOD7/DPA4 with JAZ proteins in yeast, the sequences encoding the C-terminal regions of SOD7 (amino acids 151 to 268) and DPA4 (amino acids 154 to 282) were ligated to the sequence encoding the Gal4 DNA-binding domain of the bait vector (BD-SOD7$^{151\text{-}268}$ and BD-DPA4$^{154\text{-}282}$), whereas the full-length JAZ-encoding sequences were inserted into pGADT7 to generate the prey constructs (AD-JAZ). To identify the region(s) responsible for the interaction between JAZ1 and SOD7, sequences encoding the truncated forms of JAZ1 were incorporated into pGADT7. To assess the potential interaction between SOD7 and MYC proteins, the sequences encoding the full-length or truncated SOD7 were cloned into pGADT7 to generate prey vectors (AD-SOD7, AD-SOD7$^{1\text{-}150}$, and AD-SOD7$^{151\text{-}268}$), whereas the sequences encoding the full-length or truncated forms of MYC2, MYC3, and MYC4 were inserted into pGBKT7 to produce bait vectors (BD-MYC2, BD-MYC2$^{1\text{-}188}$, BD-MYC2$^{189\text{-}445}$, BD-MYC2$^{446\text{-}624}$, BD-MYC3$^{375\text{-}593}$, and BD-MYC4$^{171\text{-}590}$).

To investigate the possible interaction between SOD7 and ABI5 or CO, the sequences encoding the full-length ABI5 or the C-terminal region of CO were cloned into pGBKT7 to produce bait vectors (BD-ABI5 and BD-CO$^{176\text{-}373}$). The Y2H assay was performed according to Clontech's Matchmaker Gold Yeast Two-Hybrid user manual as described by Du et al. (2023). Specifically, yeast strain AH109 cells were co-transformed with the bait and prey vectors. Protein interactions were indicated by the ability of the transformed cells to grow on a dropout medium lacking Leu, Trp, His, and Ade with or without 3-aminotriazole after a 4-d incubation. The primers used for cloning are listed in Supplementary Data Set 2.

BiFC assays

Pro35S was used to direct the insertion of the coding sequences for the YFP C-terminal (64 amino acids) region (cYFP) and the YFP N-terminal (173 amino acids) region (nYFP) into separate pFGC5941 plasmids to produce pFGC-cYFP and pFGC-nYFP, respectively (Kim et al. 2008). The sequences encoding the full-length or truncated SOD7, DPA4, JAZ1, JAZ8, or JAZ9 were inserted into pFGC-cYFP for the production of the following fusion proteins: SOD7-cYFP, SOD7$^{1\text{-}150}$-cYFP, SOD7$^{151\text{-}268}$-cYFP, JAZ1-cYFP, JAZ8-cYFP, and JAZ9-cYFP. Similarly, sequences encoding the full-length or truncated SOD7, MYC2, and DPA4 were inserted into pFGC-nYFP for the production of the following fusion proteins: SOD7-nYFP, SOD7$^{1\text{-}150}$-nYFP, SOD7$^{151\text{-}268}$-nYFP, DPA4-nYFP, MYC2-nYFP, and MYC2$^{151\text{-}268}$-nYFP.

The recombinant plasmids were inserted into *A. tumefaciens* (strain EHA105) cells, which were used for the infiltration of *N. benthamiana* leaves as previously described (Yang et al. 2021). The leaves were analyzed 48 h post infiltration, with YFP and DAPI fluorescence detected using the Fluoview FV1000 confocal laser scanning microscope (Olympus). For the DAPI staining, infected leaves were stained with a 10 mM DAPI solution for 5 min before the microscopic examination. The YFP signals were detected with an excitation wavelength of 488 nm (the intensity was 24% and the gains were 1) and an emission wavelength between 510 and 530 nm. The DAPI signals were detected with an excitation wavelength of 405 nm (the intensity was 15% and the gains were 1) and an emission wavelength between 420 and 440 nm. Experiments were performed more than 3 times using different batches of *N. benthamiana* plants. Each biological replicate contained more than 12 infiltrated plants, and more than 600 cells were examined. The primers used for cloning are listed in Supplementary Data Set 2.

CoIP assays

Proteins were extracted from 10-d-old transgenic Arabidopsis plants simultaneously overexpressing *JAZ1* and *SOD7* (*JAZ1-ΔJas SOD7-OE-8*) or *MYC2* and *SOD7* (*MYC2-4Myc SOD7-OE-8*) under the control of *Pro35S*. The proteins were extracted using an extraction buffer consisting of 50 mM Tris-HCl (pH 7.4), 1 mM EDTA, 150 mM NaCl, 10% (v/v) glycerol, 0.1% (v/v) Triton X-100, 1 mM PMSF, and 1× Roche protease inhibitor cocktail. Immunoprecipitation experiments were performed using Protein A/G Plus agarose beads (catalog no. D1217; Santa Cruz Biotechnology), according to the manufacturer's protocol as previously described (Huang et al. 2025). Briefly, Protein A/G Plus agarose beads were used to preclear cell lysates, after which the anti-MYC antibody (1:250) in extraction buffer was added and the beads were incubated overnight at 4 °C. The agarose beads were washed 3 times with extraction buffer, and then the CoIP proteins were detected by immunoblotting using the anti-Flag antibody (1:10,000). The primers used for cloning are listed in Supplementary Data Set 2.

Y1H assays

The Y1H assays were performed using the Matchmaker Yeast One-Hybrid System Kit (Clontech) according to the manufacturer's instructions. The putative *KLU* promoter fragments were cloned into the pAbAi vector to generate pAbAi-pKLU-1, pAbAi-pKLU-2, pAbAi-KLU-3, and pAbAi-KLU-4, which were linearized using *BstBI* and then inserted into Y1HGold yeast cells. Next, the full-length *MYC2* coding sequence was inserted into pGADT7. The resulting AD-MYC2 construct was incorporated into yeast cells carrying pAbAi-pKLU-1, pAbAi-pKLU-2, pAbAi-KLU-3, and pAbAi-KLU-4. The co-transformed cells at different concentrations were cultured for 3 d on synthetic defined/–Leu medium containing 200 μg/L aureobasidin A (AbA) in plates. Positive clones were detected on media inoculated with different yeast cell concentrations [i.e. dilutions ranging from 10^0 (OD_{600} = 0.8) to 10^{-3}]. The primers used for cloning are listed in Supplementary Data Set 2.

ChIP assays

The ChIP assays were conducted essentially as previously described (Mukhopadhyay et al. 2008; Hu et al. 2019). Specifically, 10-d-old Col-0, *SOD7-OE-8*, *MYC2-4Myc*, or *MYC2-4Myc SOD7-OE-8* seedlings were treated with 1% (w/v) formaldehyde (i.e. crosslinking step) and then their chromatin was isolated (Zhang et al.

2015b). The anti-Flag antibody (1:1,000), anti-Myc antibody (1:1,000), or IgG antibody (i.e. negative control; 1:1,000) were used to immunoprecipitate the protein–DNA (target promoter) complexes, after which the precipitated DNA was purified using a PCR purification kit (Qiagen) for the RT-qPCR analysis. To quantitatively analyze the SOD7–DNA (target promoter) or MYC2–DNA binding, RT-qPCR analyses were performed, with the 3′ untranslated regions of *ACTIN2* or *ACTIN7* serving as endogenous controls. The relative quantity was calculated in terms of the DNA binding ratio. The results presented herein were obtained from 3 independent experiments using different batches of plants. The primers used for the ChIP assays are listed in Supplementary Tables S1 and S2.

Transient transcriptional activation assays

The putative *KLU* promoter sequence (proKLU; 2,000 bp) was amplified from Col-0 genomic DNA and cloned into the pGreenII 0800-LUC vector to generate the reporter gene construct *proKLU:LUC* (Hellens et al. 2005). The full-length *SOD7*, *JAZ1*, *JAZ9*, *GFP*, *MYC2*, and *MYC4* coding sequences were amplified by PCR and cloned into the pGreenII 62-SK vector for the expression of the effectors under the control of *Pro35S* (Supplementary Fig. S3). Different combinations of recombinant plasmids were used for the transfection of leaf mesophyll protoplasts prepared from Col-0 or *JAZ1-ΔJas* plants as previously described (Sheen 2001). Transfected cells were cultured for 16 h under light, and then relative *LUC* activity was detected using the Dual-Luciferase Reporter Assay system (Promega), which measured the activities of firefly LUC and the internal control *Renilla reniformis* LUC. The primers used for generating constructs are listed in Supplementary Data Set 2.

Analysis of the effect of salinity stress on seed size

Seedlings of various Arabidopsis genotypes were cultivated in soil under long-day conditions for 14 d. To evaluate the impact of salinity stress on seed size, the plants were subsequently subjected to a treatment regimen where 75 mM NaCl was applied every 3 d, starting from the initiation of the experiment and continuing until mature seeds were harvested. A mock treatment group, where an equivalent amount of water was applied instead of NaCl, served as a control to isolate the specific effects of salinity stress. Upon reaching maturity, the seeds were collected and subjected to size measurement to analyze any differences in seed size induced by the salinity stress treatment.

Statistical analysis

Statistical analysis was performed by one-way or two-way ANOVA using Tukey's honest significant difference (HSD) as a post hoc test. Statistically significant differences were defined as those with $P < 0.05$. The lowercase letters above the column show significant differences ($P < 0.05$) among the different samples. The results are shown in Supplementary Data Set 3. The effects of the interaction between MYC2 and SOD7 on seed size, cotyledon size, petal size, transcriptional regulation, and *KLU* gene expression were examined. All analyses of multifactorial variance were performed using the generalized linear model procedure in SPSS (version for Windows). The model results showed significant interaction effects ($P < 0.05$) or highly significant interaction effects ($P < 0.01$) between MYC2 and SOD7 (Supplementary Data Set 1).

Accession numbers

Arabidopsis Genome Initiative numbers for the genes discussed in this article are as follows: *COI1*, AT2G39940; *JAZ1*, AT1G19180; *JAZ2*, AT1G74950; *JAZ3*, AT3G17860; *JAZ4*, AT1G48500; *JAZ5*, AT1G17380; *JAZ6*, AT1G72450; *JAZ7*, AT2G34600; *JAZ8*, AT1G30135; *JAZ9*, AT1G70700; *JAZ10*, AT5G13220; *JAZ11*, AT3G43440; *JAZ12*, AT5G20900; *MYC2*, AT1G32640; *MYC3*, AT5G46760; *MYC4*, AT4G17880; *SOD7*, AT3G11580; *DPA4*, AT5G06250; *KLU*, AT1G13710; *INO*, AT1G23420; *PHYB*, AT2G18790.

Acknowledgments

The authors thank Daoxin Xie (Tsinghua University), Roberto Solano (Campus Universidad Autónoma), Chuanyou Li (Institute of Genetics and Developmental Biology, Chinese Academy of Sciences), and Diqiu Yu (Yunan University) for sharing research materials. They also thank the Central Laboratory of Xishuangbanna Tropical Botanical Garden, Chinese Academy of Sciences for technical support. The authors thank Platform for Plant Multidimensional Imaging and Diversity of Kunming Institute of Botany, Chinese Academy of Sciences for technical support. We thank Liwen Bianji (Edanz) (www.liwenbianji.cn) for editing the English text of a draft of this manuscript and Sofie Cannon for technical assistance with seed size measurements.

Author contributions

Y.H., X.H., and J.Z. designed this study and wrote the manuscript. J.Z., J.Y., X.H., K.H., C.Y., J.D., J.C.D., and Q.F. performed experiments. Y.H., X.H., J.Z., J.Y., R.Y., and G.A.H. analyzed and interpreted the data and revised the manuscript. All authors read and approved the final article.

Supplementary data

The following materials are available in the online version of this article.

Supplementary Figure S1. COI1/JAZ-mediated jasmonate signaling inhibits organ size, and *klu-11* largely rescues the organ size phenotype of *coi1-2* and *coi1-16*.

Supplementary Figure S2. Analysis of seed set, silique number, seed number per silique, and seed weight in plants with attenuated jasmonate signaling.

Supplementary Figure S3. Publicly available RNA-seq data of several jasmonate-related genes (as well as *SOD7*, *DPA4*, and *KLU*) during seed development.

Supplementary Figure S4. RT-qPCR analysis of several jasmonate-related genes (as well as *SOD7*, *DPA4*, and *KLU*) during seed development.

Supplementary Figure S5. Expression analysis of *COI1*, *JAZ*, and *MYC* genes in developing seeds (7 DAP).

Supplementary Figure S6. Expression analysis of *COI1*, *JAZ*, and *MYC* genes in developing seeds (9 DAP).

Supplementary Figure S7. Expression analysis of *COI1*, *JAZ*, and *MYC* genes in developing seeds (13 DAP).

Supplementary Figure S8. Percentage of transformed cells with YFP fluorescence in the BiFC assays presented in Figs. 4C and 7C, and physical interactions of SOD7 with MYC factors in yeast.

Supplementary Figure S9. Overexpression of *SOD7* largely rescues the seed size phenotypes of *coi1-2* and *coi1-16*.

Supplementary Figure S10. Overexpression of *SOD7* largely rescues the organ size phenotypes of the *coi1* and *JAZ1-ΔJas* plants.

Supplementary Figure S11. Immunoblot analyzing the 2Flag-SOD7 fusion protein level in *coi1*, *JAZ1-ΔJas*, and *myc234*.

Supplementary Figure S12. Accumulation of SOD7, MYC2, and MYC4 in Arabidopsis leaf mesophyll protoplasts.

Supplementary Figure S13. Overexpression of *SOD7* largely rescues the seed size phenotype of *myc234*.

Supplementary Figure S14. SOD7 and MYC synergistically control organ size, and knocking out *KLU* largely rescues the organ size phenotype of *myc234*.

Supplementary Figure S15. Generation of *sod7*^{CR}, *myc234 sod7*^{CR}*-1*, and *myc234 sod7*^{CR}*-21* mutants through CRISPR-Cas9-mediated gene editing.

Supplementary Figure S16. RT-qPCR analyses of *SOD7* and *MYC2* expression.

Supplementary Figure S17. Quantitative analysis of YFP fluorescence intensity in Fig. 10I.

Supplementary Figure S18. The effect of jasmonate on the *KLU-2HA* transgene in *KLU-OE-1* seedlings.

Supplementary Figure S19. *phyB* partially rescues the seed size phenotype of *jazQ*.

Supplementary Figure S20. Seed germination phenotypes of *SOD7*-overexpressing plants upon ABA treatment or under salinity or osmotic stress conditions.

Supplementary Table S1. Information for detecting SOD7 binding to the *KLU* promoter.

Supplementary Table S2. Information for detecting MYC2 binding to the *KLU* promoter.

Supplementary Table S3. Primers used for RT-qPCR analyses.

Supplementary Data Set 1. Analyses of the interactive effects between MYC2 and SOD7 on seed size.

Supplementary Data Set 2. Primers used for generating various constructs.

Supplementary Data Set 3. ANOVA tables.

Funding

This work was supported by the National Natural Science Foundation of China (grant 32270613, 32370606, and 31922009), the Natural Science Foundation of Hunan Province (grant 2024JJ3007), the Yunnan Province Applied Basic Research Program Project (grant 202201AS070051 and 202305AS350010), Youth Innovation Promotion Association Chinese Academy of Sciences (2022399), and the Chemical Sciences, Geosciences, and Biosciences Division, Office of Basic Energy Sciences, Office of Science, United States Department of Energy through grant DE-FG02-91ER20021.

Conflict of interest statement. All authors state that they have no conflict of interest in relation on this research.

Data availability

All data supporting the findings of this study are available within the article and its supplementary materials.

References

Adamski NM, Anastasiou E, Eriksson S, O'Neill CM, Lenhard M. Local maternal control of seed size by KLUH/CYP78A5-dependent growth signaling. *Proc Natl Acad Sci U S A*. 2009:106(47):20115–20120. https://doi.org/10.1073/pnas.0907024106

An C, Li L, Zhai Q, You Y, Deng L, Wu F, Chen R, Jiang H, Wang H, Chen Q, et al. Mediator subunit MED25 links the jasmonate receptor to transcriptionally active chromatin. *Proc Natl Acad Sci U S A*. 2017:114(42):E8930–E8939. https://doi.org/10.1073/pnas.1710885114

Anastasiou E, Kenz S, Gerstung M, MacLean D, Timmer J, Fleck C, Lenhard M. Control of plant organ size by KLUH/CYP78A5-dependent intercellular signaling. *Dev Cell*. 2007:13(6):843–856. https://doi.org/10.1016/j.devcel.2007.10.001

Balbi V, Devoto A. Jasmonate signalling network in *Arabidopsis thaliana*: crucial regulatory nodes and new physiological scenarios. *New Phytol*. 2008:177(2):301–619. https://doi.org/10.1111/j.1469-8137.2007.02292.x

Barrero JM, Talbot MJ, White RG, Jacobsen JV, Gubler F. Anatomical and transcriptomic studies of the coleorhiza reveal the importance of this tissue in regulating dormancy in barley. *Plant Physiol*. 2009:150(2):1006–1021. https://doi.org/10.1104/pp.109.137901

Boter M, Golz JF, Giménez-Ibañez S, Fernandez-Barbero G, Franco-Zorrilla JM, Solano R. FILAMENTOUS FLOWER is a direct target of JAZ3 and modulates responses to jasmonate. *Plant Cell*. 2015:27(11):3160–3174. https://doi.org/10.1105/tpc.15.00220

Boter M, Ruíz-Rivero O, Abdeen A, Prat S. Conserved MYC transcription factors play a key role in jasmonate signaling both in tomato and Arabidopsis. *Genes Dev*. 2004:18(13):1577–1591. https://doi.org/10.1101/gad.297704

Cai Q, Yuan Z, Chen M, Yin C, Luo Z, Zhao X, Liang W, Hu J, Zhang D. Jasmonic acid regulates spikelet development in rice. *Nat Commun*. 2014:5(1):3476. https://doi.org/10.1038/ncomms4476

Campos ML, Yoshida Y, Major IT, de Oliveira Ferreira D, Weraduwage SM, Froehlich JE, Johnson BF, Kramer DM, Jander G, Sharkey TD, et al. Rewiring of jasmonate and phytochrome B signalling uncouples plant growth-defense tradeoffs. *Nat Commun*. 2016:7(1):12570. https://doi.org/10.1038/ncomms12570

Cao Y, Liu L, Ma K, Wang W, Lv H, Gao M, Wang X, Zhang X, Ren S, Zhang N, et al. The jasmonate-induced bHLH gene SlJIG functions in terpene biosynthesis and resistance to insects and fungus. *J Integr Plant Biol*. 2022:64(5):1102–1115. https://doi.org/10.1111/jipb.13248

Chaudhury AM, Berger F. Maternal control of seed development. *Semin Cell Dev Biol*. 2001:12(5):381–386. https://doi.org/10.1006/scdb.2001.0267

Chen Q, Sun J, Zhai Q, Zhou W, Qi L, Xu L, Wang B, Chen R, Jiang H, Qi J, et al. The basic helix-loop-helix transcription factor MYC2 directly represses *PLETHORA* expression during jasmonate-mediated modulation of the root stem cell niche in Arabidopsis. *Plant Cell*. 2011:23(9):3335–3352. https://doi.org/10.1105/tpc.111.089870

Chen R, Jiang H, Li L, Zhai Q, Qi L, Zhou W, Liu X, Li H, Zheng W, Sun J, et al. The Arabidopsis mediator subunit MED25 differentially regulates jasmonate and abscisic acid signaling through interacting with the MYC2 and ABI5 transcription factors. *Plant Cell*. 2012:24(7):2898–2916. https://doi.org/10.1105/tpc.112.098277

Chen S, Zhang N, Zhang Q, Zhou G, Tian H, Hussain S, Ahmed S, Wang T, Wang S. Genome editing to integrate seed size and abiotic stress tolerance traits in Arabidopsis reveals a role for DPA4 and SOD7 in the regulation of inflorescence architecture. *Int J Mol Sci*. 2019:20(11):2695. https://doi.org/10.3390/ijms20112695

Chen Y, Yan Y, Wu T, Zhang G, Yin H, Chen W, Wang S, Chang F, Gou J. Cloning of wheat keto-acyl thiolase 2B reveals a role of jasmonic acid in grain weight determination. *Nat Commun*. 2020:11(1):6266. https://doi.org/10.1038/s41467-020-20133-z

Cheng H, Song S, Xiao L, Soo HM, Cheng Z, Xie D, Peng J. Gibberellin acts through jasmonate to control the expression of *MYB21*, *MYB24*, and *MYB57* to promote stamen filament growth in Arabidopsis. *PLoS Genet*. 2009:5(3):e1000440. https://doi.org/10.1371/journal.pgen.1000440

Cheng Z, Sun L, Qi T, Zhang B, Peng W, Liu Y, Xie D. The bHLH transcription factor MYC3 interacts with the jasmonate ZIM-domain proteins to mediate jasmonate response in Arabidopsis. *Mol Plant*. 2011:4(2):279–288. https://doi.org/10.1093/mp/ssq073

Cheng Z, Zhao X, Shao X, Wang F, Zhou C, Liu Y, Zhang Y, Zhang X. Abscisic acid regulates early seed development in Arabidopsis by ABI5-mediated transcription of *SHORT HYPOCOTYL UNDER BLUE1*. *Plant Cell*. 2014:26(3):1053–1068. https://doi.org/10.1105/tpc.113.121566

Chini A, Fonseca S, Fernández G, Adie B, Chico JM, Lorenzo O, García-Casado G, López-Vidriero I, Lozano FM, Ponce MR, et al. The JAZ family of repressors is the missing link in jasmonate signaling. *Nature*. 2007:448(7154):666–671. https://doi.org/10.1038/nature06006

Chini A, Gimenez-Ibanez S, Goossens A, Solano R. Redundancy and specificity in jasmonate signaling. *Curr Opin Plant Biol*. 2016:33:147–156. https://doi.org/10.1016/j.pbi.2016.07.005

Dave A, Hernández ML, He Z, Andriotis VM, Vaistij FE, Larson TR, Graham IA. 12-oxo-Phytodienoic acid accumulation during seed development represses seed germination in Arabidopsis. *Plant Cell*. 2011:23(2):583–599. https://doi.org/10.1105/tpc.110.081489

Dave A, Vaistij FE, Gilday AD, Penfield SD, Graham IA. Regulation of *Arabidopsis thaliana* seed dormancy and germination by 12-oxo-phytodienoic acid. *J Exp Bot*. 2016:67(8):2277–2284. https://doi.org/10.1093/jxb/erw028

Dombrecht B, Xue GP, Sprague SJ, Kirkegaard JA, Ross JJ, Reid JB, Fitt GP, Sewelam N, Schenk PM, Manners JM, et al. MYC2 differentially modulates diverse jasmonate-dependent functions in Arabidopsis. *Plant Cell*. 2007:19(7):2225–2245. https://doi.org/10.1105/tpc.106.048017

Du J, Zhu X, He K, Kui M, Zhang J, Han X, Fu Q, Jiang Y, Hu Y. CONSTANS interacts with and antagonizes ABF transcription factors during salt stress under long-day conditions. *Plant Physiol*. 2023:193(2):1675–1694. https://doi.org/10.1093/plphys/kiad370

Eltayeb Habora ME, Eltayeb AE, Oka M, Tsujimoto H, Tanaka K. Cloning of allene oxide cyclase gene from *Leymus mollis* and analysis of its expression in wheat-*Leymus* chromosome addition lines. *Breed Sci*. 2013:63(1):68–76. https://doi.org/10.1270/jsbbs.63.68

Eriksson S, Stransfeld L, Adamski NM, Breuninger H, Lenhard M. KLUH/CYP78A5-dependent growth signaling coordinates floral organ growth in Arabidopsis. *Curr Biol*. 2010:20(6):527–532. https://doi.org/10.1016/j.cub.2010.01.039

Fan C, Xing Y, Mao H, Lu T, Han B, Xu C, Li X, Zhang Q. *GS3*, a major QTL for grain length and weight and minor QTL for grain width and thickness in rice, encodes a putative transmembrane protein. *Theor Appl Genet*. 2006:112(6):1164–1171. https://doi.org/10.1007/s00122-006-0218-1

Farmer EE, Dubugnon L. Detritivorous crustaceans become herbivores on jasmonate-deficient plants. *Proc Natl Acad Sci U S A*. 2009:106(3):935–940. https://doi.org/10.1073/pnas.0812182106

Fernández-Calvo P, Chini A, Fernández-Barbero G, Chico J-M, Gimenez-Ibanez S, Geerinck J, Eeckhout D, Schweizer F, Godoy M, Franco-Zorrilla JM, et al. The Arabidopsis bHLH transcription factors MYC3 and MYC4 are targets of JAZ repressors and act additively with MYC2 in the activation of jasmonate responses. *Plant Cell*. 2011:23(2):701–715. https://doi.org/10.1105/tpc.110.080788

Figueiredo DD, Köhler C. Auxin: a molecular trigger of seed development. *Genes Dev*. 2018:32(7-8):479–490. https://doi.org/10.1101/gad.312546.118

Finkelstein RR, Gampala SSL, Rock CD. Abscisic acid signaling in seeds and seedlings. *Plant Cell*. 2002:14(suppl 1):S15–S45. https://doi.org/10.1105/tpc.010441

Fonseca S, Chico JM, Solano R. The jasmonate pathway: the ligand, the receptor and the core signaling module. *Curr Opin Plant Biol*. 2009:12(5):539–547. https://doi.org/10.1016/j.pbi.2009.07.013

Garcia D, Fitz Gerald JN, Berger F. Maternal control of integument cell elongation and zygotic control of endosperm growth are coordinated to determine seed size in Arabidopsis. *Plant Cell*. 2005:17(1):52–60. https://doi.org/10.1105/tpc.104.027136

Garcia D, Saingery V, Chambrier P, Mayer U, Jurgens G, Berger F. Arabidopsis *haiku* mutants reveal new controls of seed size by endosperm. *Plant Physiol*. 2003:131(4):1661–1670. https://doi.org/10.1104/pp.102.018762

Gegas VC, Nazari A, Griffiths S, Simmonds J, Fish L, Orford S, Sayers L, Doonan JH, Snape JW. A genetic framework for grain size and shape variation in wheat. *Plant Cell*. 2010:22(4):1046–1056. https://doi.org/10.1105/tpc.110.074153

Gomez MD, Cored I, Barro-Trastoy D, Sanchez-Matilla J, Tornero P, Perez-Amador MA. DELLA proteins positively regulate seed size in Arabidopsis. *Development*. 2023:150:dev201853. https://doi.org/10.1242/dev.201853

Gomez MD, Ventimilla D, Sacristan R, Perez-Amador MA. Gibberellins regulate ovule integument development by interfering with the transcription factor ATS. *Plant Physiol*. 2016:172(4):2403–2415. https://doi.org/10.1104/pp.16.01231

Goossens J, Swinnen G, Vanden Bossche R, Pauwels L, Goossens A. Change of a conserved amino acid in the MYC2 and MYC3 transcription factors leads to release of JAZ repression and increased activity. *New Phytol*. 2015:206(4):1229–1237. https://doi.org/10.1111/nph.13398

Guo Q, Major IT, Howe GA. Resolution of growth-defense conflict: mechanistic insights from jasmonate signaling. *Curr Opin Plant Biol*. 2018a:44:72–81. https://doi.org/10.1016/j.pbi.2018.02.009

Guo Q, Major IT, Kapali G, Howe GA. MYC transcription factors coordinate tryptophan-dependent defence responses and compromise seed yield in Arabidopsis. *New Phytol*. 2022:236(1):132–145. https://doi.org/10.1111/nph.18293

Guo Q, Yoshida Y, Major IT, Wang K, Sugimoto K, Kapali G, Havko NE, Benning C, Howe GA. JAZ repressors of metabolic defense promote growth and reproductive fitness in Arabidopsis. *Proc Natl Acad Sci U S A*. 2018b:115(45):E10768–E10777. https://doi.org/10.1073/pnas.1811828115

Han X, Hu Y, Zhang G, Jiang Y, Chen X, Yu D. Jasmonate negatively regulates stomatal development in Arabidopsis cotyledons. *Plant Physiol*. 2018:176(4):2871–2885. https://doi.org/10.1104/pp.17.00444

Han X, Kui M, He K, Yang M, Du J, Jiang Y, Hu Y. Jasmonate-regulated root growth inhibition and root hair elongation. *J Exp Bot*. 2023a:74(4):1176–1185. https://doi.org/10.1093/jxb/erac441

Han X, Kui M, Xu T, Ye J, Du J, Yang M, Jiang Y, Hu Y. CO interacts with JAZ repressors and bHLH subgroup IIId factors to negatively regulate jasmonate signaling in Arabidopsis seedlings. *Plant Cell*. 2023b:35(2):852–873. https://doi.org/10.1093/plcell/koac331

Han X, Zhang M, Yang M, Hu Y. Arabidopsis JAZ proteins interact with and suppress RHD6 transcription factor to regulate jasmonate-stimulated root hair development. *Plant Cell*. 2020:32(4):1049–1062. https://doi.org/10.1105/tpc.19.00617

Haughn G, Chaudhury A. Genetic analysis of seed coat development in Arabidopsis. *Trends Plant Sci*. 2005:10(10):472–477. https://doi.org/10.1016/j.tplants.2005.08.005

He K, Du J, Han X, Li H, Kui M, Zhang J, Huang Z, Fu Q, Jiang Y, Hu Y. PHOSPHATE STARVATION RESPONSE1 (PHR1) interacts with

JASMONATE ZIM-DOMAIN (JAZ) and MYC2 to modulate phosphate deficiency-induced jasmonate signaling in Arabidopsis. *Plant Cell*. 2023:35(6):2132–2156. https://doi.org/10.1093/plcell/koad057

He Z, Zeng J, Ren Y, Chen D, Li W, Gao F, Cao Y, Luo T, Yuan G, Wu X, et al. *OsGIF1* positively regulates the sizes of stems, leaves, and grains in rice. *Front Plant Sci*. 2017:8:1730. https://doi.org/10.3389/fpls.2017.01730

Hellens RP, Allan AC, Friel EN, Bolitho K, Grafton K, Templeton MD, Karunairetnam S, Gleave AP, Laing WA. Transient expression vectors for functional genomics, quantification of promoter activity and RNA silencing in plants. *Plant Methods*. 2005:1(1):13. https://doi.org/10.1186/1746-4811-1-13

Howe GA, Major IT, Koo AJ. Modularity in jasmonate signaling for multistress resilience. *Annu Rev Plant Biol*. 2018:69(1):387–415. https://doi.org/10.1146/annurev-arplant-042817-040047

Hu S, Yang H, Gao H, Yan J, Xie D. Control of seed size by jasmonate. *Sci China Life Sci*. 2021:64(8):1215–1226. https://doi.org/10.1007/s11427-020-1899-8

Hu S, Yu K, Yan J, Shan X, Xie D. Jasmonate perception: ligand-receptor interaction, regulation, and evolution. *Mol Plant*. 2023:16:23–42. https://doi.org/10.1016/j.molp.2022.08.011

Hu Y, Han X, Yang M, Zhang M, Pan J, Yu D. The transcription factor INDUCER OF CBF EXPRESSION1 interacts with ABSCISIC ACID INSENSITIVE5 and DELLA proteins to fine-tune abscisic acid signaling during seed germination in Arabidopsis. *Plant Cell*. 2019:31(7):1520–1538. https://doi.org/10.1105/tpc.18.00825

Hu Y, Jiang L, Wang F, Yu D. Jasmonate regulates the INDUCER OF CBF EXPRESSION–C-REPEAT BINDING FACTOR/DRE BINDING FACTOR1 cascade and freezing tolerance in Arabidopsis. *Plant Cell*. 2013:25(8):2907–2924. https://doi.org/10.1105/tpc.113.112631

Hu Y, Zhou L, Huang M, He X, Yang Y, Liu X, Li Y, Hou X. Gibberellins play an essential role in late embryogenesis of Arabidopsis. *Nat Plants*. 2018:4(5):289–298. https://doi.org/10.1038/s41477-018-0143-8

Huang H, Chen Y, Wang S, Qi T, Song S. Jasmonate action and crosstalk in flower development and fertility. *J Exp Bot*. 2023:74(4):1186–1197. https://doi.org/10.1093/jxb/erac251

Huang H, Liu B, Liu L, Song S. Jasmonate action in plant growth and development. *J Exp Bot*. 2017:68(6):1349–1359. https://doi.org/10.1093/jxb/erw495

Huang Z, Han X, He K, Ye J, Yu C, Xu T, Zhang J, Du J, Fu Q, Hu Y. Nitrate attenuates abscisic acid signaling via NIN-LIKE PROTEIN8 in Arabidopsis seed germination. *Plant Cell*. 2025:37(3):koaf046. https://doi.org/10.1093/plcell/koaf046

Huo X, Wu S, Zhu Z, Liu F, Fu Y, Cai H, Sun X, Gu P, Xie D, Tan L, et al. NOG1 increases grain production in rice. *Nat Commun*. 2017:8(1):1497. https://doi.org/10.1038/s41467-017-01501-8

Hutchison CE, Li J, Argueso C, Gonzalez M, Lee E, Lewis MW, Maxwell BB, Perdue TD, Schaller GE, Alonso JM, et al. The Arabidopsis histidine phosphotransfer proteins are redundant positive regulators of cytokinin signaling. *Plant Cell*. 2006:18(11):3073–3087. https://doi.org/10.1105/tpc.106.045674

Jiang L, Yoshida T, Stiegert S, Jing Y, Alseekh S, Lenhard M, Pérez-Alfocea F, Fernie AR. Multi-omics approach reveals the contribution of KLU to leaf longevity and drought tolerance. *Plant Physiol*. 2021:185(2):352–368. https://doi.org/10.1093/plphys/kiaa034

Jiang W, Huang H, Hu Y, Zhu S, Wang Z, Lin W. Brassinosteroid regulates seed size and shape in Arabidopsis. *Plant Physiol*. 2013:162(4):1965–1977. https://doi.org/10.1104/pp.113.217703

Jiang Y, Liang G, Yang S, Yu D. Arabidopsis WRKY57 functions as a node of convergence for jasmonic acid- and auxin-mediated signaling in jasmonic acid-induced leaf senescence. *Plant Cell*. 2014:26(1):230–245. https://doi.org/10.1105/tpc.113.117838

Ju L, Jing Y, Shi P, Liu J, Chen J, Yan J, Chu J, Chen K, Sun J. JAZ proteins modulate seed germination through interacting with ABI5 in bread wheat and Arabidopsis. *New Phytol*. 2019:223(1):246–260. https://doi.org/10.1111/nph.15757

Kang X, Li W, Zhou Y, Ni M. A WRKY transcription factor recruits the SYG1-like protein SHB1 to activate gene expression and seed cavity enlargement. *PLoS Genet*. 2013:9(3):e1003347. https://doi.org/10.1371/journal.pgen.1003347

Kanno Y, Jikumaru Y, Hanada A, Nambara E, Abrams SR, Kamiya Y, Seo M. Comprehensive hormone profiling in developing Arabidopsis seeds: examination of the site of ABA biosynthesis, ABA transport and hormone interactions. *Plant Cell Physiol*. 2010:51(12):1988–2001. https://doi.org/10.1093/pcp/pcq158

Katsir L, Chung HS, Koo AJ, Howe GA. Jasmonate signaling: a conserved mechanism of hormone sensing. *Curr Opin Plant Biol*. 2008:11(4):428–435. https://doi.org/10.1016/j.pbi.2008.05.004

Kazan K, Manners JM. MYC2: the master in action. *Mol Plant*. 2013:6(3):686–703. https://doi.org/10.1093/mp/sss128

Ke J, Ma H, Gu X, Thelen A, Brunzelle J, Li J, Xu H, Melcher K. Structural basis for recognition of diverse transcriptional repressors by the TOPLESS family of corepressors. *Sci Adv*. 2015:1(6):e1500107. https://doi.org/10.1126/sciadv.1500107

Kim KC, Lai Z, Fan B, Chen Z. Arabidopsis WRKY38 and WRKY62 transcription factors interact with Histone Deacetylase 19 in basal defense. *Plant Cell*. 2008:20(9):2357–2371. https://doi.org/10.1105/tpc.107.055566

Krock B, Schmidt S, Hertweck C, Baldwin IT. Vegetation derived abscisic acid and four terpenes enforce dormancy in seeds of the post-fire annual, *Nicotiana attenuata*. *Seed Sci Res*. 2002:12(4):239–252. https://doi.org/10.1079/SSR2002117

Lee BH, Wynn AN, Franks RG, Hwang YS, Lim J, Kim JH. The *Arabidopsis thaliana GRF-INTERACTING FACTOR* gene family plays an essential role in control of male and female reproductive development. *Dev Biol*. 2014:386(1):12–36. https://doi.org/10.1016/j.ydbio.2013.12.009

Lee SH, Sakuraba Y, Lee T, Kim KW, An G, Lee HY, Paek NC. Mutation of *Oryza sativa CORONATINE INSENSITIVE 1b* (*OsCOI1b*) delays leaf senescence. *J Integr Plant Biol*. 2015:57(6):562–576. https://doi.org/10.1111/jipb.12276

Li C, Du J, Xu H, Feng Z, Chater CCC, Duan Y, Yang Y, Sun X. UVR8-TCP4-LOX2 module regulates UV-B tolerance in Arabidopsis. *J Integr Plant Biol*. 2024:66(5):897–908. https://doi.org/10.1111/jipb.13648

Li J, Nie X, Tan JL, Berger F. Integration of epigenetic and genetic controls of seed size by cytokinin in Arabidopsis. *Proc Natl Acad Sci U S A*. 2013:110(38):15479–15484. https://doi.org/10.1073/pnas.1305175110

Li L, Zhao Y, McCaig BC, Wingerd BA, Wang J, Whalon ME, Pichersky E, Howe GA. The tomato homolog of CORONATINE-INSENSITIVE1 is required for the maternal control of seed maturation, jasmonate-signaled defense responses, and glandular trichome development. *Plant Cell*. 2004:16(1):126–143. https://doi.org/10.1105/tpc.017954

Li M, Yu G, Cao C, Liu P. Metabolism, signaling, and transport of jasmonates. *Plant Commun*. 2021:2(5):100231. https://doi.org/10.1016/j.xplc.2021.100231

Li N, Li Y. Signaling pathways of seed size control in plants. *Curr Opin Plant Biol*. 2016:33:23–32. https://doi.org/10.1016/j.pbi.2016.05.008

Li N, Xu R, Li Y. Molecular networks of seed size control in plants. *Annu Rev Plant Biol*. 2019:70(1):435–463. https://doi.org/10.1146/annurev-arplant-050718-095851

Lin C, Lan C, Li X, Xie W, Lin F, Liang Y, Tao Z. A pair of nuclear factor Y transcription factors act as positive regulators in jasmonate signaling and disease resistance in Arabidopsis. *J Integr Plant Biol*. 2024:66(9):2042–2057. https://doi.org/10.1111/jipb.13732

Linkies A, Graeber K, Knight C, Leubner-Metzger G. The evolution of seeds. *New Phytol*. 2010:186(4):817–831. https://doi.org/10.1111/j.1469-8137.2010.03249.x

Liu Y, Du M, Deng L, Shen J, Fang M, Chen Q, Lu Y, Wang Q, Li C, Zhai Q. MYC2 regulates the termination of jasmonate signaling via an autoregulatory negative feedback loop. *Plant Cell*. 2019:31(1):106–127. https://doi.org/10.1105/tpc.18.00405

Liu Z, Li N, Zhang Y, Li Y. Transcriptional repression of GIF1 by the KIX-PPD-MYC repressor complex controls seed size in Arabidopsis. *Nat Commun*. 2020:11(1):1846. https://doi.org/10.1038/s41467-020-15603-3

Lopes MA, Larkins BA. Endosperm origin, development, and function. *Plant Cell*. 1993:5(10):1383–1399. https://doi.org/10.1105/tpc.5.10.1383

Lorenzo O, Chico JM, Sanchez-Serrano JJ, Solano R. JASMONATE-INSENSITIVE1 encodes a MYC transcription factor essential to discriminate between different jasmonate-regulated defense responses in Arabidopsis. *Plant Cell*. 2004:16(7):1938–1950. https://doi.org/10.1105/tpc.022319

Luo M, Dennis ES, Berger F, Peacock WJ, Chaudhury A. *MINISEED3 (MINI3)*, a WRKY family gene, and *HAIKU2 (IKU2)*, a leucine-rich repeat *(LRR) KINASE* gene, are regulators of seed size in Arabidopsis. *Proc Natl Acad Sci U S A*. 2005:102(48):17531–17536. https://doi.org/10.1073/pnas.0508418102

Maes L, Inzé D, Goossens A. Functional specialization of the TRANSPARENT TESTA GLABRA1 network allows differential hormonal control of laminal and marginal trichome initiation in Arabidopsis rosette leaves. *Plant Physiol*. 2008:148(3):1453–1464. https://doi.org/10.1104/pp.108.125385

Mao Y, Liu Y, Chen D, Chen F, Fang X, Hong G, Wang L, Wang J, Chen X. Jasmonate response decay and defense metabolite accumulation contributes to age-regulated dynamics of plant insect resistance. *Nat Commun*. 2017:8(1):13925. https://doi.org/10.1038/ncomms13925

McCarty M. Transforming biology. *Mol Med*. 1995:1(4):342–343. https://doi.org/10.1007/BF03401571

McConn M, Browse J. The critical requirement for linolenic acid is pollen development, not photosynthesis, in an Arabidopsis mutant. *Plant Cell*. 1996:8(3):403–416. https://doi.org/10.2307/3870321

Mei S, Zhang M, Ye J, Du J, Jiang Y, Hu Y. Auxin contributes to jasmonate-mediated regulation of abscisic acid signaling during seed germination in Arabidopsis. *Plant Cell*. 2023:35(3):1110–1133. https://doi.org/10.1093/plcell/koac362

Moles AT, Ackerly DD, Webb CO, Tweddle JC, Dickie JB, Pitman AJ, Westoby M. Factors that shape seed mass evolution. *Proc Natl Acad Sci U S A*. 2005:102(30):10540–10544. https://doi.org/10.1073/pnas.0501473102

Moreno JE, Shyu C, Campos ML, Patel LC, Chung HS, Yao J, He SY, Howe GA. Negative feedback control of jasmonate signaling by an alternative splice variant of JAZ10. *Plant Physiol*. 2013:162(2):1006–1017. https://doi.org/10.1104/pp.113.218164

Mukhopadhyay A, Deplancke B, Walhout AJ, Tissenbaum HA. Chromatin immunoprecipitation (ChIP) coupled to detection by quantitative real-time PCR to study transcription factor binding to DNA in *Caenorhabditis elegans*. *Nat Protoc*. 2008:3(4):698–709. https://doi.org/10.1038/nprot.2008.38

Nguyen HT, Cheaib M, Fournel M, Rios M, Gantet P, Laplaze L, Guyomarc'h S, Riemann M, Heitz T, Petitot A-S, et al. Genetic analysis of the rice jasmonate receptors reveals specialized functions for *OsCOI2*. *PLoS One*. 2023:8:e0291385. https://doi.org/10.1371/journal.pone.0291385

Niu YJ, Figueroa P, Browse J. Characterization of JAZ-interacting bHLH transcription factors that regulate jasmonate responses in Arabidopsis. *J Exp Bot*. 2011:62(6):2143–2154. https://doi.org/10.1093/jxb/erq408

Nobusawa T, Kamei M, Ueda H, Matsushima N, Yamatani H, Kusaba M. Highly pleiotropic functions of CYP78As and AMP1 are regulated in non-cell-autonomous/organ-specific manners. *Plant Physiol*. 2021:186(1):767–781. https://doi.org/10.1093/plphys/kiab067

Norastehnia A, Sajedi RH, Nojavan-Asghari M. Inhibitory effects of methyl jasmonate on seed germination in maize (*Zea mays*): effect on a-amylase activity and ethylene production. *Gen Appl Plant Physiol*. 2007:33:13–23.

Orsi CH, Tanksley SD. Natural variation in an ABC transporter gene associated with seed size evolution in tomato species. *PLoS Genet*. 2009:5(1):e1000347. https://doi.org/10.1371/journal.pgen.1000347

Pan J, Hu Y, Wang H, Guo Q, Chen Y, Howe GA, Yu D. Molecular mechanism underlying the synergetic effect of jasmonate on abscisic acid signaling during seed germination in Arabidopsis. *Plant Cell*. 2020:32(12):3846–3865. https://doi.org/10.1105/tpc.19.00838

Pan J, Wang H, You Q, Cao R, Sun G, Yu D. Jasmonate-regulated seed germination and crosstalk with other phytohormones. *J Exp Bot*. 2023:74(4):1162–1175. https://doi.org/10.1093/jxb/erac440

Pauwels L, Barbero GF, Geerinck J, Tilleman S, Grunewald W, Pérez AC, Chico JM, Bossche RV, Sewell J, Gil E, et al. NINJA connects the co-repressor TOPLESS to jasmonate signaling. *Nature*. 2010:464(7289):788–791. https://doi.org/10.1038/nature08854

Poretska O, Yang S, Pitorre D, Poppenberger B, Sieberer T. AMP1 and CYP78A5/7 act through a common pathway to govern cell fate maintenance in *Arabidopsis thaliana*. *PLoS Genet*. 2020:16(9):e1009043. https://doi.org/10.1371/journal.pgen.1009043

Preston CA, Betts H, Baldwi IT. Methyl jasmonate as an allelopathic agent: sagebrush inhibits germination of a neighboring tobacco, *Nicotiana attenuata*. *J Chem Ecol*. 2002:28(11):2343–2369. https://doi.org/10.1023/A:1021065703276

Putterill J, Robson F, Lee K, Simon R, Coupland G. The CONSTANS gene of Arabidopsis promotes flowering and encodes a protein showing similarities to zinc finger transcription factors. *Cell*. 1995:80(6):847–857. https://doi.org/10.1016/0092-8674(95)90288-0

Qi T, Huang H, Song S, Xie D. Regulation of jasmonate-mediated stamen development and seed production by a bHLH-MYB complex in Arabidopsis. *Plant Cell*. 2015:27(6):1620–1633. https://doi.org/10.1105/tpc.15.00116

Qi T, Huang H, Wu D, Yan J, Qi Y, Song S, Xie D. Arabidopsis DELLA and JAZ proteins bind the WD-repeat/bHLH/MYB complex to modulate gibberellin and jasmonate signaling synergy. *Plant Cell*. 2014:26(3):1118–1133. https://doi.org/10.1105/tpc.113.121731

Qi T, Song S, Ren Q, Wu D, Huang H, Chen Y, Fan M, Peng W, Ren C, Xie D. The jasmonate-ZIM-domain proteins interact with the WD-Repeat/bHLH/MYB complexes to regulate jasmonate-mediated anthocyanin accumulation and trichome initiation in *Arabidopsis thaliana*. *Plant Cell*. 2011:23(5):1795–1814. https://doi.org/10.1105/tpc.111.083261

Reiser L, Fischer RL. The ovule and the embryo sac. *Plant Cell*. 1993:5(10):1291–1301. https://doi.org/10.2307/3869782

Riefler M, Novak O, Strnad M, Schmülling T. Arabidopsis cytokinin receptor mutants reveal functions in shoot growth, leaf senescence, seed size, germination, root development, and cytokinin metabolism. *Plant Cell*. 2005:18(1):40–54. https://doi.org/10.1105/tpc.105.037796

Robert HS, Park C, Gutièrrez CL, Wójcikowska B, Pěnčík A, Novák O, Chen J, Grunewald W, Dresselhaus T, Friml J, et al. Maternal auxin supply contributes to early embryo patterning in Arabidopsis. *Nat Plant*. 2018:4(8):548–553. https://doi.org/10.1038/s41477-018-0204-z

Sanders PM, Lee PY, Biesgen C, Boone JD, Beals TP, Weiler EW, Goldberg RB. The Arabidopsis DELAYED DEHISCENCE1 gene encodes an enzyme in the jasmonic acid synthesis pathway. *Plant Cell*. 2000:12(7):1041–1061. https://doi.org/10.1105/tpc.12.7.1041

Schruff MC, Spielman M, Tiwari S, Adams S, Fenby N, Scott RJ. The *AUXIN RESPONSE FACTOR 2* gene of Arabidopsis links auxin signalling, cell division, and the size of seeds and other organs. *Development*. 2006:133(2):251–261. https://doi.org/10.1242/dev.02194

Schweizer F, Fernández-Calvo P, Zander M, Diez-Diaz M, Fonseca S, Glauser G, Lewsey MG, Ecker JR, Solano R, Reymond P. Arabidopsis basic helix-loop-helix transcription factors MYC2, MYC3, and MYC4 regulate glucosinolate biosynthesis, insect performance, and feeding behavior. *Plant Cell*. 2013:25(8):3117–3132. https://doi.org/10.1105/tpc.113.115139

Scott RJ, Spielman M, Bailey J, Dickinson HG. Parent-of-origin effects on seed development in *Arabidopsis thaliana*. *Development*. 1998:125(17):3329–3341. https://doi.org/10.1242/dev.125.17.3329

Serrano-Bueno G, de Los Reyes P, Chini A, Ferreras-Garrucho G, Sánchez de Medina-Hernández V, Boter M, Solano R, Valverde F. Regulation of floral senescence in Arabidopsis by coordinated action of CONSTANS and jasmonate signaling. *Mol Plant*. 2022:15(11):1710–1724. https://doi.org/10.1016/j.molp.2022.09.017

Sheard LB, Tan X, Mao H, Withers J, Ben-Nissan G, Hinds TR, Kobayashi Y, Hsu F-F, Sharon M, Browse J, et al. Jasmonate perception by inositol-phosphate-potentiated COI1-JAZ co-receptor. *Nature*. 2010:468(7322):400–405. https://doi.org/10.1038/nature09430

Sheen J. Signal transduction in maize and Arabidopsis mesophyll protoplasts. *Plant Physiol*. 2001:127(4):1466–1475. https://doi.org/10.1104/pp.010820

Shyu C, Figueroa P, Depew CL, Cooke TF, Sheard LB, Moreno JE, Katsir L, Zheng N, Browse J, Howe GA. JAZ8 lacks a canonical degron and has an EAR motif that mediates transcriptional repression of jasmonate responses in Arabidopsis. *Plant Cell*. 2012:24(2):536–550. https://doi.org/10.1105/tpc.111.093005

Simon R, Igeño MI, Coupland G. Activation of floral meristem identity genes in Arabidopsis. *Nature*. 1996:384(6604):59–62. https://doi.org/10.1038/384059a0

Song J, Pang S, Xue B, Rong D, Qi T, Huang H, Song S. The AMS/DYT1-MYB module interacts with the MED25-MYC-MYB complexes to inhibit jasmonate-regulated floral defense in Arabidopsis. *J Integr Plant Biol*. 2025:67(2):408–422. https://doi.org/10.1111/jipb.13818

Song S, Qi T, Fan M, Zhang X, Gao H, Huang H, Wu D, Guo H, Xie D. The bHLH subgroup IIId factors negatively regulate jasmonate-mediated plant defense and development. *PLoS Genet*. 2013:9(7):e1003653. https://doi.org/10.1371/journal.pgen.1003653

Song S, Qi T, Huang H, Ren Q, Wu D, Chang C, Peng W, Liu Y, Peng J, Xie D. The jasmonate-ZIM domain proteins interact with the R2R3-MYB transcription factors MYB21 and MYB24 to affect jasmonate-regulated stamen development in Arabidopsis. *Plant Cell*. 2011:23(3):1000–1013. https://doi.org/10.1105/tpc.111.083089

Song X, Huang W, Shi M, Zhu M, Lin H. A QTL for rice grain width and weight encodes a previously unknown RING-type E3 ubiquitin ligase. *Nat Genet*. 2007:39(5):623–630. https://doi.org/10.1038/ng2014

Staswick P, Su W, Howell S. Methyl jasmonate inhibition of root growth and induction of a leaf protein are decreased in an *Arabidopsis thaliana* mutant. *Proc Natl Acad Sci U S A*. 1992:89(15):6837–6840. https://doi.org/10.1073/pnas.89.15.6837

Stintzi A, Browse J. The Arabidopsis male-sterile mutant, *opr3*, lacks the 12-oxophytodienoic acid reductase required for jasmonate synthesis. *Proc Natl Acad Sci U S A*. 2000:97(19):10625–10630. https://doi.org/10.1073/pnas.190264497

Suárez-López P, Wheatley K, Robson F, Onouchi H, Valverde F, Coupland G. CONSTANS mediates between the circadian clock and the control of flowering in Arabidopsis. *Nature*. 2001:410(6832):1116–1120. https://doi.org/10.1038/35074138

Sun Y, Zheng Y, Yao H, Ma Z, Xiao M, Wang H, Liu Y. Light and jasmonic acid coordinately regulate the phosphate responses under shade and phosphate starvation conditions in Arabidopsis. *Plant Direct*. 2023:7(6):e504. https://doi.org/10.1002/pld3.504

Thines B, Katsir L, Melotto M, Niu Y, Mandaokar A, Liu G, Nomura K, He SY, Howe GA, Browse J. JAZ repressor proteins are targets of the $SCF^{(CO11)}$ complex during jasmonate signaling. *Nature*. 2007:448(7154):661–665. https://doi.org/10.1038/nature05960

Traw MB, Bergelson J. Interactive effects of jasmonic acid, salicylic acid, and gibberellin on induction of trichomes in Arabidopsis. *Plant Physiol*. 2003:133(3):1367–1375. https://doi.org/10.1104/pp.103.027086

Varshney V, Hazra A, Rao V, Ghosh S, Kamble NU, Achary RK, Gautam S, Majee M. The Arabidopsis F-box protein SKIP31 modulates seed maturation and seed vigor by targeting JAZ proteins independently of jasmonic acid-isoleucine. *Plant Cell*. 2023:35(10):3712–3738. https://doi.org/10.1093/plcell/koad199

Villanueva JM, Broadhvest J, Hauser BA, Meister RJ, Schneitz K, Gasser CS. INNER NO OUTER regulates abaxial- adaxial patterning in Arabidopsis ovules. *Genes Dev*. 1999:13(23):3160–3169. https://doi.org/10.1101/gad.13.23.3160

Wang A, Garcia D, Zhang H, Feng K, Chaudhury A, Berger F, Peacock WJ, Dennis ES, Luo M. The VQ motif protein IKU1 regulates endosperm growth and seed size in Arabidopsis. *Plant J*. 2010:63(4):670–679. https://doi.org/10.1111/j.1365-313X.2010.04271.x

Wang H, Li S, Li Y, Xu Y, Wang Y, Zhang R, Sun W, Chen Q, Wang X, Li C, et al. MED25 connects enhancer-promoter looping and MYC2-dependent activation of jasmonate signaling. *Nat Plants*. 2019:5(6):616–625. https://doi.org/10.1038/s41477-019-0441-9

Wang H, Li Y, Pan J, Lou D, Hu Y, Yu D. The bHLH transcription factors MYC2, MYC3, and MYC4 are required for jasmonate-mediated inhibition of glowering in Arabidopsis. *Mol Plant*. 2017:10(11):1461–1464. https://doi.org/10.1016/j.molp.2017.08.007

Wang J, Li Y, Hu Y, Zhu S. Jasmonate induces translation of the Arabidopsis transfer RNA-binding protein YUELAO1, which activates MYC2 in jasmonate signaling. *Plant Cell*. 2024:37(1):koae294. https://doi.org/10.1093/plcell/koae294

Wang J, Schwab R, Czech B, Mica E, Weigel D. Dual effects of miR156-targeted SPL genes and CYP78A5/KLUH on plastochron length and organ size in *Arabidopsis thaliana*. *Plant Cell*. 2008:20(5):1231–1243. https://doi.org/10.1105/tpc.108.058180

Wang X, Chen Y, Liu S, Fu W, Zhuang Y, Xu J, Lou Y, Baldwin IT, Li R. Functional dissection of rice jasmonate receptors involved in development and defense. *New Phytol*. 2023:238(5):2144–2158. https://doi.org/10.1111/nph.18860

Wasternack C. Determination of sex by jasmonate. *J Integr Plant Biol*. 2020:62(2):162–164. https://doi.org/10.1111/jipb.12840

Wasternack C, Forner S, Strnad M, Hause B. Jasmonates in flower and seed development. *Biochimie*. 2013:95(1):79–85. https://doi.org/10.1016/j.biochi.2012.06.005

Wasternack C, Hause B. Jasmonates: biosynthesis, perception, signal transduction and action in plant stress response, growth and development. *Ann Bot*. 2013:111(6):1021–1058. https://doi.org/10.1093/aob/mct067

Wilen RW, van Rooijen GJ, Pearce DW, Pharis RP, Holbrook LA, Moloney MM. Effects of jasmonic acid on embryo-specific processes in *brassica* and *linum* oilseeds. *Plant Physiol*. 1991:95(2):399–405. https://doi.org/10.1104/pp.95.2.399

Wu F, Deng L, Zhai Q, Zhao J, Chen Q, Li C. Mediator subunit MED25 couples alternative splicing of JAZ genes with fine-tuning of jasmonate signaling. *Plant Cell*. 2020:32(2):429–448. https://doi.org/10.1105/tpc.19.00583

Xiao W, Brown RC, Lemmon BE, Harada JJ, Goldberg RB, Fischer RL. Regulation of seed size by hypomethylation of maternal and paternal genomes. *Plant Physiol*. 2006:142(3):1160–1168. https://doi.org/10.1104/pp.106.088849

Xie D, Feys BF, James S, Nieto-Rostro M, Turner JG. *COI1*: an Arabidopsis gene required for jasmonate-regulated defense and fertility. *Science*. 1998:280(5366):1091–1094. https://doi.org/10.1126/science.280.5366.1091

Xu L, Liu F, Lechner E, Genschik P, Crosby WL, Ma H, Peng W, Huang D, Xie D. The $SCF^{(COI1)}$ ubiqutin-ligase complexes are required for jasmonate response in Arabidopsis. *Plant Cell*. 2002:14(8):1919–1935. https://doi.org/10.1105/tpc.003368

Yan J, Li H, Li S, Yao R, Deng H, Xie Q, Xie D. The Arabidopsis F-Box protein CORONATINE INSENSITIVE1 is stabilized by SCF^{COI1} and degraded via the 26S proteasome pathway. *Plant Cell*. 2013:25(2):486–498. https://doi.org/10.1105/tpc.112.105486

Yan J, Zhang C, Gu M, Bai Z, Zhang W, Qi T, Cheng Z, Peng W, Luo H, Nan F, et al. The Arabidopsis CORONATINE INSENSITIVE1 protein is a jasmonate receptor. *Plant Cell*. 2009:21(8):2220–2236. https://doi.org/10.1105/tpc.109.065730

Yang DL, Yao J, Mei C-S, Tong X-H, Zeng L-J, Li Q, Xiao L-T, Sun T, Li J, Deng X-W, et al. Plant hormone jasmonate prioritizes defense over growth by interfering with gibberellin signaling cascade. *Proc Natl Acad Sci U S A*. 2012:109(19):E1192–E1200. https://doi.org/10.1073/pnas.1201616109

Yang M, Han X, Yang J, Jiang Y, Hu Y. The Arabidopsis circadian clock protein PRR5 interacts with and stimulates ABI5 to modulate abscisic acid signaling during seed germination. *Plant Cell*. 2021:33(9):3022–3041. https://doi.org/10.1093/plcell/koab168

Yoo SD, Cho YH, Sheen J. Arabidopsis mesophyll protoplasts: a versatile cell system for transient gene expression analysis. *Nat Protoc*. 2007:2(7):1565–1572. https://doi.org/10.1038/nprot.2007.199

You Y, Zhai Q, An C, Li C. LEUNIG_HOMOLOG mediates MYC2-dependent transcriptional activation in cooperation with the coactivators HAC1 and MED25. *Plant Cell*. 2019:31(9):2187–2205. https://doi.org/10.1105/tpc.19.00115

Yu B, He X, Tang Y, Chen Z, Zhou L, Li X, Zhang C, Huang X, Yang Y, Zhang W, et al. Photoperiod controls plant seed size in a CONSTANS-dependent manner. *Nat Plants*. 2023:9(2):343–354. https://doi.org/10.1038/s41477-023-01350-y

Zander M, Lewsey MG, Clark NM, Yin L, Bartlett A, Saldierna Guzmán JP, Hann E, Langford AE, Jow B, Wise A, et al. Integrated multi-omics framework of the plant response to jasmonic acid. *Nat Plants*. 2020:6(3):290–302. https://doi.org/10.1038/s41477-020-0605-7

Zhai Q, Deng L, Li C. Mediator subunit MED25: at the nexus of jasmonate signaling. *Curr Opin Plant Biol*. 2020:57:78–86. https://doi.org/10.1016/j.pbi.2020.06.006

Zhai Q, Yan Y, Tan D, Chen R, Sun J, Gao L, Dong M, Wang Y, Li C. Phosphorylation-coupled proteolysis of the transcription factor MYC2 is important for jasmonate-signaled plant immunity. *PLoS Genet*. 2013:9(4):e1003422. https://doi.org/10.1371/journal.pgen.1003422

Zhai Q, Zhang X, Wu F, Feng H, Deng L, Xu L, Zhang M, Wang Q, Li C. Transcriptional mechanism of jasmonate receptor COI1-mediated delay of flowering time in Arabidopsis. *Plant Cell*. 2015:27(10):2814–2828. https://doi.org/10.1105/tpc.15.00619

Zhang B, Li C, Li Y, Yu H. Mobile TERMINAL FLOWER1 determines seed size in Arabidopsis. *Nat Plants*. 2020a:6(9):1146–1157. https://doi.org/10.1038/s41477-020-0749-5

Zhang F, Ke J, Zhang L, Chen R, Sugimoto K, Howe GA, Xu HE, Zhou M, He SY, Melcher K. Structural insights into alternative splicing-mediated desensitization of jasmonate signaling. *Proc Natl Acad Sci U S A*. 2017b:114(7):1720–1725. https://doi.org/10.1073/pnas.1616938114

Zhang F, Yao J, Ke J, Zhang L, Lam VQ, Xin X-F, Zhou XE, Chen J, Brunzelle J, Griffin PR, et al. Structural basis of JAZ repression of MYC transcription factors in jasmonate signalling. *Nature*. 2015b:525(7568):269–273. https://doi.org/10.1038/nature14661

Zhang H, Zhang F, Yu Y, Feng L, Jia J, Liu B, Li B, Guo H, Zhai J. A comprehensive online database for exploring ~20,000 public Arabidopsis RNA-seq libraries. *Mol Plant*. 2020b:13(9):1231–1233. https://doi.org/10.1016/j.molp.2020.08.001

Zhang J, Zhang X, Liu X, Pai Q, Wang Y, Wu X. Molecular network for regulation of seed size in plants. *Int J Mol Sci*. 2023:24(13):10666. https://doi.org/10.3390/ijms241310666

Zhang L, Zhang F, Melotto M, Yao J, He SY. Jasmonate signaling and manipulation by pathogens and insects. *J Exp Bot*. 2017a:68(6):1371–1385. https://doi.org/10.1093/jxb/erw478

Zhang Q, Du J, Han X, Hu Y. Transcription factor ABF3 modulates salinity stress-enhanced jasmonate signaling in Arabidopsis. *Plant Divers*. 2024:46(6):791–803. https://doi.org/10.1016/j.pld.2024.05.003

Zhang Y, Du L, Xu R, Cui R, Hao J, Sun C, Li Y. Transcription factors SOD7/NGAL2 and DPA4/NGAL3 act redundantly to regulate seed size by directly repressing *KLU* expression in *Arabidopsis thaliana*. *Plant Cell*. 2015a:27(3):620–632. https://doi.org/10.1105/tpc.114.135368

Zhao L, Cai H, Su Z, Wang L, Huang X, Zhang M, Chen P, Dai X, Zhao H, Palanivelu R, et al. *KLU* suppresses megasporocyte cell fate through SWR1-mediated activation of *WRKY28* expression in Arabidopsis. *Proc Natl Acad Sci U S A*. 2018:115(3):E526–E535. https://doi.org/10.1073/pnas.1716054115

Zhao Y, Dong W, Zhang N, Ai X, Wang M, Huang Z, Xiao L, Xia G. A wheat allene oxide cyclase gene enhances salinity tolerance via jasmonate signaling. *Plant Physiol*. 2014:164(2):1068–1076. https://doi.org/10.1104/pp.113.227595

Zheng L, Wu H, Wang A, Zhang Y, Liu Z, Ling H, Song X, Li Y. The SOD7/DPA4–GIF1 module coordinates organ growth and iron uptake in Arabidopsis. *Nat Plants*. 2023:9(8):1318–1332. https://doi.org/10.1038/s41477-023-01475-0

Zhou W, Lozano-Torres JL, Blilou I, Zhang X, Zhai Q, Smant G, Li C, Scheres B. A jasmonate signaling network activates root stem cells and promotes regeneration. *Cell*. 2019:177(4):942–956.e14. https://doi.org/10.1016/j.cell.2019.03.006

Zhou X, Zhang Y, Yao J, Zheng J, Zhou Y, He Q, Moreno J, Lam VQ, Cao X, Sugimoto K, et al. Assembly of JAZ-JAZ and JAZ-NINJA complexes in jasmonate signaling. *Plant Commun*. 2023:4(6):100639. https://doi.org/10.1016/j.xplc.2023.100639

Zhou Y, Zhang X, Kang X, Zhao X, Ni M. SHORT HYPOCOTYL UNDER BLUE1 associates with *MINISEED3* and *HAIKU2* promoters in *vivo* to regulate Arabidopsis seed development. *Plant Cell*. 2009:21(1):106–117. https://doi.org/10.1105/tpc.108.064972

Zhu Z, An F, Feng Y, Li P, Xue L, A M, Jiang Z, Kim J-M, To TK, Li W, et al. Derepression of ethylene-stabilized transcription factors (EIN3/EIL1) mediates jasmonate and ethylene signaling synergy in Arabidopsis. *Proc Natl Acad Sci U S A*. 2011:108(30):12539–12544. https://doi.org/10.1073/pnas.1103959108

Zuo J, Li J. Molecular genetic dissection of quantitative trait loci regulating rice grain size. *Annu Rev Genet*. 2014:48(1):99–118. https://doi.org/10.1146/annurev-genet-120213-092138